NTNU

Norwegian University of
Science and Technology

Analysis of Ammonium and Nitrate with Ion Selective Electrodes (ISE) in Recirculating Aquaculture Systems (RAS) and a Test of Ag - TiO_2 Nanotube Composite Material as Antifouling Sensor Protection.

Kristin Søiland

Chemical Engineering and Biotechnology
Submission date: June 2018
Supervisor: Øyvind Mikkelsen, IKJ

Norwegian University of Science and Technology
Department of Chemistry

Preface

This master thesis in industrial chemistry and biotechnology with specialisation in analytical chemistry was written at the Department of Chemistry at the Norwegian University of Science and Technology (NTNU). The analyses were carried out at the Faculty of Chemistry at NTNU and at Nofima in Sunndalsøra. The project was a part of the centre for research-based innovation CtrlAQUA.

Trondheim, June 2018

Kristin Søiland

Kristin Søiland

NTNU
Norwegian University of
Science and Technology

CtrlAQUA

Acknowledgment

During this project, I have learned to work independently in the laboratory, planned, collected and analyzed water samples. I have gained deeper insight into how to organize and implement bigger research projects within the field of aquaculture. Without NTNUs expertise and good collaboration with Nofima, this project would not be possible. I would like to thank Professor Øyvind Mikkelsen at NTNU for excellent supervising and good support this semester. I would also like to thank Britt Kristin Reiten for spectrophotometric analysis of NH_4-N and help with installation of my equipment in the recirculating aquaculture system (RAS), and Valeria Ivanova for letting me test the sensors in the flow through system (FTS) for smolt. Also huge thank to PhD candidate Sharada Navada and Erasmus student Claudia Spanu for helping me collecting samples in Sunndalsøra, and PhD candidate Xiaoxue Zhang for providing PDMS-TiO_2-Ag coated caps for the antifouling experiment. Thanks to Syverin Lierhagen for analyzing samples on ICP-MS.

Abstract

Keeping salmon farming in closed recirculating systems, the challenge related to salmon lice, escape and leakage of nutrients will be dramatically reduced. A high content of nitrogen species deriving from nutrients and excrements can cause formation of ammonia, that is toxic for salmon. The industry demands fast and reliable analysis of these species. In this master thesis, the use of HACH ion selective electrodes (ISE) for nitrate (ISENO3181) and ammonium (ISENH4181) have been tested. Two tests were done in a recirculating aquaculture system (RAS) at Nofima in Sunndalsøra with 12‰ salinity, where challenges related to interfering ions and biofouling were investigated. One experiment with no antifouling treatment, and one experiment where vibration and a nylon filter was used as antifouling treatment was done. In addition to the RAS experiments, a flow through system (FTS) with fresh water was used to test a composite material of TiO_2 nanorods with silver nanoparticles attached (PDMS-TiO_2/Ag) as antifouling sensor protection. The release of silver ions from the silver particles was investigated adding a PDMS-TiO_2/Ag coated Teflon cap to a brackish water solution. The silver concentration was determined by inductively coupled plasma mass spectrometry (ICP-MS). Samples from the RAS and FTS were also analyzed by ICP-MS to investigate eventual accumulation of metals. The samples were also analyzed by ion chromatography (IC) to quantify the ammonium and nitrate content compared to the ISE measurements. None of the metals in RAS or FTS exceeded the background levels for Norwegian coastal waters. There was found an accumulation of Zn and Cu in the RAS with a slope of 0.38 and 0.02 $\mu gL^{-1}day^{-1}$ respectively. Drift due to biofouling occurred in all experiments. In RAS the biofouling process started already after the first day. In the FTS the biofouling was visible after two weeks. When the ISE and IC results were compared, the presence of interfering ions was most significant in RAS. The $NH_4{}^+$ electrode was more affected by the salinity change in RAS than the $NO_3{}^-$ electrode. The use of vibration and a nylon filter protecting the sensing elements, resulted in a more stable drift successively estimated using baseline reduction by minimum least squares regression (MLR). The PDMS-TiO_2/Ag coated caps did not have a visible antifouling effect. In the experiment where the release of Ag^+ was investigated, the increase was significant with a p-value equal to 0.012 for the two beakers with coated caps compared to p=0.11 for two blank tests. To achieve an antifouling effect, the cap design needs to be improved. In the FTS the ISE did detect small variations in the ammonium concentration as a result of the salmons' daytime activity. The method was fast and effective in the freshwater system. More tests regarding antifouling and the presence of interfering ions need to be done to fully elucidate ISEs potential in aquaculture.

Sammendrag

Ved å holde laksen lengre i lukkede oppdrettsanlegg, utfordringer knyttet til lakselus, rømming og utslipp av mat og medisiner vil reduseres. Høye konsentrasjoner av nitrogenforbindelser fra fôring og ekskrementer kan føre til dannelse av ammoniakk, som er giftig for laksen. For industrien er det viktig med hurtige og pålitelige målinger av disse forbindelsene. I denne masteroppgaven har bruken av ioneselektive elektroder (ISE) fra HACH for analyse av ammonium (ISENH4181) og nitrat (ISEN03181) i oppdrettsnæringen blitt undersøkt for interferenser og påvirkning av begroing. Det ble gjort to tester i et resirkuleringsanlegg (RAS) hos Nofima i Sunndalsøra med 12‰ salinitet. I det første eksperimentet ble det ikke brukt noe behandling for begroing, mens i det andre eksperimentet ble brukt vibrering og et nylonfilter. I tillegg ble det gjennomført to eksperimenter i et gjennomstrømningsanlegg (FTS) i ferskvann, hvor det første var uten noe behandling. I det andre eksperimentet ble et kompositttmateriale av TiO_2 nanostaver med nanosølv partikler (PDMS-TiO_2/Ag) testet som beskyttelse mot begroing. Kompositttmaterialet ble belagt på teflon hetter. Hvor mye sølv som ble frigjort ble undersøkt ved å legge en hette i et begerglass med brakkvannsløsning. Sølvkonsentrasjonen ble bestemt ved hjelp av ICP-MS. Prøver fra RAS og FTS ble også analysert ved hjelp av ICP-MS for å undersøke eventuell akkumulering av metaller og undersøke om konsentrasjonene oversteg bakgrunnsnivåene for norsk kystvann. Prøvene ble også analysert ved hjelp av ionekromatografi (IC) for å bestemme nitrat og ammoniumkonsentrasjonene. Ingen av metallene oversteg bakgrunsverdiene, og kun Zn og Cu hadde en signifikant stigning med henholdsvis 0.38 og 0.02 $\mu gL^{-1}day^{-1}$ i RAS. I RAS var begroningen synlig allerede etter en dag. I FTS var den ikke synlig før etter to uker. Etter sammenligning med IC resultatene, ble det påvist en signifikant konsentrasjon av interfererende ioner i begge systemene. Spesielt i RAS på grunn av det høye saltinnholdet. Ammoniumelektroden var mest påvirket av saltinnholdet i forhold til nitratelektroden. Bruken av vibrering og nylonfilter ga en mer stabil begroingsprosess, og driften kunne estimeres ved hjelp av minste kvadraters metode. PDMS-TiO_2/Ag materialet som ble brukt på teflon hettene hadde ingen synlig effekt mot begroing. Frigjøringen av sølv ble derimot målt til å være signifikant med en p-verdi på 0.012 for to hetter med belegget, sammenlignet med 0.11 for to hetter uten. Designet på hettene trenger forbedring, samt at flere tester av dette materialet som begroingshemmende materiale må gjøres. De ioneselektive elektrodene i FTS klatre å detektere små variasjoner i ammoniumkonsentrasjonen som følge av laksens dag og natt aktivitetsforskjell. ISE er en mer effektiv og hurtig analysemetode for disse forbindelsene, men flere tester med antigroende materialet og hvilke interferenser som finnes i systemet trenger videre undersøkelse.

Table of Contents

Acronyms and Abbreviations

AgNP	Silver nano particles
CCS	Closed containment aquaculture system
FTS	Flow through system
GRM	Gan-Ruan-Mo baseline correction method
IC	Ion chromatography
ICP-MS	Inductively coupled plasma mass spectrometry
ISE	Ion selective electrode
MBBR	Moving bed biofilm reactor
MLR	Minimum least squares regression
MSD	mass spectrometry detector
m/z	mass to charge ratio
NTNU	Norwegian University of Science and Technology
PCA	Principal component analysis
PDMS	Polydimethylsiloxane
PVC	Polyvinylchloride
RAS	Recirculating aquaculture system
SFI	Centre for research-based innovation
TAN	Total ammonia nitrogen
TBT	Tributyltin
TOC	Total organic carbon
TN	Total nitrogen
WHO	Wold Health Organization
NO_3-N	Concentration of nitrate as nitrogen
NH_4-N	Concentration of ammonium as nitrogen
E	Potential
R	Gas constant
T	Temperature
F	Farady constant
z	Ion charge
a	Activity
γ	Activity coefficient
α	Effective diameter of hydrated ion
μ	Ionic strength

1 Introduction

In 2016 1.3 million tons of sea food was produced by Norwegian aquaculture companies according to numbers form Statistics Norway [1]. The majority of this food is grown in open cages in the sea to obtain a fresh environment for the fish. There are some challenges related to fish farming in open cages that need to be eliminated, or at least reduced, to protect the environment, the wild stock and to keep a sustainable production. For instance, open cages increase the risk of fish escape, that leads to a genetic weakening of the wild stock [2] [3]. Even though more efficient feeding equipment has been developed, and a better utilization of the leaking nutrients can be used, the leakage of nutrients and medicines are still of great concern [4][5]. Parasites, salmon lice and new diseases also occur more often in cages where the fish lives extreamly close to each other, and will spread easily to wild species as well as within the cage [6][7]. Fish farming in open cages can threaten the wild stock and the ecosystem in the fish farms' surroundings [8]. One way of producing seafood in a more sustainable way could be using a recirculating aquaculture system (RAS) [9].

1.1 CtrlAQUA

This project has been a part of a Centre for Research-based Innovation (SFI) called CtrlAQUA at Nofima, where the goal is to make the production of salmon in closed systems more reliable and economical using new technology and biological innovations. The centre works with both land based recirculating systems and sea based closed systems (closed-containment aquaculture system CCS), focusing on the post-smolt stage, where the salmon is most sensitive and first introduced to sea water [10]. In both systems are water being pumped up from the deep to prevent the presence of salmon lice [11]. Researches are facing challenges related to water treatment, fish welfare and optimizing the growth in closed systems. In CtrlAQUA researchers are working with new technology in order to solve todays challenges.

1.2 Nitrification

The main purification steps needed in a recirculating aquaculture system are removal of biological matter, CO_2 and ammonium, and extra supply of oxygen [12]. The biological process where bacteria are being used to oxidize ammonium to nitrite and nitrate is called nitrification. The method used in RAS to remove ammonium is by a bio membrane that consists of these bacteria [13]. The bacteria are gown on plates with a high surface area, and mixed with the

water in a moving bed biofilm reactor (MBBR) [14]. The desire to keep salmon on land for a longer time, to the post-smolt stage, require a system suitable for seawater. To make sure the concentration of ammonium doesn't reach a toxic level, an easy way of measuring ammonium and nitrate is an advantage. Real time measurements with ion selective electrodes (ISE) in brackish water are challenging because of the high concentration of interfering ions such as sodium and chlorine [15]. Over time the presence of biofouling and drifting makes the readings unreliable. Techniques used to prevent biofouling and compensate for drifting are necessary when ISE are going to be used in RAS.

1.3 Objective

The main objective of this master thesis is to examine the possibilities using ISE for ammonium and nitrate analysis in RAS for salmon smolt and post smolt production. Challenges related to drifting and biofouling will be investigated using ion chromatography (IC) as an alternative analytical method. Mathematical compensation and antifouling material will be used to respectively compensate for drifting and reduce or avoid biofouling.

2 Theory

In this section, the presence of nitrogen species in natural waters will be presented. The analytical methods, such as IC and ISE for ammonia and nitrate analysis, will be discussed. The principle used to detect metal concentrations in water samples using ICP-MS and the statistical methods that have been used will also be presented.

2.1 Ammonium in Natural Waters

The distribution of the various nitrogen species in water depends on different factors like the temperature, redox potential, and the alkalinity. Figure 2.1 (a) shows the concentration of different nitrogen species in an aqueous system depending on the negative logarithm of the redox potential, pϵ, when pH=7, while Figure 2.1(b) shows the predominant species depending on both pH and pϵ. In addition to the pH and pϵ conditions, biological activity can also reduce or oxidise these species. Less than 2% of the nitrogen on earth is biologically available, and on a reactive state, which means bound to C, H or O. The way of converting nitrogen from the atmosphere to a reactive state is called biological fixation, for instance the process where N_2 is reduced to NH_4^+ [16]. The bacteria Nitrosomanas is an aerobic bacteria deriving its energy from the oxidation of NH_4^+ to NO_2^-. Another example is the bacteria Nitrobacter, that catalyses the next oxidation step from NO_2^- to NO_3^- [17].

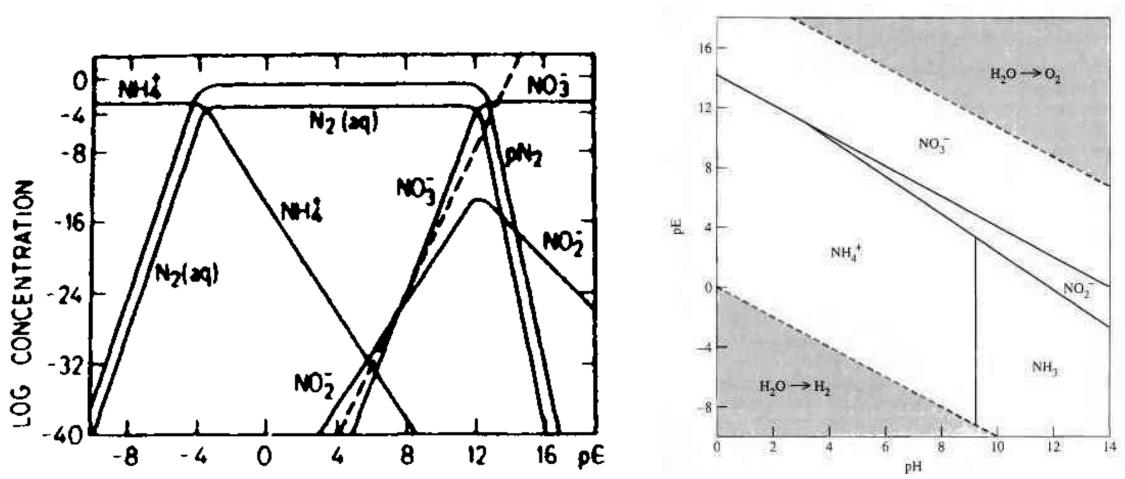

(a) **(b)**

Figure 2.1: (a) Equilibrium concentrations of redox components of nitrogen species as a function of pϵ at pH= 7. (b) Predominant nitrogen species in natural waters depending on pH and pϵ conditions. [17]

In closed fish farms, ammonium comes from urine, feces and nutrients. Because the circulation of water, total ammonia nitrogen (TAN) reaches higher concentrations than in open cages [9]. Unionised ammonia is most toxic to fish, and salmon is found to be one of the most vulnerable species of those grown in fish farms. High concentrations of NH_3 can cause a disturbance in the metabolism, respiration and ion balance [18][19][20]. The Norwegian Directorate of Fisheries (Fiskeridirektoratet) has recommended an optimum concentration less than 2 μg/L NH_3-N, and a maximum acceptable concentration up to 25 μg/L NH_3-N in water used to grow salmon [21].

The ionisation of ammonia is dependent on pH, as shown in Figure 2.2, which is based on ammonia's equilibrium constant. In seawater, the pH is between 7.5 to 8.4 [22]. The chemical equilibrium equation is given in Equation 2.1 and 2.2. The dissociation constant for ammonium ion, K_a, is $5.75 \cdot 10^{-10}$ at 25 °C [23]. Calculation of the ammonium concentration versus the ammonia concentration in this pH range for normal seawater, shows that 98 to 87 % of the species is at the ionic and less toxic form.

$$NH_4{}^+ \rightarrow NH_3 + H^+ \tag{2.1}$$

$$K_a = \frac{NH_3H^+}{NH_4{}^+} \tag{2.2}$$

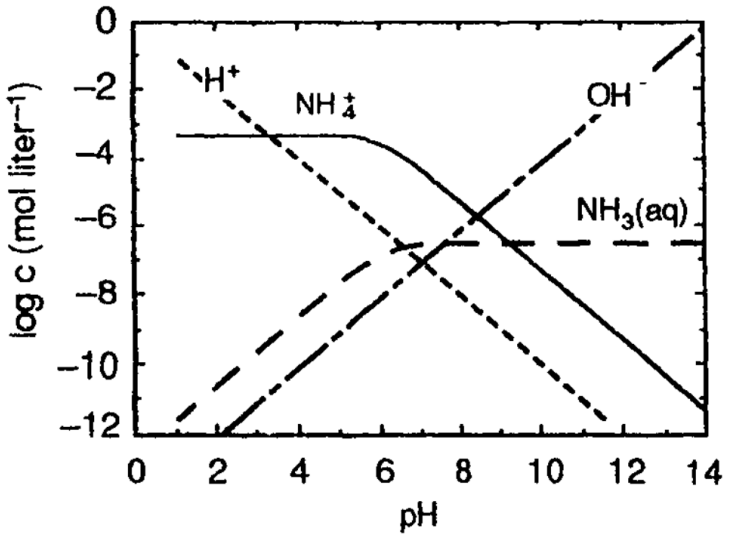

Figure 2.2: Graphical presentation of the pH dependency of the ionisation of ammonia to ammonium [17].

2.2 Ion Selective Electrodes (ISE)

An ion selective membrane electrode (ISE) uses the principal of potentiometry to measure the activity of an analyte ion in an aqueous solution. The measuring device consists of a reference electrode, an ion selective indicator electrode and a potentiometer, as shown in Figure 2.3. The reference electrode is usually placed inside the ion selective electrode of practical reasons [15].

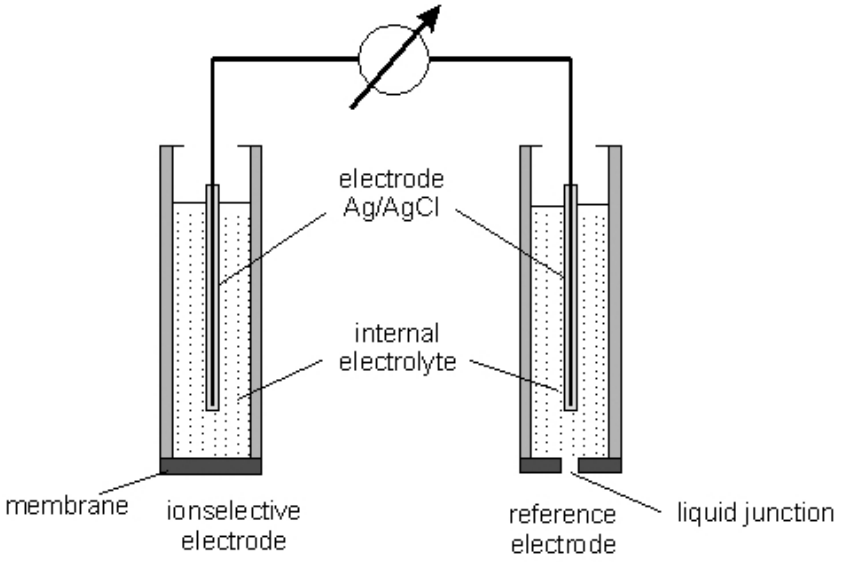

Figure 2.3: Typical electrode system for measuring ions with an ion selective membrane electrode, where a potentiometer is used to measure the difference in potential [24].

When putting the electrode in an analyte solution, the different concentration of the target ion inside and outside the membrane causes an electrical potential, that can be measured compared to the reference electrode. The measured potential, E_{ind}, is a sum of the boundary potential over the membrane, E_b, the reference potential, E_{ref}, and an often negligible asymmetry potential, E_{asym}, see Equation 2.3.

$$E_{\text{ind}} = E_{\text{b}} + E_{\text{ref}} + E_{\text{asym}} \tag{2.3}$$

The activity can be calculated using Nernst equation, given in Equation 2.4 [15].

$$E_{\text{b}} = E_{\text{ref}} - \frac{RT}{zF} \ln \left(\frac{a_1}{a_2}\right) \tag{2.4}$$

Where R is the gas constant, T the temperature, F Faraday constant, z the ions charge and a_1 and a_2 are the activities of the target ion in the external analyte and internal standard solution,

respectively. When using this method on saline samples, the ion strength must be considered. High ion strength increases the activity, while the concentration does not change, $a = \gamma c$, where γ is the species activity coefficient expressed by Debye-Hückel equation, Equation 2.5.

$$-\log\gamma = \frac{0.51z^2\sqrt{\mu}}{1 + 3.3\alpha\sqrt{\mu}} \tag{2.5}$$

Where α is the effective diameter of the hydrated ion, and μ the ionic strength. For dilute solutions, where the ion strength is less than 0.01 M, the term $1 + \sqrt{\mu} \approx 1$, and simplifies Equation 2.5 to the so called Debye-Hückel Limiting Law as given in Equation 2.6.

$$-\log\gamma = 0.51z^2\sqrt{\mu} \tag{2.6}$$

When an ISE is used in saline waters, it is important to be aware of the presence of interfering ions. The selectivity of an interfering ion compared to the the analyte ion is described by the selectivity coefficient, K. Especially in sea water and brackish water, the concentration of interfering ions are high. The most interfering ions for NH_4^+ and NO_3^- electrodes are given in Table 2.1. If the selectivity coefficient is equal to one, the interfering ion and the analyte ion contributes equally to the measured concentration, while a selectivity coefficient equal to 0.01, the electrode is 100 times more sensitive to the analyte compared to the interfering ion [25].

Table 2.1: Common interfering ions and their selectivity coefficient, K, for NH_4^+ and NO_3^- ISE [26].

NH4+		NO3-	
Ion	K	Ion	K
Potassium	0.1	Iodide	10
Sodium	0.002	Bromide	0.1
Magnesium	0.0002	Chloride	0.006
Calcium	0.00006	Nitrite	0.001

2.3 Ion Chromatography (IC)

The analytical method ion chromatography allows separation of small anions and cations. The chromatographic system consists of a column with a stationary phase separating the analyte species, a mobile phase transporting the analyte through the system, and a detector to identify the samples retention time and signal strength. A typical setup is shown in Figure 2.4. Based on

known standards, the species can be identified and quantified using a calibration curve, where the signal of the detector assumes to be linear dependent on the concentration. A common detector used in ion chromatography is a conductivity detector. Most small ions have weak UV-vis absorbance, hence a UV-detector would not be suitable [27].

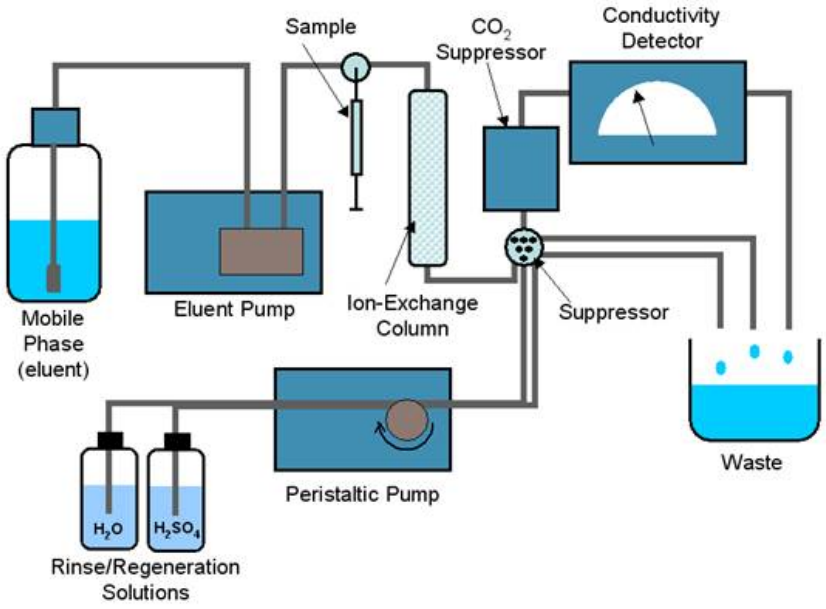

Figure 2.4: A typical setup used in an ion chromatograph [28].

The conductivity detector consists of two electrodes with applied potential, measuring the resistant when charged ions pass the cell. The detector measures all changes in conductivity caused by any passing ions. The presence of competing ions in the mobile phase, often used sodium carbonate, will increase the background conductivity. A suppressor column can be used prior the detector to eliminate the background contribution from the mobile phase ions. For anion alaysis, the eluents cations are replaced by protons from a diluted acid in the supressor. Carbonate in the mobile phase is then present as carbonic acid when it reaches the detector. Use of a suppressor increases the sensitivity and the detectors linear calibration range, and is often beneficial in an IC-system [27][29][30].

When ions are being analyzed, the stationary phase consists of opposite charged functional groups, which separates the analyte ions based on their affinity to the stationary phase. Separating small anions like nitrite and nitrate, a column made of polyvinyl alcohol with positively charged functional groups, like quaternary ammonium, can be used. A mixture of water and sodium carbonate are common to use as a mobile phase, because carbonates function as a pH buffer, and is easy to suppress before detection[31]. Species with high affinity to the station-

ary phase have long retention time, and species with weak affinity have short retention time. Assuming an anion analysis where the mobile phase anions and the sample anions, A^-, are in equilibrium with the stationary phase cations groups SP^+ like equation 2.7, the selectivity coefficient is given by Equation 2.8.

$$SF^+E^- + A^- = SF^+A^- + E^- \tag{2.7}$$

$$K_E^A = \frac{A_s E_m}{A_m E_s} \tag{2.8}$$

Where $[A]_s$ and $[A]_m$ are concentrations of anions in stationary and mobile phases in equilibrium, respectively, and $[E]_m$ and $[E]_s$ are the concentration of competing eluent ions in mobile and stationary phase [32]. The retention times of the different analyte anions are dependent on the selectivity coefficient, concentration of the competing ion and exchange capacity of the columns stationary phase. Increasing either the selectivity coefficient, ion exchange capacity of the stationary phase or concentration of competing anions, the retention time is decreased [27].

2.4 Inductively Coupled Plasma Mass Spectrometry (ICP-MS)

In Norwegian fish farms, the concentration of different metals and heavy metals are strictly regulated, and must be controlled to not exceed toxic levels concerning the salmons life and the environment [33]. Pollution of metals and heavy metals in sea water and fresh water are classified in five categories by the Norwegian environmental agency, see Table 2.2. The first two classes are background levels and levels of non-toxic concentrations, while class three to five can result in chronic toxic effects over time, acute toxic effects and finally lethal effects [34]. The classification system can be used as a guidance related to fish welfare and allowance of emissions to the environment. Detection of metal in very low concentrations can be challenging. An analytical method with sensitivity and accuracy necessary for measuring low metal concentrations in salty water samples is inductively coupled plasma with mass spectrometry detection (ICP-MS).

Table 2.2: Classification of condition for Norwegian coastal waters in mg/L [34]

Element	**Class I**	**Class II**	**Class III**	**Class IV**	**Class V**
Cadmium (Cd)	0.03	0.2	Footnote 1	Footnote 2	Footnote 2
Lead (Pb)	0.02	1.3	14	57	>57
Nickel (Ni)	0.5	8.6	34	67	>67
Mercury (Hg)	0.001	0.047	0.07	0.14	>0.14
Copper (Cu)	0.3	2.6	2.6	5.2	>5.2
Zinc (Zn)	1.5	3.4	6	60	>60
Chromium (Cr)	0.1	3.4	36	358	>58
Arsenic (As)	0.15	0.6	8.5	85	>85

[1] Depends on water hardness: <0.45 when <40mg $CaCO_3$/L, 0.45 when 40-50 mg $CaCO_3$/L, 0.60 when 50-100 mg$CaCO_3$/L, 0.9 when 100-200 mg $CaCO_3$/L and 1.5 when >200mg $CaCO_3$/L

[2] Depends on water hardness: <4.5 when <40mg $CaCO_3$/L, 4.5 when 40-50 mg $CaCO_3$/L, 6.0 when 50-100 mg$CaCO_3$/L, 9.0 when 100-200 mg $CaCO_3$/L and 15 when >200mg $CaCO_3$/L

The ICP-MS instrument is an advanced and relatively expensive instrument, which requires lots of training to operate. The instrument comes with different detectors and extra equipment to make the analysis suitable for a varied and diverse sample range [35]. A simple scheme of the ICP-MS instrument is given in Figure 2.5. After injection, the sample reaches a nebulizer, where the sample is spread out to an aerosol, and mixed with argon gas. The aerosol passes through a spray chamber, where the larger droplets are removed. The small aerosol droplets are transferred to the plasma torch, consisting of an inner and an outer flow of argon gas. The inner flow is mixed with the analyte, and is ionised by a spark from a Tesla coil. The positively charged ions and their electrons interacts with a magnetic field produced by a water-cooled induction coil powered by radio frequency. Resistance in the flow of charge causes ohmic heating resulting in a plasma at atmospheric pressure. The temperature can reach 6000 K to 8000 K in 2 ms. The outer argon flow cools the outer quarts walls in the plasma torch and prevent it from melting. As the sample is ionised, it passes an interface region in close vacuum consisting of metallic cones called skimmer cones. Here the ion beam is focused in to the MS detector, and neutral species and photons can be removed [36] [15].

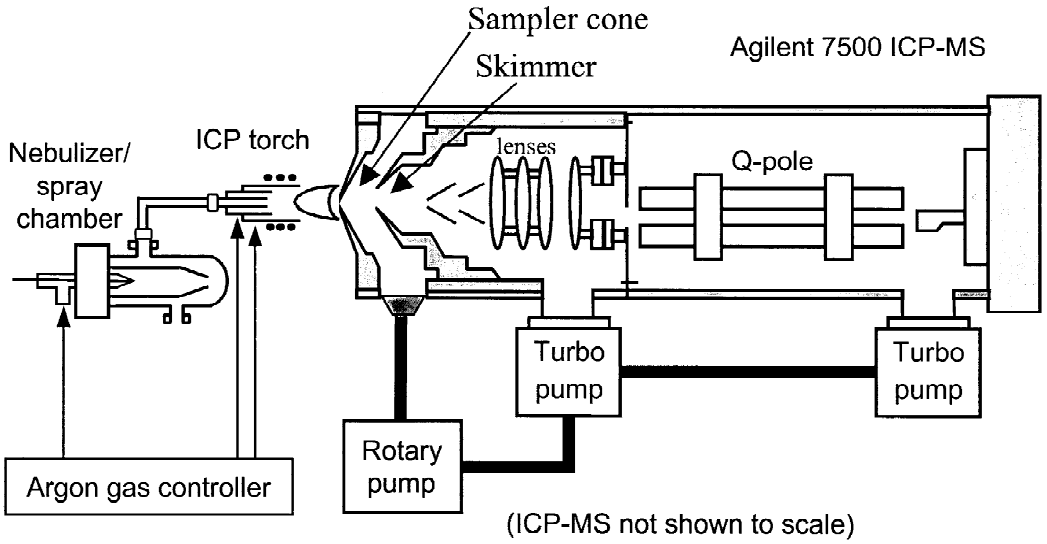

Figure 2.5: A simple scheme of the vital components in the ICP-MS instrument [37].

The MS detector identifies the metal ions based on their mass to charge ratio (mx). The first MS detector, invented by Francis William Aston, had a magnetic sector deflecting the ions by applying a magnetic field. An accelerated ion entering the magnetic sector is deflected with respect to both mass and charge. A heavy ion is deflected less than a light ion. For this invention, Aston received the Nobel Prize in chemistry in 1922 [38]. Newer MSDs have one magnetic sector and one electric sector increasing the sensitivity. The electric sector separates the elements with respect to charge, regardless of mass. Focusing slits and elements forces ions of same charge to follow the same path in the electric sector. These instruments are called double-focusing MSD [39].

The most common mass filters in today's ICP-MS instruments is the quadrupole mass filter. The filter consists of four rods mounted parallel and at the corners of a square. With applied AC and DC voltage at opposite pairs of rods, only one mass to charge ratio can pass the filter at a time. An illustration of a quadrupole mass filter is given in Figure 2.6 An alternating voltage can switch very fast, and can scan over the mass range from 1 atomic mass unit (amu) to 2400 amu in just one second [40]. Each element with a given mz ratio is subsequently counted in the detector, which forms an electric signal proportional to the concentration in the sample [39].

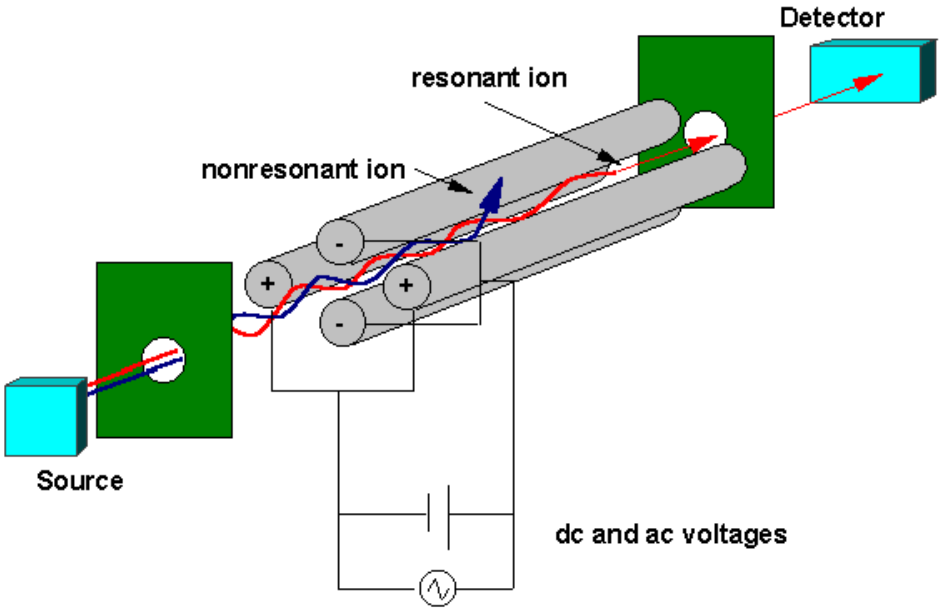

Figure 2.6: Illustration of a quadrupole mass filter used in a MSD [41].

2.5 Biofouling

Biofouling is caused by the growth of a biofilm on the surface of any substance in contact with water [42]. Adsorption of inorganic and organic macromolecules forms a film where microbial cells and bacteria can settle. This first step is called microfouling, and recruits the growth of larger organisms, such as algal spores and invertebrate larvae, which forms the macrofouling [42] [43]. The number of species causing biofouling varies in the literature. There has been found 4000 different species in marine biofouling. What kind of species are dependent on local factors such as temperature, salinity and current [44]. In RAS the presence of nutrition and high biological activity are factors beneficial for biofouling [45]. The biofilm on sensors installed in the system grows rapidly, and after two weeks, it can already affect the results significantly [46].

Several methods of antifouling are already applied in different industries. One of the best known antifouling product, tributyltin (TBT), was found to have a negative effect on growth, reproduction, development and survival of several species. The product is therefore not beneficial in salmon farming [47]. Today the use of TBT is very restricted, to reduce the risk of accumulation in the ecosystem. Copper was found to be a successively replacement for TBT on moored sensors [48]. The release of copper ions has an antibacterial effect inhibiting the biological activity on the surface [49]. Release of significant amount of copper ions in recirculating system could possibly disrupt the fish swimming pattern and cause deformities

[50]. Both copper and TBT are most often added to paint coatings, which seldom can be used directly on the sensors measuring device.

To avoid the use of toxic chemicals used as antifouling, mechanically and chemical cleaning methods can be used. Brushes [51] [52] or water jets [53] can be installed to clean the sensors regularly. Some sensors are fragile to chemicals and mechanical rubbing, which makes these methods damaging. For instance, the glass bulb on the pH electrode or the membrane in ISE are not supposed to withstand such treatment. A cleaning method like these could reduce the sensors lifetime [54].

2.6 PDMS-TiO_2/Ag as Antifouling Material

Silver nano particles have been used as an antibacterial agent for several years. The antibacterial effect of nanoparticles is shape and size dependent, and found to be more efficient than free Ag^+ ions and AgCl colloids [55] [56]. The mechanism causing the toxic effect is slightly different than free Ag^+ ions. The ions interrupt the bacteria' enzyme activity and membrane permeability by attaching to the negatively charged cell wall, which causes cell lysis and death [57]. The oxidation of silver nano particles causes Ag^+ release, but the AgNPs do also have other properties that causes toxic effects. In investigations of nano silvers effect on E. coli bacteria, the particles were observed attached to the cell wall, but also penetrated into the cell, resulting in a more effective inhibition than free ions [58][59].

AgNPs are popular to use as an antibacterial agent because the material is known as harmless to mammalian cells in low concentration, but the mechanism is not fully understood [60]. The use of AgNP has grown relatively fast, and new applications are rapidly found. Today, AgNP are found in many consumer products available all over the world. For instance, in food containers, textile, electronics, cosmetics and medical products [61]. The wide use of NPs increases the exposure to humans and other mammalians. Several studies have found AgNPs to have negative effect on mammalian cells as well [62], especially smaller particles (<10 nm) [63]. The particles enter the ecosystem mainly through our waste waters. From there, they enter the food chain through the animals respiration or diet. The risk of bioaccumulation and biomagnification is not fully understood, but some studies can not eliminate the risk of at least accumulation in biological tissue [64].

TiO_2 nano rods has been of industrial interests several years, because of the many beneficial properties as self-cleaning, anti-bacterial, anti-reflecting and anti-fogging [65]. To keep the nanomaterial immobilized, a polydimethylsiloxane (PDMS) is used in a composite, which makes the material superhydrophobic. The use of superhydrophobic surfaces as self-cleaning material is inspired from natural phenomena in i.e. plant leaves. Water droplets absorbs dust and organic matter as they repel. [66]. The combination of TiO_2 and AgNP in a composite material enhance the self-cleaning and antibacterial properties. TiO_2 nano rods are syntesized from TiO_2 particles [67]. The AgNPs are attached by adding silver nitrate and trisodium citrate to the TiO_2 nano rods mixture. Figure 2.7 shows a schematic illustration how the synthesis can be done [68].

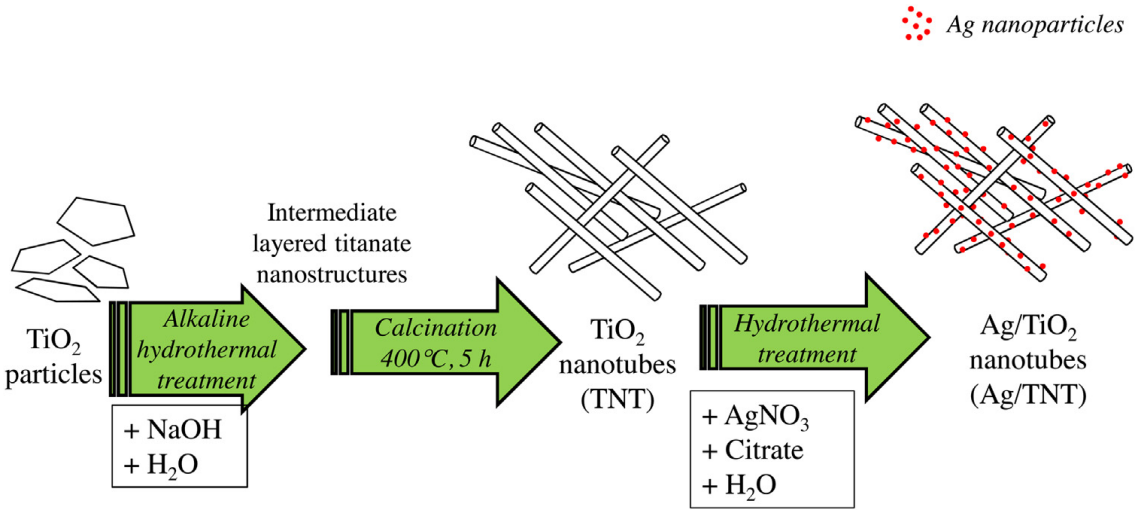

Figure 2.7: A schematic illustration how the synthesis of Ag/TiO_2 nanotubes can be done [68].

2.7 Baseline Correction

For most kinds of electrochemical, optical and potensiometric sensors, drift will occur when the sensor is used over time. This phenomenon is in most cases related to an offset in the measured data, with relatively constant change over time [69]. How fast, and how much depends on the type of sensor, and in what environment it is used. Cleaning and calibration is necessary to retain accurate measurements. When a sensor is installed under water or of other reasons out of reach, frequent calibration can be demanding. Estimation of the offset caused by drifting can be an option to reduce the calibration frequency [70] [71].

There are mainly two approaches that are being used to remove baseline drift. Either numerical differentiation or subtracting a smooth fitted curve to get an estimate of the real signal. Numeric differentiation, such as Savitsky-Golay filters, can be used to remove a baseline drift, but a method including numerical differentiation can also result in amplifying the noise [72] [73]. Minimum least squares regression (MLR) can alternatively be used to fit a polynomial to the dataset. The baseline can in most cases be estimated by a polynomial of relatively low degree. By subtracting the estimated polynomial from the dataset, the baseline is removed. If there are peaks in the dataset, high spikes will increase the value of the polynomial. To avoid a polynomial with higher value than the base line, a method called Gan-Ruan-mo can be used [74] [75] [71].

To avoid signals influencing the prediction of the base line, a polynomial fitting first presented by Gan, Ruan and Mo (GRM) can be used. The algorithm uses an improved iterative polynomial fitting to make an estimate of the base line. The method is suitable in dataset with sharp and distinct peaks in positive direction. If a signal, y(x), is expressed as Equation 2.9 [71].

$$yx = bx + sx + \epsilon \tag{2.9}$$

Where y(x) is the measured signal, s(x) is the true signal, b(x) is the base line and ϵ is general error. Using polynomials, the baseline can be subtracted from the measured signal, and the true signal is obtained. Polynomial fitting with a series of variables are done in matrix form. The equation looks like $\mathbf{y} = \mathbf{Xa}$, where $\mathbf{y}$ and $\mathbf{a}$ are vectors with length m and n, while $\mathbf{X}$ is a matrix with dimensions $n \times m$, as displayed in Equation 2.10 [71].

$$\begin{bmatrix} yx_1 \\ yx_2 \\ yx_3 \\ \dots \\ yx_m \end{bmatrix} = \begin{bmatrix} 1 & x_1 & x_1^2 & \dots & x_1^n \\ 1 & x_2 & x_2^2 & \dots & x_2^n \\ \dots & \dots & \dots & \dots & \dots \\ 1 & x_m & x_m^2 & \dots & x_1^m \end{bmatrix} \begin{bmatrix} a_0 \\ a_1 \\ a_2 \\ \dots \\ a_n \end{bmatrix} \tag{2.10}$$

An estimate of $\mathbf{y}$, $\hat{\mathbf{b}}$, can then be calculated using least square method, as given in Equation 2.11 [73].

$$\hat{\mathbf{b}} = \mathbf{X}\mathbf{X}^{\mathbf{T}}\mathbf{X}^{-\mathbf{1}}\mathbf{X}^{\mathbf{T}}\mathbf{y} \tag{2.11}$$

A pseudocode of the GRM-method and a script suitable for the program R is given in Appendix A.

2.8 Principal Component Analysis (PCA)

Working with large dataset with multiple variables can be challenging. PCA is a powerful tool used to simplify huge data tables to discover interesting relationships and trends. Sometimes just a few latent variables can explain almost all the variation in the data, which makes it possible to reduce and compress the data. The method allows us to visualize data with multiple dimensions in order to see patterns, relationships, and clusters. Even new samples can be predicted and classified using PCA.

PCA is used to project data with multiple variables onto a lower dimensional space, by using latent variables covering most of the variance. The latent variables can be described using scores and loadings. The scores are the coordinates using the principal components as a new coordinate system, and the loadings are the direction of the latent variable. See Figure 2.8 as an example of a latent variable with a 3D dataset. A plot of the scores can be used to detect clusters, potential outliers and other groupings within the data set. By inspecting the loadings plot, correlated variables can be detected. If the angle between two variables in the loadings plot is close to zero, they are positively correlated, close to 180, negatively correlated, while a 90-degree angle indicates no correlation.

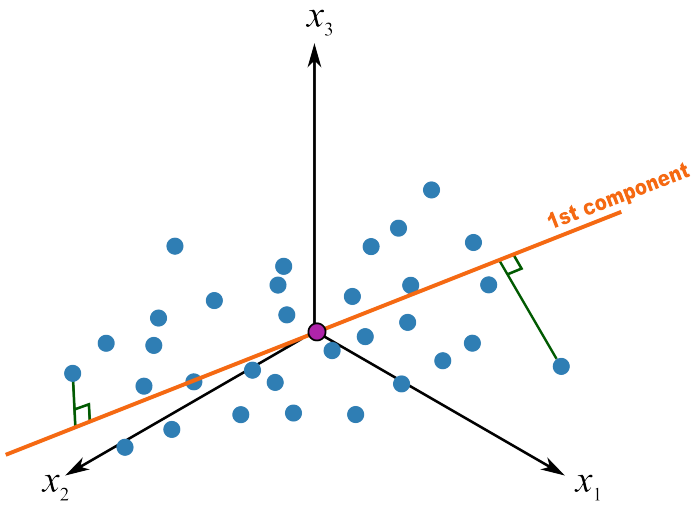

Figure 2.8: First principle component in a 3D data set [76].

3 Materials and Methods

Ion selective electrodes from HACH, selective for total ammonia (ISENH4181) and nitrate (ISENO3181) were tested in two different systems at Nofima in Sunndalsøra. One recirculated system (RAS) for post-smolt in brackish water, and one flow-through system (FTS) for smolt in fresh water.

Two samples for IC analysis were taken approximately twice a week, following the same sampling procedure described in Section 3.4. The sensors were cleaned and calibrated after each experiment, as described in Section 3.3. Four different experiments were done with the same sensors two in RAS and two in FTS. A summary of the experiments is given in Table 3.1, and the systems are further described in Section 3.1 and 3.2.

Table 3.1: A summary of the experimental setup at Nofima, where four tests with ISEs were done to measure NH_4^+ and NO_3^- in smolt and post-smolt cages. Both a recirculating system (RAS) and a flow-through system (FTS) were used.

Date	Days	System	Salinity [‰]	Antifouling treatment
05.02-26.02	22	RAS	12	None
26.02-08.03	11	RAS	12	Vibration and nylon filter
09.03-18.04[1]	40[1]	FTS	0	None
18.04-09.05	22	FTS	0	PDMS-TiO_2/Ag coated caps

[1] Logging of data ended 23.03, after 15 days because of an unknown technical error.

3.1 Recirculating Aquaculture System (RAS)

The RAS at Nofima consists of two water treatment installations, RAS1 and RAS2. Water from 12 tanks with approximately 2400 salmons in total were treated in the system. During the test period, the fish were grown from a size of 50g to 450g. To obtain the same condition in all tanks, some of the water was mixed before re-entering the fish tanks. The electrodes were tested in RAS2, but there has been assumed to be the same conditions in both systems because of the cross-mixing.

The electrodes were placed in the water treatment system in between the filter removing biomass, and the MBBR converting ammonia to nitrite and nitrate. This tank was cleaned three times a

week because of the biofouling. The sensors were not supposed to be touched in this routine. A water flow of ca. 600 L/min was treated in RAS2, and of them, 17 L/min was new water mixed with fresh water and seawater. A rod was used to attach the electrodes to avoid them touching the tank walls, as shown in Picture 3.1. Because of an ongoing experiment in the fish tanks, the salinity and pH were measured every day with sensors from WTW. Analysis of total ammonia nitrogen (TAN) was done every second day by Nofima employees using a Spectroquant® ammonium test kit and a PhotoLab® 6100 VIS spectrophotometer. The first experiment lasted in 22 days, where no antifouling treatment was used.

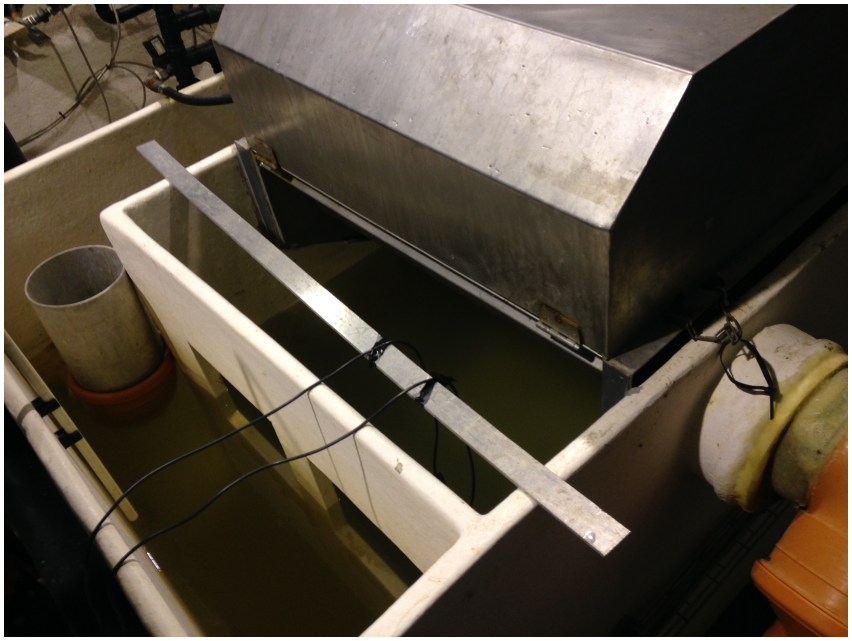

Figure 3.1: The two sensors were attached to a metall rod to keep them away from the walls. The water had passed the biofilter, and were about to enter the MBBR.

In the second experiment, a nylon filter and vibration were used to examine the effect on biofouling. Nylon from a nylon tights was attached as a loose bag over the sensing element using plastic strips, as shown in Picture 3.2. A vibrating element from a shaver was attached to the sensor with electric tape. A voltage source was connected to provide a constant voltage of 1.5 V as the sensors were placed in the water system. The experiment lasted in 10 days before the RAS was emptied, end the experiment had to be ended.

Figure 3.2: Before the second experiment in RAS where a nylon filter and vibration were used to examine the effect on biofouling.

3.2 Flow Through System (FTS)

Because Nofimas projects in RAS was finished after the first two experiments, a flow through system (FTS) for smolt was used for the next two tests. In this tank, approximately 1000 salmons were grown from the size of 100 g to 300 g. A total flow of 300 L/min fresh water was continuously flowing through the tank. In the first 10 days of the first experiment, the salmon was exposed to 12 hours light and feeding from 9 am to 9 pm. After these first 10 days, the light was turned on at all time and continuous feeding started. A picture of the electrodes in the system is given in Figure 3.3. The electrodes were first tested without any treatment to avoid biofouling. Because the biofouling was much less significant in this system, the sensors were lifted above the water level to check and document the biofouling process every week. The sensors were tested in 40 days, but the logging ended after 15 days because of an unknown technical error in the multimeter.

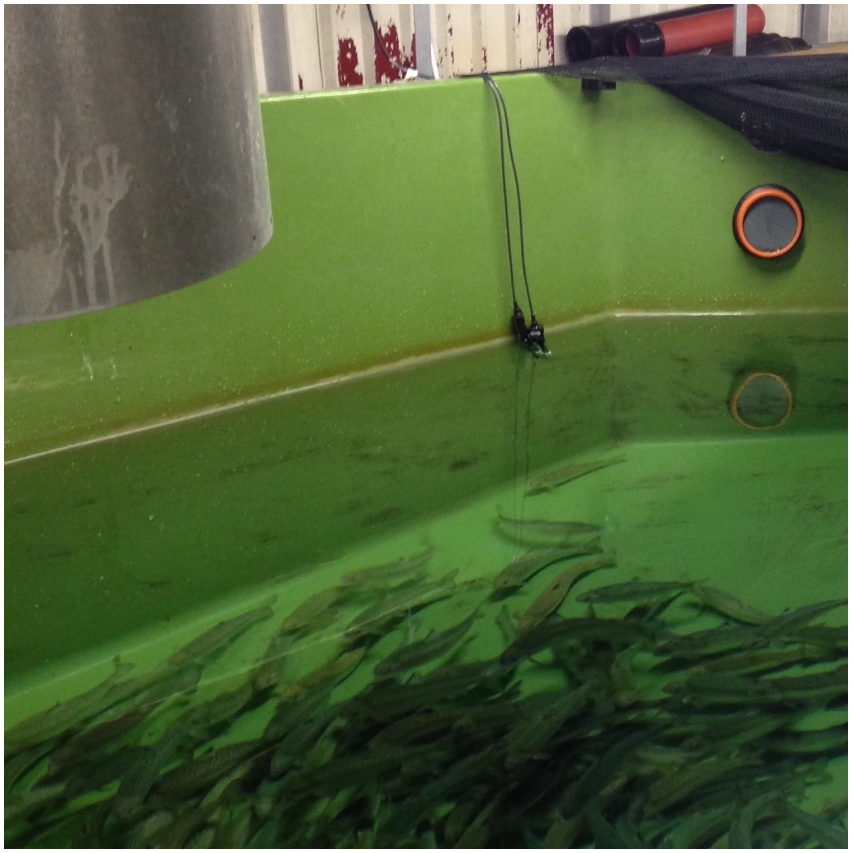

Figure 3.3: In the flow through system, the electrodes were placed directly in the fish tank.

In the second experiment, sensor caps designed by a PhD-candidate at NTNU were tested to see their effect on biofouling. The caps were made in Teflon, and coated with PDMS-TiO_2/Ag. A needle was used to open some of the holes after the coating process. A picture of one of the caps is given in Figure 3.4. The sensors were pushed into the cap until it reached the holes. To avoid air bubbles inside the cap, they were slid on under water. The sensors were not lifted above the water during this experiment.

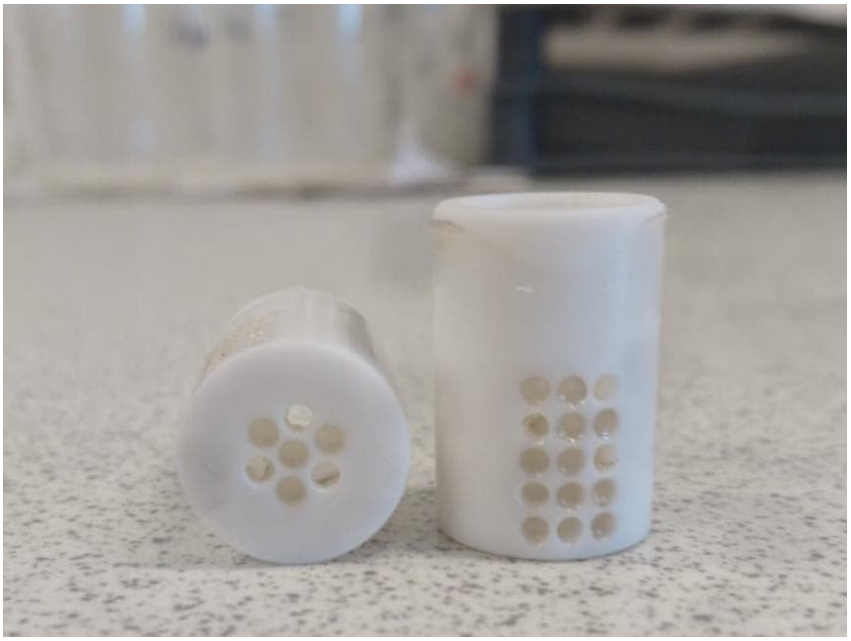

Figure 3.4: The Teflon caps coated with PDMS-TiO_2/Ag. Some of the holes had to be reopened with a needle after coating.

3.3 Cleaning and Calibration of ISE

The electrodes were cleaned and calibrated before a new experiment was started. Any biofilm was removed using a soft sponge and water. To avoid the biofilm from drying inn, the cleaning was done within few minutes after the experiment was done. Before calibration, the electrodes were left in the most concentrated calibration solution (100 mg/L) for conditioning in at least 20 minutes. The electrodes were rinsed gently with Milli-Q water and dried carefully with paper.

The calibration was done, using HACH calibration solutions with 1, 10 and 100 mg/L NO_3-N and 10 and 100 mg/L NH_4-N. The electrodes were first rinsed with Milli-Q water, and dried gently with a piece of paper. Starting with the lowest calibration standard, the electrode was first rinsed with a small amount of the lowest calibration standard, before the first calibration step was measured. 25 mL of each standard was added a small beaker (50 mL), and HACH salt buffers suitable for respectively NH_4^+ and NO_3^- was added to the beaker to increase the ionic strength. The solutions were stirred gently before the electrode was added. The electrode was used to stir the solution, without touching the glass walls, while the concentration was measured. The calibration was done with increasing concentration, and the procedure was done with one electrode at a time.

3.4 Sampling for IC and ICP-MS

Two duplicate samples for IC were taken approximately twice a week. Analysis of nitrate and ammonium could not be done simultaneously, and with two duplicate samples, one could be analyzed at a time. A sample was taken using a plastic syringe (50 mL). The syringe and sample tube (50 mL) were rinsed a few times with sample. The samples were filtrated using a 0.45μm VWR syringe filter and stored in a 50 mL metal free centrifuge tubes also produced by VWR. The filter was rinsed with 5-10 mL sample before the vials were filled and frozen at -20 °C. Before the IC analysis, the samples were defrosted in refrigerator and analyzed within 6 hours. ICP-MS samples were taken using the same filter and syringe. A 15 mL VWR metal free centrifuge tube was filled and conserved with three droplets of concentrated ultra pure nitric acid before analysis.

To validate the samples stability over time, two samples were analyzed four times over a time period of 20 hours. The samples were stored in the autosampler vials at room temperature, to find out how long the samples can be stored in the autosampler before analysis. The result of this test is given in Appendix C.

3.5 IC Analysis

The analysis of anions and cations were done using a Metrohm 940 Professional IC Vario with a 941 Eluent Production Module and 919 IC Autosampler plus. The instrumental setup is given in Table 3.2. A column separating anions, Metrosep A Supp 7 – 250/4.0, with polyvinyl alcohol with quaternary ammonium groups as carrier material and a particle size of 5 μm was used. The column had dimensions 250 x 4.0 mm and used a mobile phase consisting of 3.6 mM solution of sodium carbonate diluted from a concentrate solution from Fluka Analytical. For cation analysis, a Metrosep C6 – 250/4.0 column with polybutadienemaleic acid as carrier material on spherical silica gel particles with a size of 5 μm was used. The column had the same dimensions, and a 1.7 mM solution of nitric acid diluted from a concentrated Fluka Analytical solution, was used as mobile phase. The instrument used a conductivity detector with a suppressor column in front, using a 0.1 M H_2SO_4 suppressor solution for the anion analysis. The cation and anion analysis could not be done simultaneously, therefore a manual replacement of column and mobile phase was necessary before analyzing the opposite ion.

Table 3.2: Instrumental setup for analysis of anions and cations in brackish water and fresh water samples with Metrohm 940 Professional IC Vario.

Parameter	**Anion analysis**	**Cation analysis**
Injection type	loop	loop
Sample volume	20 μL	20 μL
Mobile phase	3.6 mM Na_2CO_3	1.7 mM HNO_3
Column temperature	45 °C	30 °C
Detector temperature	40 °C	40 °C
Detector cell constant	16.2 cm^{-1}	16.2 cm^{-1}
Pressure	10 MPa	10 MPa
Flow rate	0.7 mL/min	0.9 mL/min
Recording time	38 min	40 min

3.5.1 Preparation of Calibration Standards

Fluka analytical calibration standards for IC with 1000 mg/L $NO_3{}^-$, Br^-, F^-,$NO_2{}^-$, and $SO_4{}^-$ were used to make calibration curves. A solution of NaCl (1000 mg/L) was used to make a calibration curve for Cl^-. Approximately 50 mL Milli-Q water was added to a 100 mL volumetric flask, and 1 mL of each calibration standard was added using a 200-1000 μL Thermo Finnpipette®, resulting in a 10 mg/L calibration solution. Each calibration standard was added following the same procedure, where a small amount of the standard was poured into the calibration standard cap, and from there pipetted over to the volumetric flask. A new pipette tip was used for each standard to avoid contamination. Subsequently, the flask was filled with Milli-Q water to the mark, and mixed. The analysis of the calibration standard was started just after preparation. Three vials were filled with the 10 mg/L solution and analyzed with 1, 2, 5, 10, 20, 50 times dilution starting with the lowest concentration.

The same procedure was followed as the calibration solution for cations was made. Fluka analytical calibration standards for Na^+, NH_4-N and Ca^+ with concentration 1000 mg/L was used. 10 mL Na^+ standard, 1 mL NH_4-N and 5 mL of the Ca^+ standard were added a volumetric flask (100 mL) and diluted with Milli-Q water.

To validate the calibration curve, and to control the IC instrument was working properly, the standard solution was analyzed regularly. The standards used to calibrate the ISEs were also analyzed by the IC as a cross check. The result of this validation samples are given in Appendix F.

3.6 Investigation of Silver Released from PDMS-TiO_2/Ag

Two Teflon caps coated with PDMS-TiO_2/Ag and two without coating were tested for silver ion leakage in brackish water conditions. A solution of 12‰ NaCl was made by adding 6 g NaCl to an Erlenmeyer flask and dissolved in 500 mL Milli-Q water. Each beaker was cleaned with Milli-Q water before they were filled with 100 mL of the brackish water solution. The volumetric measurements were done by weight. A piece of line was attached to each cap, and a glass rod was used to make the caps floating in the middle of the solution. A magnetic stirrer was added each beaker and turned on at approximately 200 rpm. The beakers were covered by Parafilm. A sample for ICP-MS was taken after 1.5 and 10 hours, 2, 3, 7 and 21 days. To avoid contamination, each beaker had its associated syringe, that was rinsed with Milli-Q water after use. Because of the limited amount of solution, the syringe was used to take 4-5 mL solution into a metal-free VWR centrifuge tube (15 mL). Two droplets of ultra-pure nitric acid were used to conserve the samples before analysis. The beakers were weighed before and after each sample to calculate the exact volume left in the beaker. A picture of the setup is given in Figure 3.5.

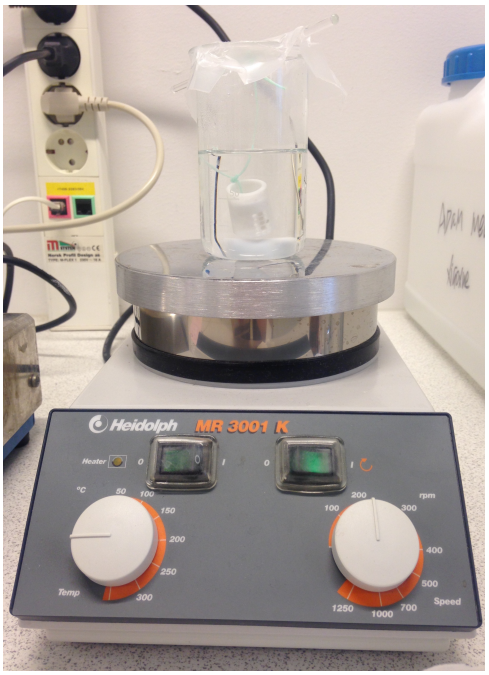

Figure 3.5: Setup used to investigate the release of Ag^+ ions from the antifouling material PDMS-TiO_2/Ag.

4 Results

The biofouling process in RAS and FTS are shown with pictures in Section 4.1. In Section 4.2 the raw data from the ISE sensors are plotted as a function of time, and the concentrations found by IC are included to compare the results. The result from a baseline correction for one of the experiments with the NO_3^- sensor is also included. In Section 4.3 ICP-MS results are plotted to investigate a possible accumulation of metals in this RAS. Finally, the ICP-MS results investigating the silver released from the PDMS-TiO_2/Ag material are presented.

4.1 Biofouling

The amount of biofouling in RAS was much more significant than in the FTS. This section is therefore further divided in the results from RAS followed by the FTS results.

4.1.1 Biofouling in RAS

The biofouling process in RAS was observed already after day one, as a slimy layer had appeared on the plastic housing. Organic matter floating in the water was observed attaching to the sensors before it loosened due to water currents. A picture of the sensing elements before and after three weeks in RAS are given in Figure 4.1, while pictures of the sensors in the water during the experiment are given in Figure 4.2.

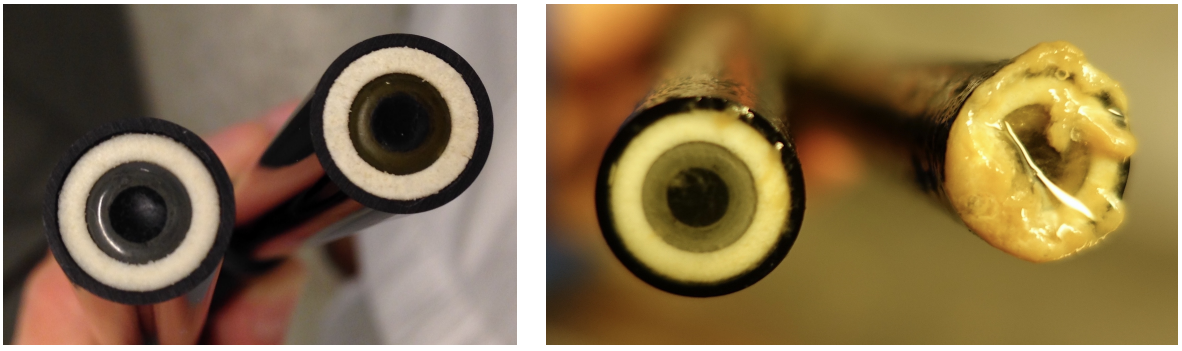

(a) **(b)**

Figure 4.1: Amount of biofouling before (a) and after (b) three weeks of analysis in RAS water treatment. A lot of the biofouling fell off as the sensors were removed from the water.

(a) **(b)** **(c)**

Figure 4.2: Pictures of the sensors in the RAS after 10 days (a), 16 days (b) and 21 days (c) without any antifouling treatment.

In the second experiment, with a nylon filter and vibration as antifouling treatment, the vibration had stopped when the experiment was ended. The vibrating elements did work as the power supply was restarted. How many days the vibration worked is not known. Even though the experiment just lasted in 11 days, biofouling had all ready appeared inside the nylon filter as shown in the two pictures in Figure 4.3. The sensing elements were covered by a slimy layer, while the surrounding pourous material had a more visible amount of biofouling.

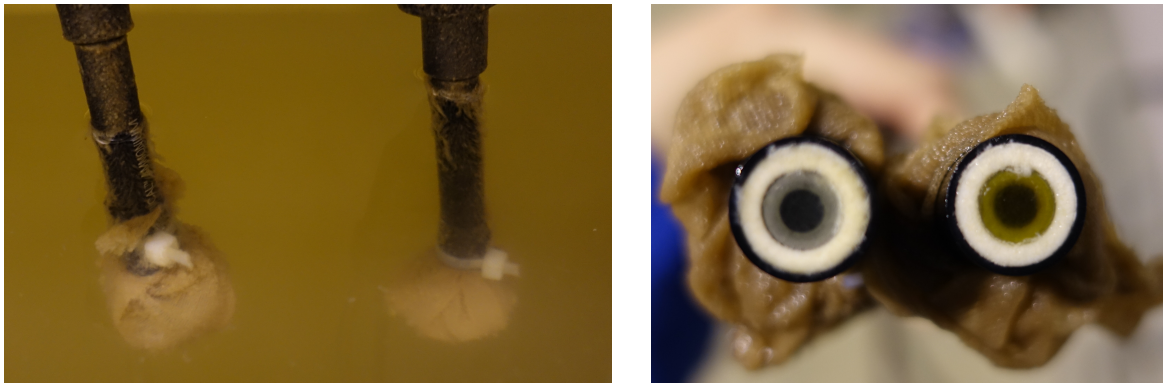

(a) **(b)**

Figure 4.3: The amount of biofouling after 11 days in RAS where the electrodes were covered by a nylon filter and had a vibrating element attached.

4.1.2 Biofouling in FTS

There was observed much less biofouling in the FTS in fresh water than in the RAS. In the first experiment without antifouling caps, no biofouling was observed the first week. The second

week a thin slimy layer was observed. After 3-4 weeks, the biofouling was visible, as shown in Figure 4.4.

(a) **(b)**

Figure 4.4: Amount of biofouling after three weeks (a) and in the end of the experiment, 5 weeks (b) in the flow through system with smolt.

In the second experiment in the FTS, the sensors were not lifted above the water line as the experiment had started, because of the risk of getting air bubbles inside the PDMS-TiO_2/Ag coated caps. After 3 weeks, there were observed a biofilm covering both sensors. The $NO_3{}^-$ sensor had more of the yellow/brown growth than the $NH_4{}^+$ sensor. There were also visible growth through some of the holes in the cap. Pictures of the sensors with and without the caps after three weeks is given in Figure 4.5.

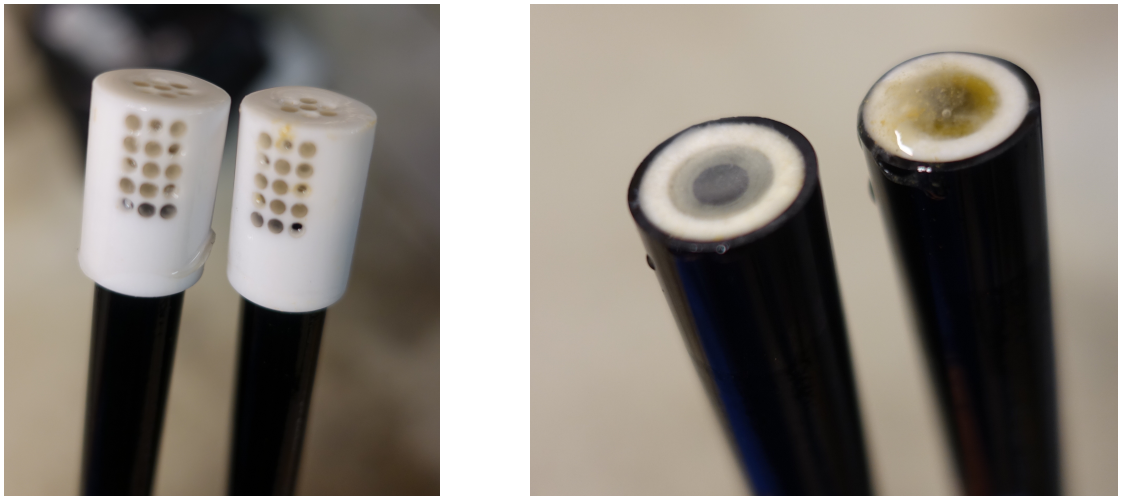

(a) **(b)**

Figure 4.5: Pictures of the sensors with and without PDMS-TiO_2/Ag coated Teflon caps after three weeks in the FTS. The $NH_4{}^+$ electrode is to the left and $NO_3{}^-$ is to the right in both pictures.

4.2 ISE and IC Results

The results from the ISEs were compared to the concentrations determined by IC. The IC chromatograms are given in Appendix H for anion analysis and Appendix I for cation analysis . This section is further divided in the RAS experiments and the FTS.

4.2.1 ISE in RAS

In the first RAS eksperiment, the salinity had a sudden change, and the regulation back to normal salinity at 12‰ lasted in 10 days. The graph in Figure 4.6 shows the change in salinity during the first experiment in RAS. In Figure 4.7 and 4.8, the ISE measurements from the NH_4^+ and NO_3^- sensor respectively are compared to the concentration quantified by IC.

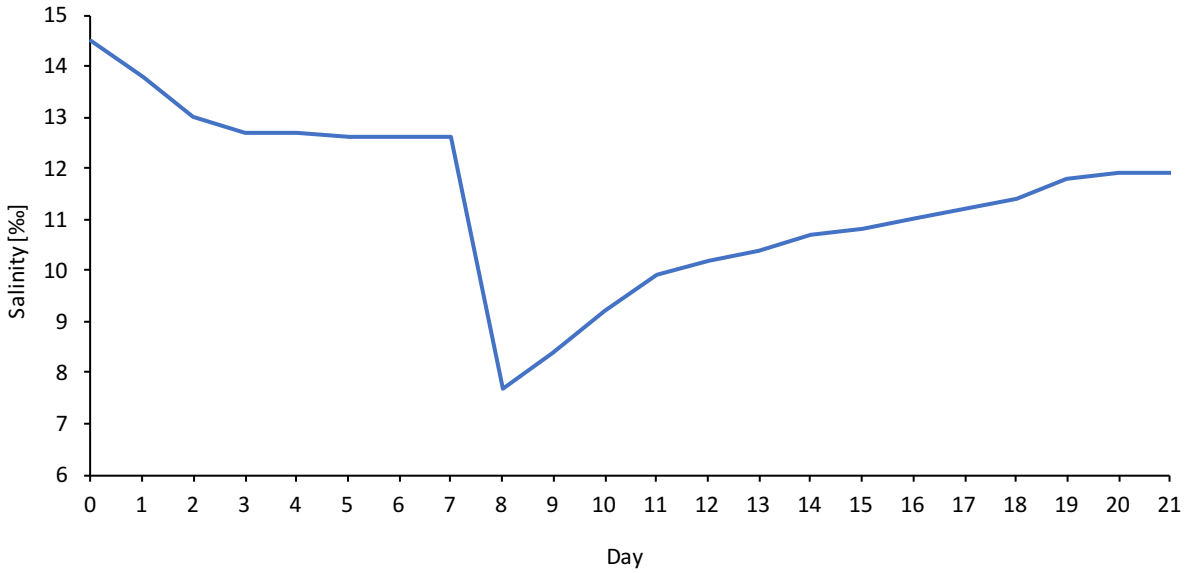

Figure 4.6: Change in salinity in RAS during the first experiment. The salinity was supposed to be stable at 12‰.

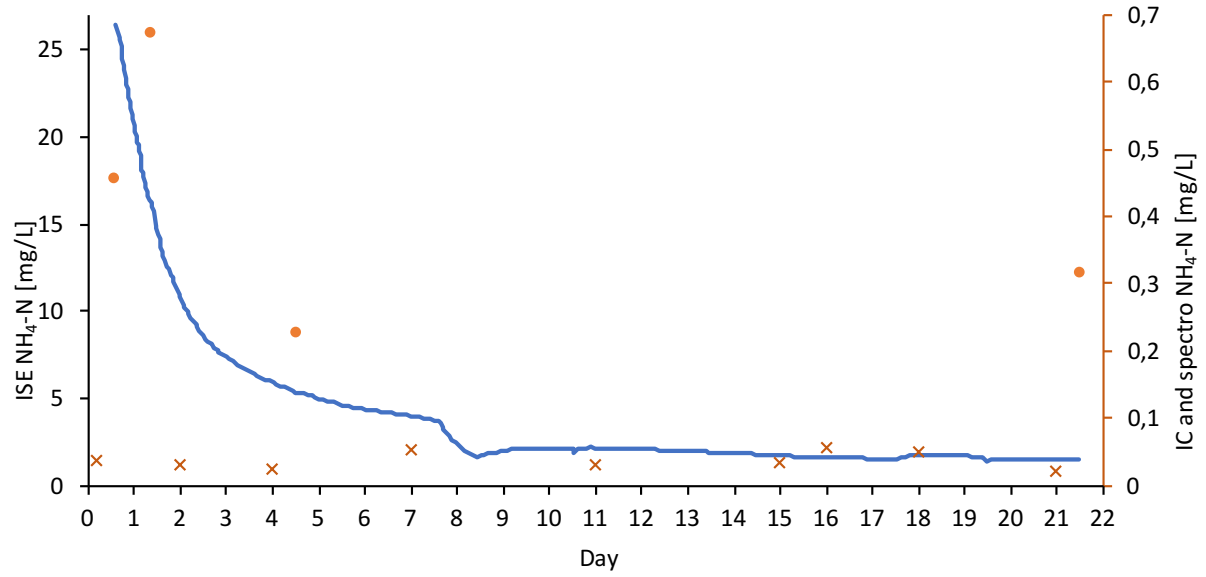

Figure 4.7: The NH_4-N concentration measured by ISE during the first experiment in RAS is plotted in blue. No antifouling treatment was used. The orange points are the concentration of NH_4-N quantified by IC, and the orange crosses are from the PhotoLab® 6100 VIS spectrophotometer at Nofima.

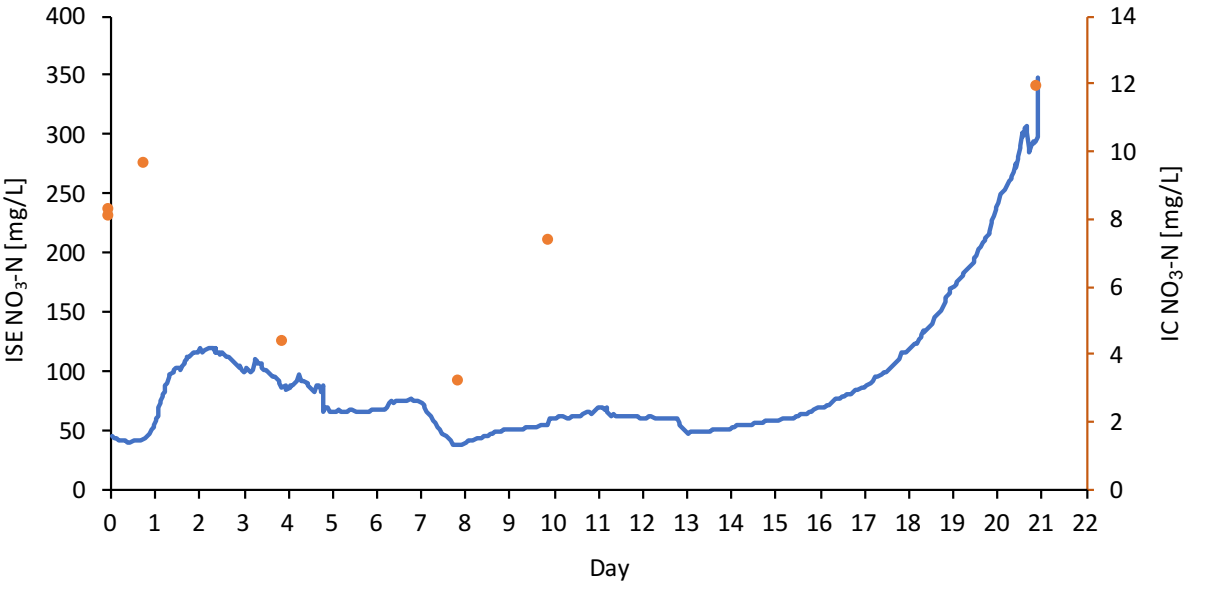

Figure 4.8: The NO_3-N concentration measured by ISE first experiment in RAS is plotted in blue. No antifouling treatment was used in this experiment. The concentration of NO3-N quantified by IC are marked as orange points, and use the y-axis to the right.

A visualisation of the correlation between the salinity and concentrations determined by IC and ISE is presented in a loading plot in Figure 4.9. The correlation factor between the salinity and NH_4-N was 0.59, while for NO_3-N and salinity it was 0.34, based on all the data from the two experiments in RAS.

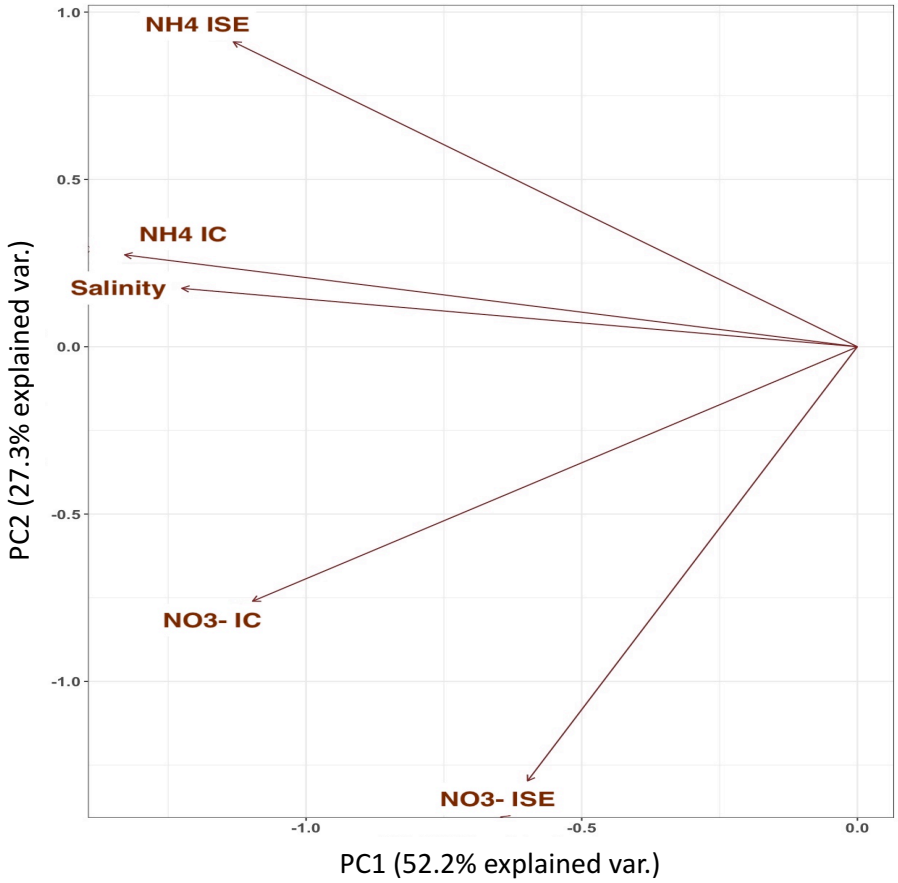

Figure 4.9: Loading plot of the NO_3-N and NH_4-N concentration quantified by IC and ISE and the change in salinity in the first RAS experiment. The parameters were scaled and centered.

In the second experiment, where vibration and a nylon filter were used as antifouling treatment, the salinity was stable at 12.3‰. The ISE results from this second experiment in RAS is shown in Figure 4.10 for NH_4-N and Figure 4.11 for NO_3-N.

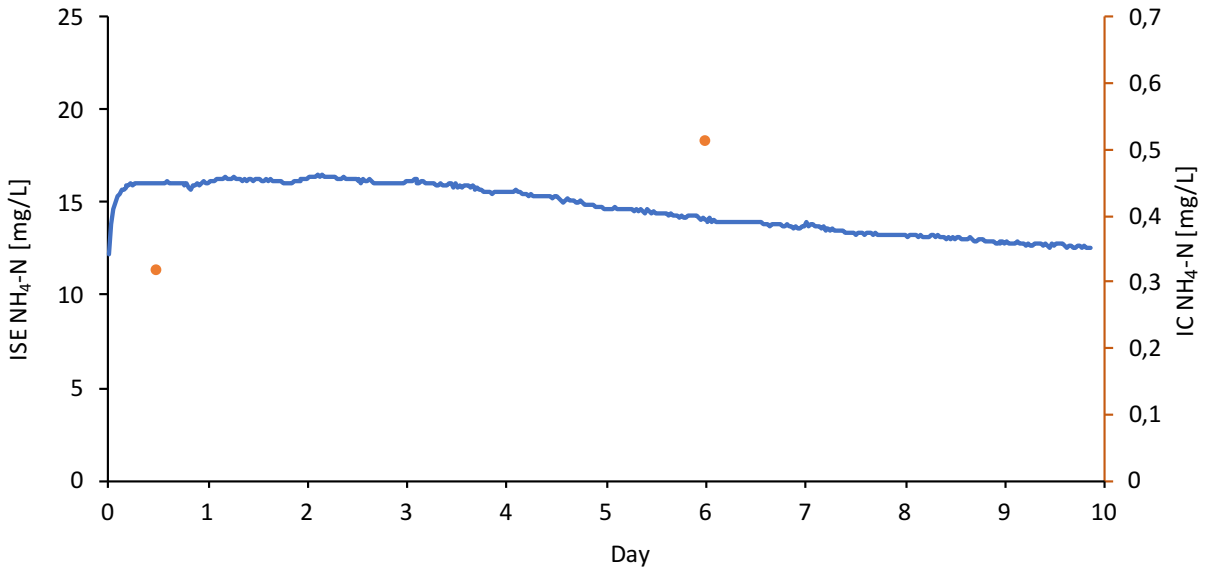

Figure 4.10: The NH_4-N concentration measured by ISE in the second experiment in RAS is plotted in blue. A nylon filter and vibration was used as antifouling treatment. The concentration of NH4-N quantified by IC are marked as orange points, and use the right y-axis.

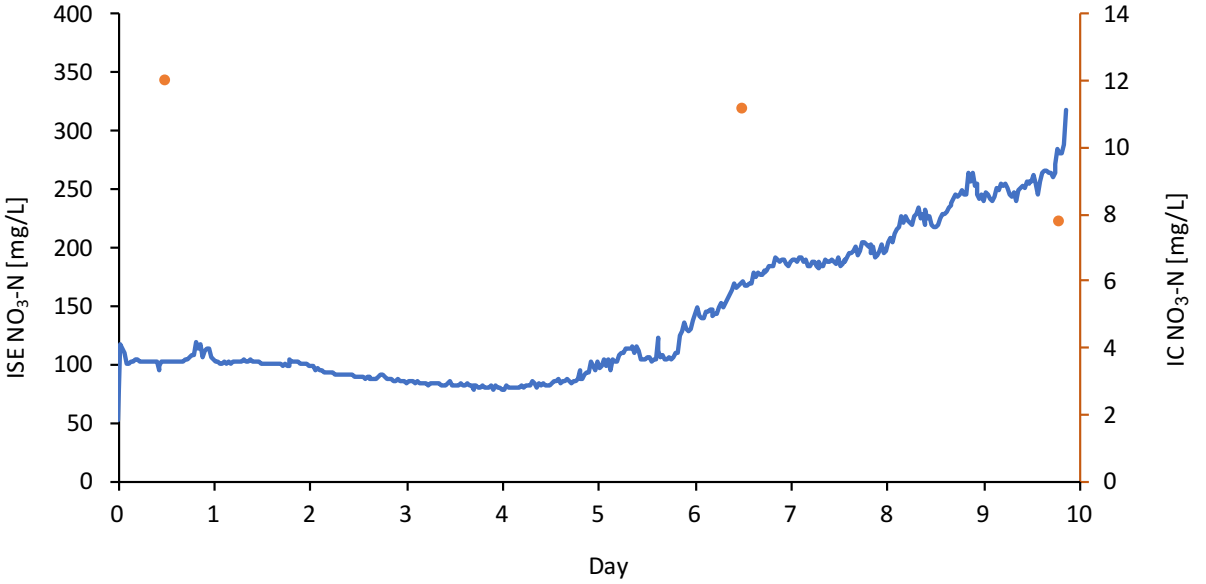

Figure 4.11: The NO_3-N concentration measured by ISE in the second experiment in RAS is plotted in blue. A nylon filter and vibration was used as antifouling treatment. The concentration of NO_3-N quantified by IC are marked as orange points, and use the right y-axis.

4.2.2 ISE in Flow Through System

The water in the FTS was observed to contain less organic matter than RAS, and the biofouling process was much slower. In the first experiment with no antifouling treatment, the ISE logging had stopped after 14 days and between day 4 to 6. The ISE data for NH_4-N is presented in Figure 4.12, and data from NO_3-N is shown in Figure 4.13.

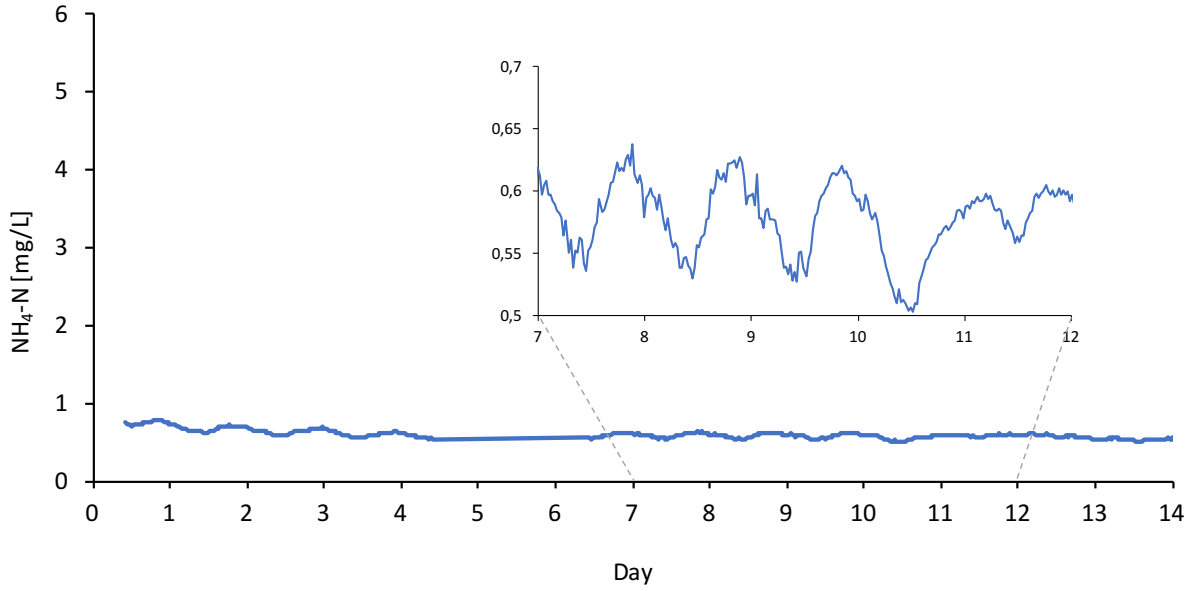

Figure 4.12: The concentration of NH_4-N in the FTS for smolt in fresh water measured with ISE. No antifouling treatment was used in this experiment.

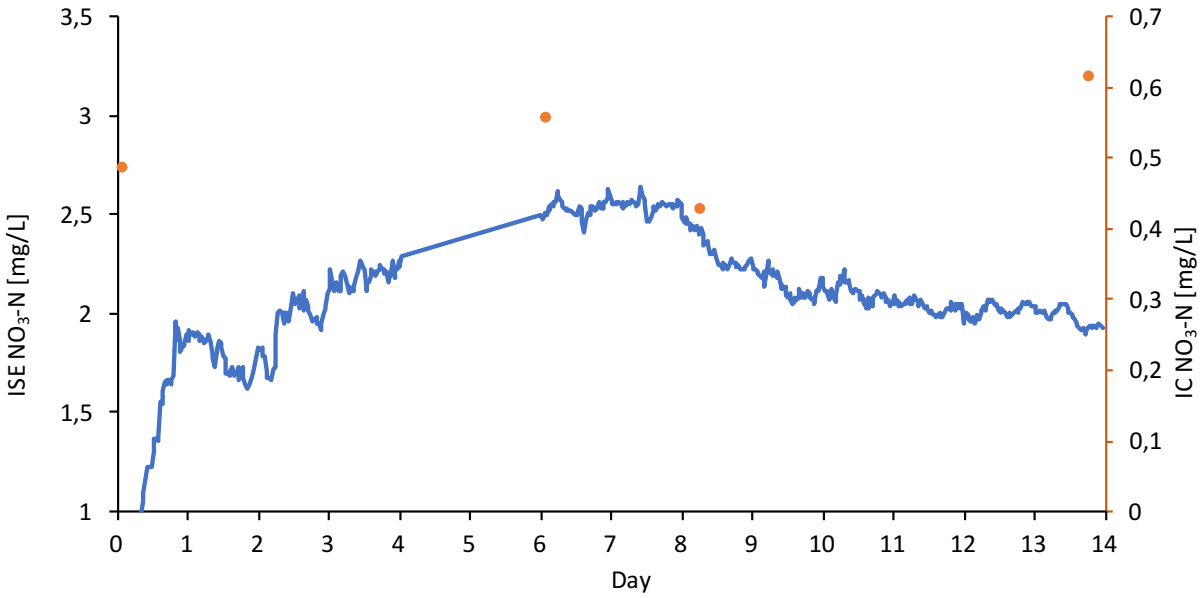

Figure 4.13: The concentration of NO_3-N in the FTS for smolt in fresh water measured with ISE. No antifouling treatment was used in this experiment. The concentration measured by IC are plotted as orange points, and use the right y-axis.

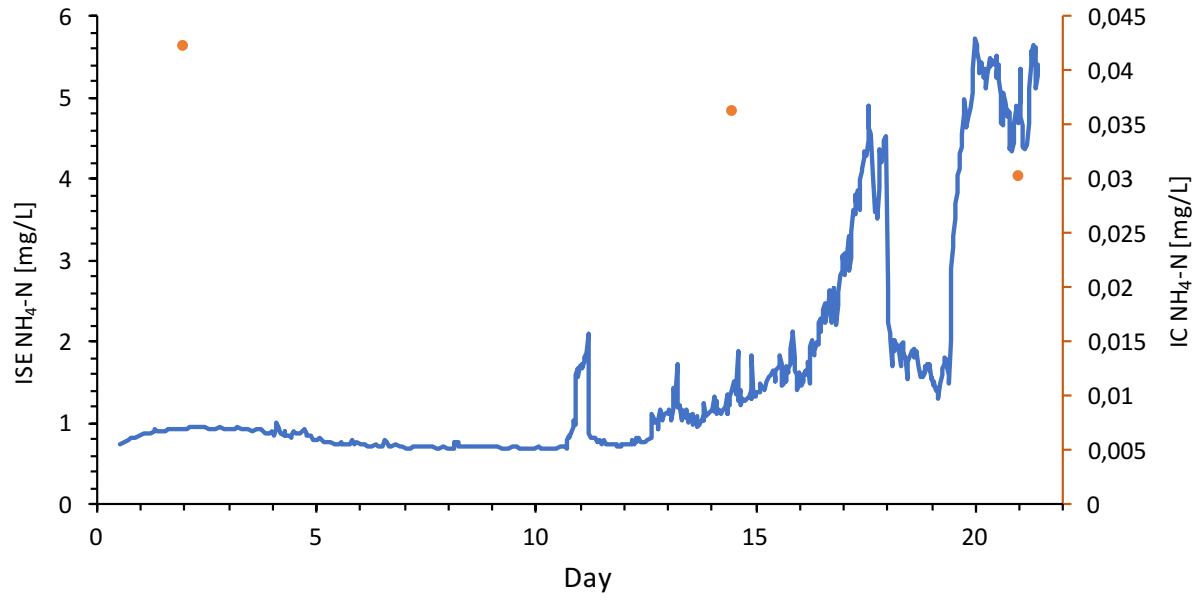

Figure 4.14: The concentration of NH_4-N in the FTS for smolt in fresh water measured with ISE. Teflon caps coated with PDMS-TiO_2/Ag were used as antifouling treatment. The concentration measured by IC are plotted as orange points, and use the right y-axis.

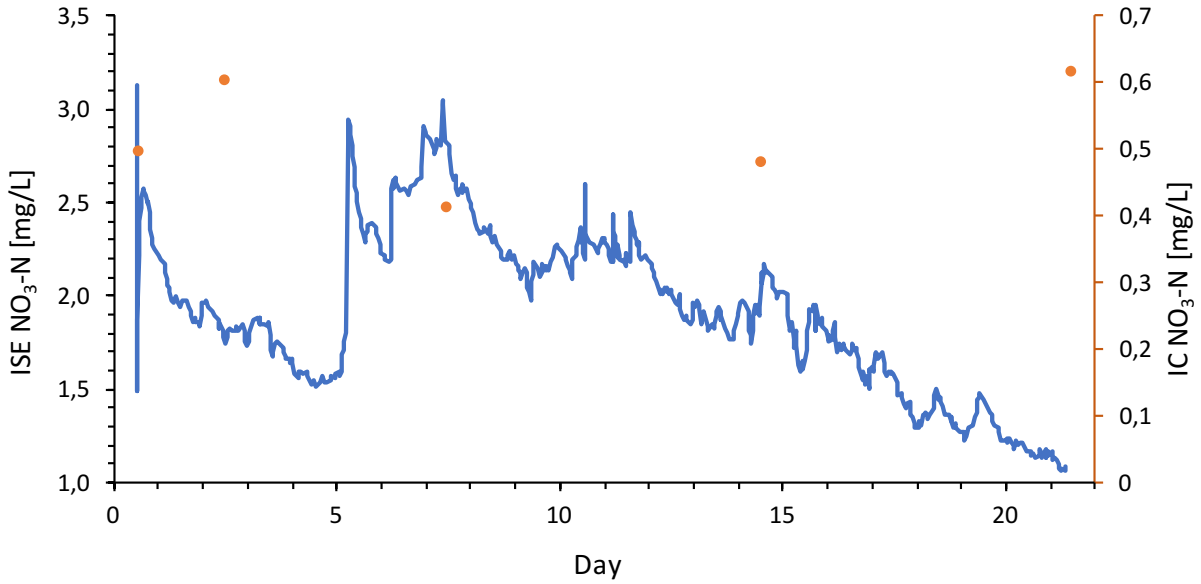

Figure 4.15: The concentration of NH_4-N in the FTS for smolt in fresh water measured with ISE. Teflon caps coated with PDMS-TiO_2/Ag were used as antifouling treatment. The concentration measured by IC are plotted as orange points, and use the right y-axis.

4.2.3 Baseline Correction

A baseline correction method described by Gan, Ruan and Mo (GRM) was used to remove the baseline drift where possible. In Figure 4.16 a baseline correction using MLR is compared to the GRM method. The data from the NO_3^- electrode in the second experiment in RAS with nylon filter and vibration was used.

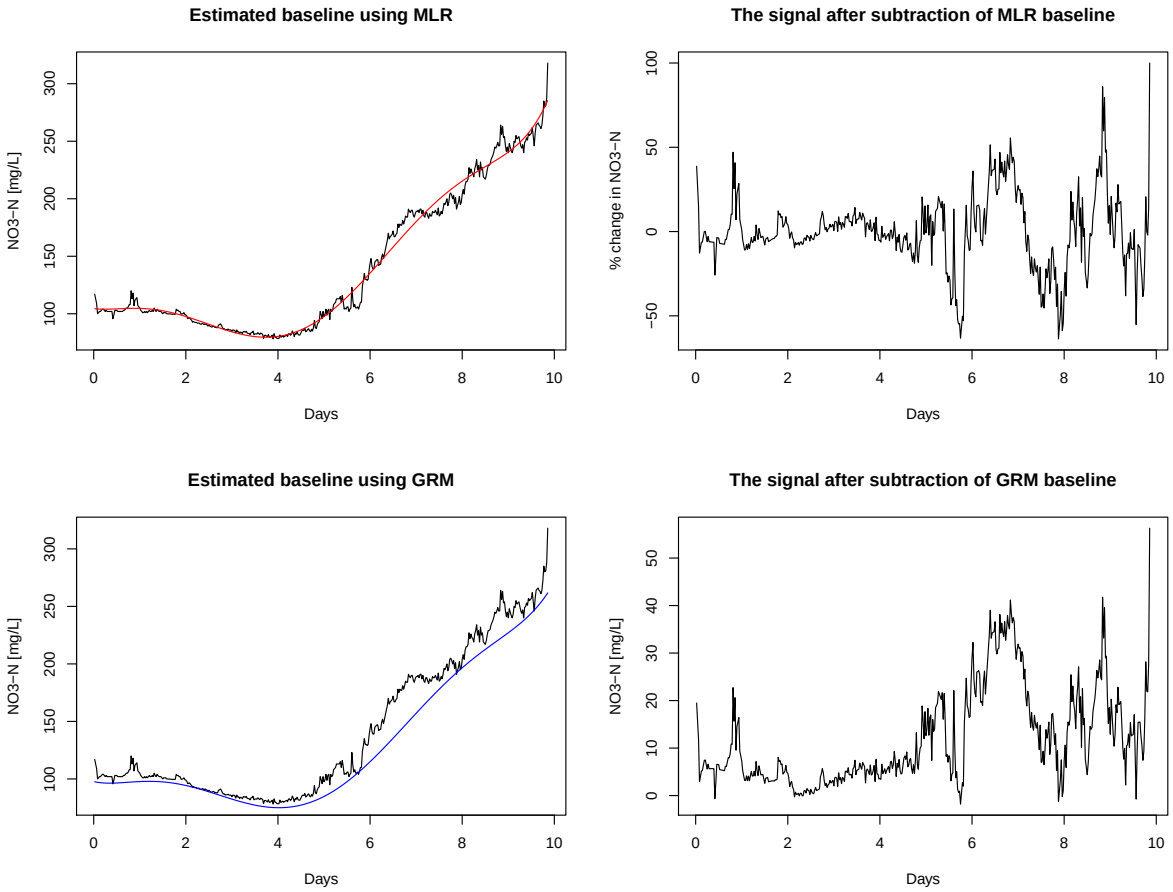

Figure 4.16: Baseline correction of data from the NO_3^- electrode in RAS comparing MLR and GRM.

4.3 Metal Concentrations in RAS

Water samples from RAS and FTS analyzed with ICP-MS Element 2 from Thermo Scientific for eight different metals Pb, Hg, Cd, Cr, Ni, Cu, Zn, Fe and As. Lead and mercury concentrations were below detection in all samples from RAS. The concentration of the other elements are given in Figure 4.17 to 4.20, and are classified based on the classification system for Norwegian costal waters in Table 4.1. The instrument analyzed the samples ten times each, and the error bars are therefore based on the instrumental variation. A duplicate sample was taken at day 2 and 22.

Table 4.1: Concentration in μg/L of eight different metals in RAS and FTS. Coloured according to he classification of Norwegian costal waters. Hg was not detected in brackish water.

System	Date	Cd	Pb	Ni	Hg	Cu	Zn	Cr	As
RAS	06.02.18	0.055	<0.008	0.53	-	0.62	5.59	0.16	0.930
RAS	05.03.18	0.057	<0.008	0.46	-	1.35	18.10	0.16	0.865
FTS	09.03.18	0.006	<0.002	0.27	0.011	0.49	1.52	0.16	<0.025
FTS	09.05.18	0.004	<0.002	0.20	0.002	0.45	3.14	0.07	<0.025

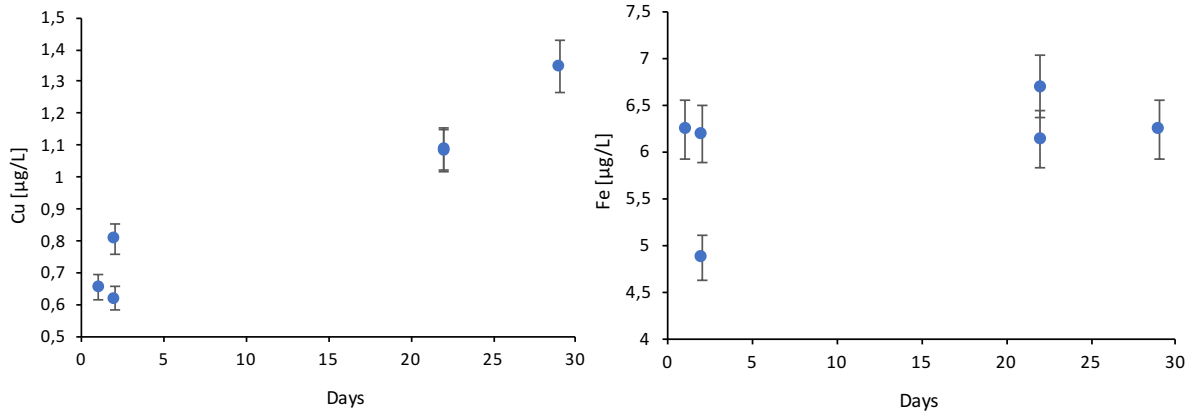

(a) **(b)**

Figure 4.17: Concentration of Cu (a) and Fe (b) in RAS quantified by ICP-MS.

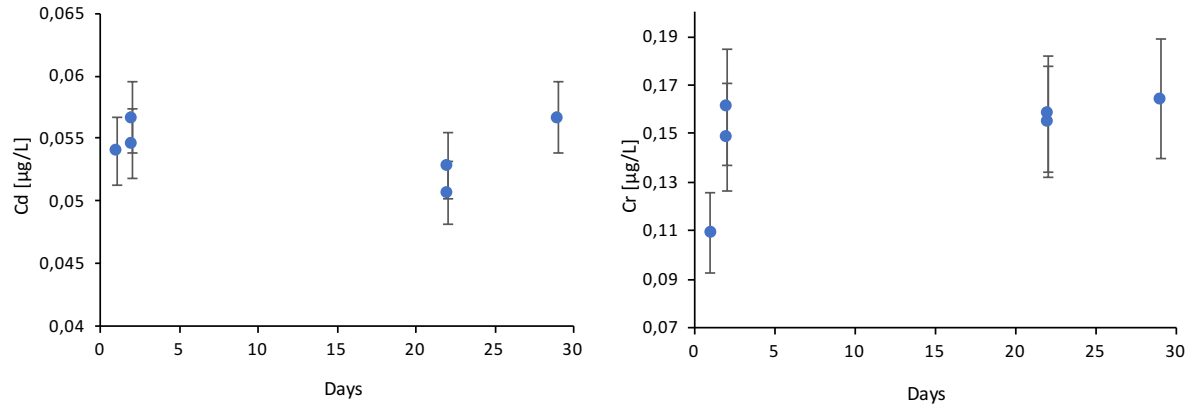

(a) **(b)**

Figure 4.18: Concentration of Cd (a) and Cr (b) in RAS quantified by ICP-MS.

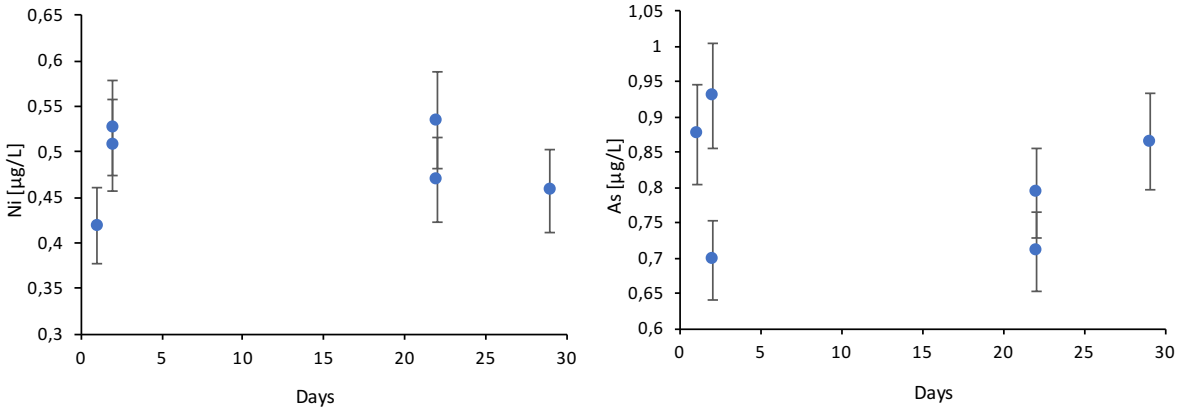

(a) **(b)**

Figure 4.19: Concentration of Ni (a) and As (b) in RAS quantified by ICP-MS.

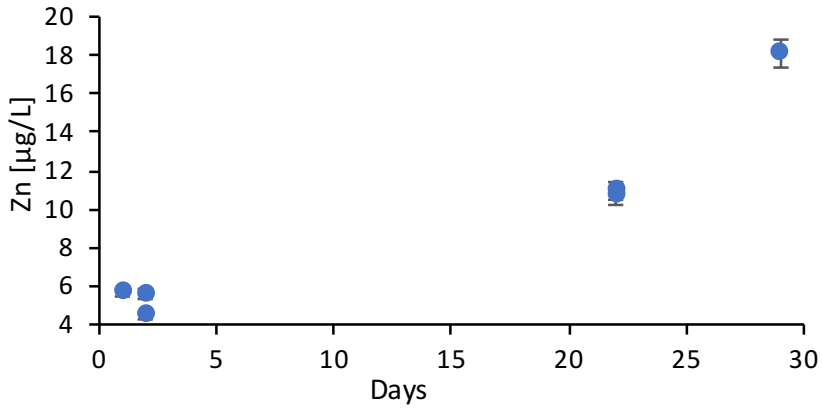

Figure 4.20: Concentration of Zn in RAS quantified by ICP-MS.

To investigate possible accumulation of these metals in RAS, a hypothesis testing if the slope in a linear regression, $\hat{\beta}$, was significant larger than zero. The null hypothesis in a t-test was H_0: $\hat{\beta} \leq 0$ with the alternative hypothesis H_1: $\hat{\beta} > 0$. With p-values lower than a significance level α=0.05, the null hypothesis was rejected. The result from this t-test is presented in Table 4.2.

Table 4.2: A linear regression investigating if different elements concentration in RAS increased through a time periode of 28 days. A t-test with null hypotesis H_0: $\hat{\beta} \leq 0$ versus an alternative hypotesis H_1: $\hat{\beta} > 0$, where $\hat{\beta}$ is the regression slope. A significance level equal to 0.05 was used and 4 degrees of freedom.

Element	$\hat{\beta}$	**P value**	**Reject H_0**
Cd	-0.00004	0.66	No
Cr	0.0008	0.15	No
Ni	-0.0001	0.53	No
Cu	0.02	0.00089	Yes
Zn	0.38	0.0029	Yes
As	-0.001	0.63	No
Fe	0.023	0.17	No

4.4 Silver Released from PDMS-TiO_2/Ag Material

The concentration of silver in the 12‰ NaCl solution used in this experiment was found to be 6.5 $\pm$ 0.4 μg/L before the solution was poured into the beakers with blank caps or PDMS-TiO_2/Ag coated caps. The concentration at a given time during the experiment is given in Figure 4.21 for each beaker. A t-test with null hypothesis H_0: $\hat{\beta} \leq 0$ versus an alternative hypothesis H_1: $\hat{\beta} > 0$, where $\hat{\beta}$ is the regression slope. was used to check if the increase in silver concentration was significant. Under a significant level of 0.05, H_0 was not rejected in the blank experiments, but rejected in the beakers coated with PDMS-TiO_2/Ag, as presented in Table 4.3.

Table 4.3: A linear regression was used to investigating the concentration of dissolved silver in a beaker with caps coated with PDMS-TiO_2/Ag. A t-test with null hypotesis H_0: $\hat{\beta} \leq 0$ versus an alternative hypothesis H_1: $\hat{\beta} > 0$, where $\hat{\beta}$ is the regression slope. A significance level equal to 0.05 was used, and 13 degrees of freedom.

Coating material	$\hat{\beta}$	**P-value**	**Reject H_0**
Blank	0.022	0.11	No
PDMS-TiO_2/Ag	0.029	0.012	Yes

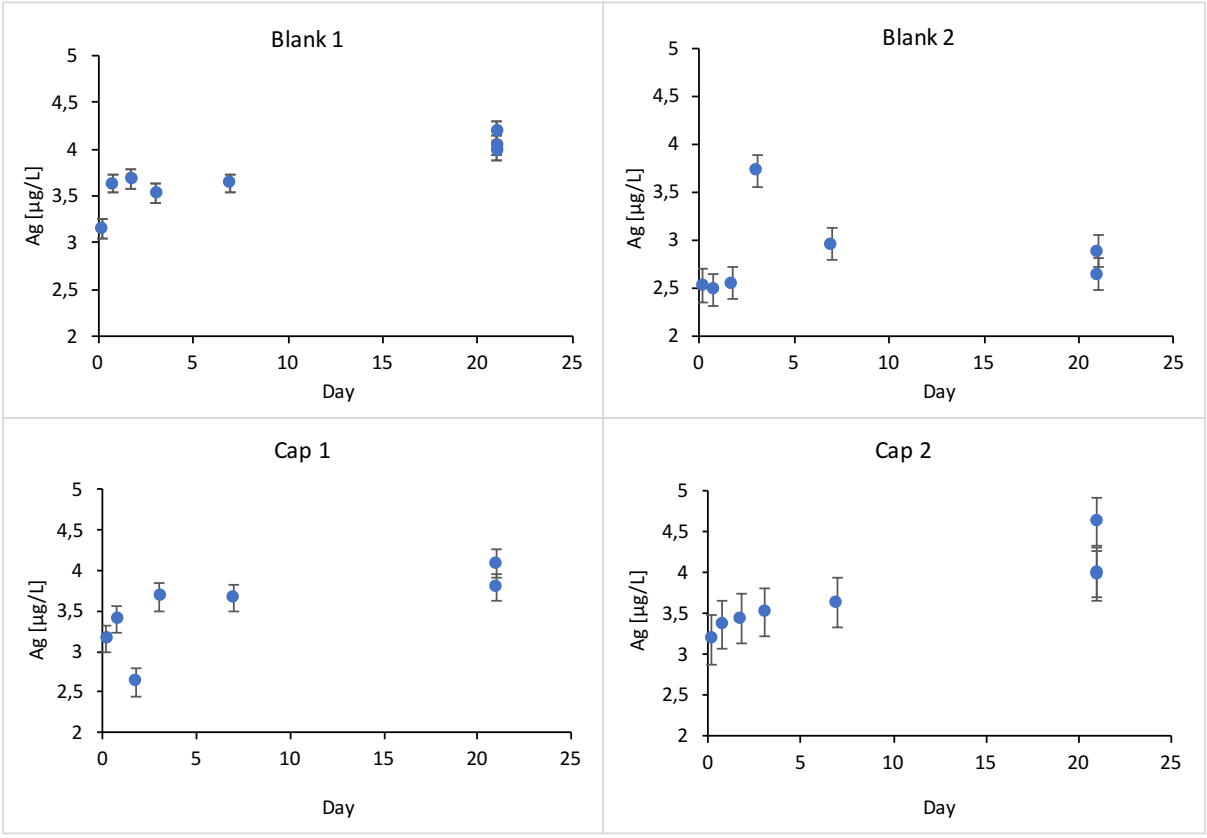

Figure 4.21: Investigation of silver released from two caps coated with PDMS-TiO_2/Ag versus two blank caps over a time periode of 21 days.

5 Discussion

5.1 Biofouling in RAS

The biofouling process in RAS was observed very quickly. Already after the first day, a slimy layer was observed on the electrodes' housings. The tank was cleaned with brushes three times a week to remove the growth on the tank walls. Particles that loosened from the tank walls under this brush-routine had a tendency to settle on the sensors. As mentioned in other articles, this process increases the biofouling possess a lot. This biofouling is relatively easy to remove by for instance water currents or brushing [77] [78]. As observed in Figure 4.8, sudden changes in NO_3-N appeared in the first experiment. Attachment and release of organic matter can explain some of the sudden variations in the ISE measurements. To prevent larger particles of organic matter to settle on the sensors, the vibrating element and filter were tested in the next experiment.

On inspecting the graph from the NO_3-N electrode in the second test in the RAS, in Figure 4.11, the early NO_3-N measurements seemed to be more stable than in the previous experiment in Figure 4.8. The use of vibration and nylon filter might reduce the sudden variations most likely caused by the attachment of organic particles in the water. The nitrate concentration was expected to be relatively stable because of the continuous feeding and cross mixing of water. The drifting occurred after 5 days in this experiment, compared to 14 days in the first experiment with no antifouling treatment. Less water recirculating inside the nylon filter might have increased a stable biofilm formation on the sensing elements.

The NH_4-N electrode was much more affected by the salinity change during the first experiment, which made it hard to compare the results from the two tests done in the RAS. In Figure 4.10 from the vibration test, the sensor seems to drift towards a lower concentration as the biofilm was growing. Further tests would need to be done to examine the biofouling effect on this sensor in brackish water.

After the experiment, there was visually observed a biofilm inside both the nylon filters on the sensing elements. Because of the relatively continuous drifting and stable measurements, the growth of this biofilm seemed to be more continues when the floating organic particles did not have the opportunity to attach to the sensing elements. The amount of biofouling was only examined by visual inspection. Presence of transparent growth not visible in wet conditions was not possible to observe. Neither what kind of growth nor where it was attached. In future experiments, an analytical method like scanning electron microscope (SEM) or similar tests

could be done gain deeper insight into the formation of the biofilm.

The vibration was not controlled during the experiment, and when the experiment was over, the vibration had stopped. For how long is unknown. It is possible that the effect was just due to the nylon filter and not by the vibration. To examine the effect of vibration, a test with vibration as the only antifouling agent could be done in later experiments. The RAS was emptied after the second experiment, and an additional test with the same conditions was not possible.

5.2 Biofouling in FTS

There was observed much less biofouling in the FTS compared to the RAS. The water temperature in FTS was ca. 6 °C compared to ca. 13 °C in RAS. Colder water, and no recirculating reduced the biological activity. Thus, algae growth was dramatically reduced [77]. After two weeks, the first biofouling was observed in the porous PTFE material surrounding the PVC membrane. Higher surface area in the rough surface and different surface properties can increase the biological activity in this material [79] [80]. In the experiment where the PDMS-TiO_2/Ag caps were tested, the biofouling was not visually inspected every week, because the sensors could not be lifted above water. When the biofouling started to impact the sensing elements were visible in the concentration measurements displayed in Figure 4.15 and 4.14. After two weeks, the drifting in the NH_4-N electrode had started. At this time, in the blank experiment, the first biofouling was observed. When it comes to the other electrode, it was hard to differentiate if the reduced NO_3-N concentration was due to drift or an actual reduction in concentration. The IC results indicates a slight increase in NO_3-N concentration, and the decrease measured by ISE was assumed to be due to the biofouling. In the blank experiment in FTS, the logging ended, not intentionally, after the first two weeks. The biofouling's effect on the measurements after three and four weeks was therefore not determined. The PDMS-TiO_2/Ag coated caps seemed to have no effect on the biofouling, because the drifting was significant already after two weeks. By visual inspection, the amount of biofouling was observed to be much like the amount of biofouling with no antifouling treatment after the first three weeks.

5.3 PDMS-TiO_2/Ag Coated Caps as Antifouling Material in FTS

To get exact measurements in real time with ISE, a continuous water flow passing the sensing element is important. With the current cap-design, the volume inside the cap was relatively large. As the caps were coated with the antifouling material, the holes needed to be re-opened

with a needle. If all the holes were opened, the whole coating peeled off. Therefore, only a few of the holes were opened, enough to obtain a water flow through the cap. To improve the design of the cap, a material with better adherent abilities to the coating material have to be used. This way, the coating material could get closer to the sensing element, and hopefully protect the sensor better against biofouling.

The cap design could also need other improvements to make sure the readings are reliable. As the caps were first slid on, air bubbles were captured in both caps, resulting in completely wrong results. If the water level was less stable, and the sensors appeared to be above the water for a short time, this would cause new air bubbles and unreliable results until the cap was reattached under water. As mentioned in the previous paragraph, the coating was not sufficient adherent to the Teflon material. As the caps was designed to perfect fit the sensor housing, the material was peeled off as the caps were first slid on. The material was folded close to the sensors sensing element, captured air bubbles and reduced the water flow. To improve the design, a material with better adhesion to the coating material and a shape avoiding air bubbles could be used.

5.4 ISE in RAS

In the beginning of the experiments in RAS, the salinity changed a lot due to variations in the incoming water. As known, an increase in ionic strength has a huge impact on the measurements by ISE [25]. As observed in the results, the ammonium electrode was much more affected by the change in salinity than the nitrate electrode. The loadings-plot created by using PCA visualizes a higher correlation between the salinity and NH_4-N, than NO_3-N. An explanation to the higher dependency in NH_4-N can be due to the presence of more interfering ions with high selectivity coefficients. As seen in Table 2.1, high concentrations of Na^+ and Cl^- can cause a significant interference in relatively high concentrations compared to the analyte ion. According to the selectivity coefficient Table, Cl^- has a larger impact on the $NO_3{}^-$ results than Na^+ has on $NH_4{}^+$. The presence of K^+ in seawater is normally about 380 ppm, while I^- is 0.05 ppm [17]. The higher interference of K^+ might cause the higher deviation in $NH_4{}^+$ than $NO_3{}^-$, in addition to the already low NH_4-N concentration compared to NO_3-N. However, the concentration of Na^+ and Cl^- will dominate the interfering in brackish water for both electrodes.

In the results from the spectrophotometer in Figure 4.7, there were observed lower and more stable concentrations than the IC results. The test kit used to quantify ammonium in these

samples, adjusted the pH to 11-12, hence ammonium was converted to ammonia. The ammonia was further reacted to a coloured complex using monochloramine, ranging from yellow to green depending on the ammonia concentration. Not fully conversion or reaction might result in a lower detected $NH_4{}^+$ concentration. Spectrometric methods have different sources of error than IC and ISE. According to the user manual, the samples did not contain interfering ions or compounds in a concentration that would affect the quantification [81]. The samples could however contain particles or other species absorbing the same wavelengths. In the test kit, both liquids and powder chemicals were added. Insufficient mixing could reduce the conversion to ammonia or the coloured complex, which would affect the quantification [15]. The spectrophotometric samples were analyzed a few minutes after sampling, and were not filtered. Chemical changes in the IC sample could occur during filtering, freezing and defrosting. The sources of error in IC is further described in section 5.7.

5.5 ISE in FTS

Fresh water contains less interfering ions than the brackish water used in RAS, because of a much lower concentration of Na^+ and Cl^-. Therefore, the results from IC and ISE were expected to have less deviation than the brackish water samples. Both NO_3-N and NH_4-N results from ISE were more similar to the IC results in this system, they were still significant higher than the IC results. To control the IC instruments measurements, the ISE calibration solution were analyzed. The measured concentration of the 10 mg/L NO_3-N solution was 10.95 mg/L by IC. The 100 mg/L NO_3-N was found to be 102.8 mg/L by IC. Because of the good correlation in this test, the deviation between ISE and IC is assumed to be because of the presence of interfering ions in the water. Because of the feeding system and the fish living in the tank, there might be some interfering ions increasing the measured concentrations by ISE. Based on to the samples from ICP-MS, the concentration of potassium was 5 mg/L to 6 mg/L, which increased the $NH_4{}^+$ concentration measured by ISE with 0.5 mg/L to 0.6 mg/L based on the selectivity coefficient for potassium. In combination with other interfering ions, some of the deviation can be explained.

The lowest calibration standard for NO_3-N was 1 mg/L and for NH_4-N it was 10 mg/L, which especially for NH_4-N was much higher than the expected concentration in fresh water. More calibration points in the lower concentration area could increase the sensitivity and accuracy for $NH_4{}^+$ quantification. The temperature in the systems were between 13 °C to 6 °C. The calibration solutions were stored, as recommended, in room temperature. The solutions

could advantageously be cooled down before calibration, as the recommended calibration temperature was $\pm$ 2 °C relative to the sample temperature. The same electrodes were used in FTS as in RAS, and the long lasting experiment, biofouling and cleaning might destroy the sensing element over time. The sensors were tested after calibration in the same calibration solutions before a new experiment was started. The sensing element could have reduced sensitivity or selectivity in the system over time, not detected in the lab after calibration. HACH expects a life time of two years without membrane replacement for both the NH_4^+ electrode and the NO_3^- electrode [26]. The sensors had been used in one year as this project was over. Therefore, the sensors age was not of a great concern.

During the first 10 days of the first experiment in the FTS, the light was turned on and the fish was fed between 9 am to 9 pm. In the results from the ISE in Figure 4.12, a variation in NH_4-N was detected in this time period, with highest amplitude value at 10 pm and lowest at 10 am. The peak in ammonia concentration was one hour after the feeding and light had been turned off. As described by A. Bergheim et al. in a research of oxygen consumption and ammonia excretion in fish farms, the peak in ammonia concentration was a few hours after feeding had ceased [82]. Ammonia excretion is a result of protein metabolism, and a variation based on feeding and diurnal variations are expected [83]. There were not analyzed any samples for cations with IC in this experiment, because of a limited amount of eluent available. However, a variation like this would be hard to detect with only a few IC samples or by the spectrophotometer.

5.6 Baseline Correction

The baseline correction was done on the NO_3-N electrode from the second experiment in RAS to investigate GRM as a baseline correction method for drifting ISE results. The other ISE raw data from the other experiments contained sudden changes most likely related to attachment or release of organic matter, salinity change or did not drift as significant as in this experiment. Hence, this data was the most suitable graph for baseline correction with GRM.

When the baseline created by MLR and GRM was subtracted, the graphs were quite similar. If the y-axis were scaled within the same range, the differences are minimal. GRM seemed to work better as a method to reduce baseline drift because the y-values are all positive and within the same range as the initial readings. The GRM also uses several iterations to fit the baseline better. If the data had contained sharp peaks, the MLR baseline had increased to an

even higher value, while the GRM still had been in this position. The output from GRM would be more reliable and demand less adjustments subsequently. Based on the few assumed true levels of $NO_3{}^-$ in RAS quantified by IC, the variation from day to day was not sufficient understood to conclude on the reliability of the corrected graph. Sharp spikes with a known $NO_3{}^-$ concentrations could be helpful to investigate the baseline corrected spectrums' reliability.

5.7 Comparison of IC and ISE Results

Baseline separation of the analyte peaks was obtained in all chromatograms used to quantification. The signal to noise ratio in the lowest calibration standard was 31.5 for NH_4-N and even higher for $NO_3{}^-$, where the noise band was not visible compared to the peak. The regression lines based on the calibration points had an R^2-value equal to 0.9979 for $NO_3{}^-$ and 0.9996 for NH_4-N, which indicates a good fit to the calibration points. An example calculation of the signal to noise ratio calculation and the calibration curves are given in Appendix C. The freshwater samples had the lowest concentration of NH_4-N, which gave a signal to noise ratio equal to 5.5. The samples do not fulfill the limit of quantification, which usually is set to 10 times the signal to noise ratio [84]. The uncertainty in the quantified NH_4-N in the freshwater samples from FTS might have a higher uncertainty than the samples from RAS.

The IC method requires expensive equipment, more sample preparation and longer time in the laboratory. As long as a good separation is achieved, possible interferences are minimal. Because of the necessary sampling and long analysis time, few data points are obtained with IC, and the results were not in real time. The continuous measuring with ISE in real time was able to detect small changes in ammonium concentration in fresh water. Compared to a sample for IC twice a week, it was not possible to detect such small changes. For instance, the variations in NH_4-N in Figure 4.12 caused by feeding and light regulation would not be possible to detect with IC. The readings were available in real time, and no sampling or sample preparation was necessary.

In IC, only the charged species are detected. When the total ammonia nitrogen was quantified, only ammonium was detected, and eventual ammonia presented were not included. The ISE measures the total ammonia nitrogen in the sample. Ammonia will be converted to ammonium before quantification [15]. The pH in RAS was 7.5. Calculation of the ammonium concentration at this pH, using Equation 2.2, 98% of the total ammonia nitrogen was presented as ammonia. The concentration of ammonia was not assumed to be significant as the two

methods have been compared.

Bacteria both from the MBBR, air, and water can be present in the frozen sample. Frozen at -20°C the bacteria are not active, but before the sample was fully frozen, while defrosting, and before the analysis any bacteria in the sample can change the concentration of the analyte ions [15]. Before analysis, the samples were filtered with a 0.45 μm filter to reduce the presence of nitrifying bacteria in the samples. The samples were stored in vials without a cap in the autosampler. Therefore, evaporation and direct contact with air might influence the stability in the sample. By analyzing the same sample after 0-21 hours after defrosting, the sample stability was examined. As shown in Appendix C the decrease in NH_4-N concentration in the samples had reached a deviation above 5% after 6 hours. Based on this test, the samples were analyzed within 6 hours after defrosting. Compared to the real time data from the ISE, chemical changes in the samples does not pose a concern.

5.8 Metal accumulation in RAS

ICP-MS detects the total amount of a metal in the sample, regardless of chemical speciation. The ICP-MS samples were filtrated with a 0.45 μm filter, thus eventual organic matter and precipitations were removed. Heavy metals bound to the organic matter were therefore not quantified. Metals dissolved in the water are more biological available, and can easily enter through the salmons' respiration system [50]. None of the samples either from RAS or FTS contained any toxic metals above background level of Norwegian coastal waters. The accumulation of Cu and Zn in RAS increased very slowly, and will not reach a toxic level in over a 100 years with the same accumulation rate. The concentration of metals in the water does not give rise to any toxic effect either in FTS or RAS.

5.9 Release of Silver from PDMS-TiO_2/Ag

This experiment was done to see if the concentration of silver ions released from the PDMS-TiO_2/Ag material was enough to result in a toxic effect in the surrounding water and not just at the material surface. If Ag^+ ions were released from the material, the concentration of dissolved Ag^+ would increase over time. A brackish water solution was used because that was where the caps was supposed to be tested initially. There was found a significant increase in silver concentration in both beakers with PDMS-TiO_2/Ag coated caps. The concentration increased from ca. 3 μg/L to 4 μg/L. One of the blank beakers had the same increase in silver concentration. In this

beaker, the silver can come from dust or other contaminations during sampling. Evaporation might also contribute to an increase in silver concentration. The amount of evaporated water was not significant compared to the increase in detected silver concentration. The t-test based on the samples from the two blank beakers combined did not result in a significant increase in silver concentration, and the material seemed to release a detectable amount of silver in its surrounding water.

The Brackish water used in the silver release experiment contained 12‰NaCl. The high concentration of Cl^-, can cause a precipitation of AgCl. AgCl attached to the glass walls or the caps were not quantified in samples analyzed with ICP-MS. AgCl solubility constant is $1.77 \cdot 10^{10}$ at room temperature, which would result in a very limited concentration of dissolved Ag^+ ions in the solution [23]. The ICP-MS quantifies silver independent of chemical speciation, and the increase in silver concentration could be silver ions, AgCl particles, other species or a combination. With relatively high volume inside the caps tested in FTS, and good water flow inside the cap, the amount of silver might not reach a toxic effect close to the sensing element.

6 Further Work

The application of ISE in aquaculture could be time-saving and have economic benefits. Because of interfering ions and biofouling, further research would be needed. If ISE should be used in RAS or other brackish water installations, a calibration method or compensation for salinity could be investigated. In fresh water, a calibration for lower concentrations would be beneficial, and the presence of interfering ions would need further research. More similar tests need to be done, to eliminate random variation and strengthen the statistical data. The statistical baseline reduction to eliminate drift caused by biofouling would also need further testing. Spiking with a known concentration of ammonia or nitrate would make it easier to examine if the quantification is polite after the baseline reduction.

The biofouling did change the ISE measurements, and more antifouling materials and methods to prevent biofouling should be tested. Different products containing AgNP, for instance training clothes, would be an interesting material to investigate. The antifouling properties of commercially available products could be compared to the PDMS-TiO_2/Ag material. The effect of vibration in combination with some of these antifouling materials could be investigated in additional experiments.

In these experiments, the biofouling was just visually inspected. The use SEM or similar analysis could give interesting information about the type and amount of biofouling and where it is attached. By analyzing the sensors and eventual antifouling caps in different time intervals, the biofouling process could be better understood.

Further testing of the PDMS-TiO_2/Ag material as antifouling protection in addition to SEM analysis would be recommended. The caps do need improvements to increase the antifouling properties on the sensors. A different design would be beneficial to avoid air bubbles inside the cap and to reduce the distance between the antifouling material and the sensing element. A material with better adhering to the coating material would be beneficial if the current cap design should be used. A more grid-like design or coated fabric could be alternatives to the current design.

Copper metal has been used in antifouling materials for years. A lower prize and low human toxicity could make copper a competitor to silver within the field of antifouling [49]. Possible immobilization of copper in the PDMS-TiO_2 material would need further research. The silver leakage from the current PDMS-TiO_2/Ag material needs to be tested in additional

experiments. Filtrating the ICP-MS samples would remove eventually precipitated particles, and would give rise to an investigation of the number of bioavailable silver ions.

7 Conclusion

In brackish water, the concentration of interfering ions are significant, and a compensation or calibration method considering these interfering ions are necessary before ISE can be used in this environment. In fresh water, the ISE can detect small changes in concentration, but further investigation of interfering ions, statistical compensation or calibration methods are necessary to obtain more accurate results. The design of the antifouling PDMS-TiO_2/Ag coated caps would need improvement to obtain reliable results from the sensor, and to improve the antifouling effect. With today's design, no antifouling effect was observed by visual inspection. There was found an increase in silver concentration in two caps' surrounding brackish water, but in what distance the toxic effect was significant is not known. There was found an accumulation of Zn and Cu in the RAS, but no metals would exceed the background concentration for Norwegian coastal waters in the lifetime of such installation.

References

[1] Statistics Norway TB, Steinset TA. Akvakultur - årlig, endelige tall - SSB;. (Accessed on 12/13/2017). https://www.ssb.no/jord-skog-jakt-og-fiskeri/statistikker/fiskeoppdrett/aar.

[2] Norwegian Environment Agency HH. Rømt oppdrettsfisk;. http://www.miljodirektoratet.no/no/Tema/Arter-og-naturtyper/Villaksportalen/Pavirkninger/Romt-oppdrettsfisk/.

[3] Taranger GL, Boxaspen K, Madhun AS, Svåsand T. Risikovurdering-miljøvirkninger av norsk fiskeoppdrett [2010], Havforskningsisnstituttet. 2011;.

[4] Wang X, Olsen LM, Reitan KI, Olsen Y. Discharge of nutrient wastes from salmon farms: environmental effects, and potential for integrated multi-trophic aquaculture. Aquac Environ Interact. 2012;2(3):267–283.

[5] Whitmarsh DJ, Cook EJ, Black KD. Searching for sustainability in aquaculture: an investigation into the economic prospects for an integrated salmon–mussel production system. Mar Policy. 2006;30(3):293–298.

[6] Salama N, Rabe B. Developing models for investigating the environmental transmission of disease-causing agents within open-cage salmon aquaculture. Aquac Environ Interact. 2013;4(2):91–115.

[7] Penston MJ, McKibben MA, Hay DW, Gillibrand PA. Observations on open-water densities of sea lice larvae in Loch Shieldaig, Western Scotland. Aquac Res. 2004;35(8):793–805.

[8] Ayer NW, Tyedmers PH. Assessing alternative aquaculture technologies: life cycle assessment of salmonid culture systems in Canada. J Clean Prod. 2009;17(3):362–373.

[9] Badiola M, Mendiola D, Bostock J. Recirculating Aquaculture Systems (RAS) analysis: Main issues on management and future challenges. Aquac Eng. 2012;51:26–35.

[10] Åsa Maria O Espmark N. Centre for Research-based Innovations in Controlled-environment Aquaculture;. (Accessed on 12/13/2017). https://nofima.no/en/prosjekt/ctrlaqua/.

[11] Zhang SY, Li G, Wu HB, Liu XG, Yao YH, Tao L, et al. An integrated recirculating aquaculture system (RAS) for land-based fish farming: The effects on water quality and

fish production. Aquac Eng. 2011 Nov;45(3):93–102. Available from: http://dx.doi.org/10.1016/j.aquaeng.2011.08.001.

[12] van Rijn J. Waste treatment in recirculating aquaculture systems. Aquac Eng. 2013;53:49–56.

[13] Nijhof M, Bovendeur J. Fixed film nitrification characteristics in sea-water recirculation fish culture systems. Aquaculture. 1990;87(2):133–143.

[14] Rusten B, Eikebrokk B, Ulgenes Y, Lygren E. Design and operations of the Kaldnes moving bed biofilm reactors. Aquac Eng. 2006 May;34(3):322–331. Available from: http://dx.doi.org/10.1016/j.aquaeng.2005.04.002.

[15] Douglas A Skoog FJH Donald M West, Crouch SR. Skoog and West's Fundamentals of Analytical Chemistry. 9th ed. Mary Finch; 2014.

[16] Galloway JN. The global nitrogen cycle: changes and consequences. Environ Pollut. 1998;102(1):15–24.

[17] Stumm W, Morgan JJ. Aquatic chemistry: chemical equilibria and rates in natural waters. 3rd ed. John Wiley & Sons; 1996.

[18] Smart G. Investigations of the toxic mechanisms of ammonia to fish–gas exchange in rainbow trout (Salmo gairdneri) exposed to acutely lethal concentrations. J Fish Biol. 1978;12(1):93–104.

[19] Alabaster J, Shurben D, Knowles G. The effect of dissolved oxygen and salinity on the toxicity of ammonia to smolts of salmon, Salmo salar L. J Fish Biol. 1979;15(6):705–712.

[20] Girard J, Payan P. Ion exchanges through respiratory and chloride cells in freshwater- and seawater-adapted teleosteans. Am J Physiol Regul Integr Comp Physiol. 1980;238(3):R260–R268.

[21] Trond Rosten TKBORBB Åse Åtland. Vannkvalitet og dyrevelferd. Trondheim: Mattilsynet; 2004.

[22] Schulz HD, Zabel M, et al. Marine geochemistry. vol. 2. Springer; 2006.

[23] Aylward G, Findlay T. SI Chemical Data. 6th ed. John Wiley & Sons; 2008.

[24] CHEMICAL SENSORS RESEARCH GROUP;. (Accessed on 12/13/2017). http://csrg.ch.pw.edu.pl/tutorials/ise/.

[25] Bakker E. Selectivity of liquid membrane ion-selective electrodes. Electroanalysis. 1997;9(1):7–12.

[26] Headquarters HCW. User Manual for Ammonia Probe Models: ISENH31801 or ISENH31803; 2013.

[27] Poole CF. The Essence of Chromatography. Elsevier; 2003.

[28] Manual ACL. Determination of Sulfur in Coal by Ion Chromatography - Analytical Chemistry Lab Manual;. (Accessed on 12/13/2017). http://sites.cord.edu/chem-330-lab-manual/experiments/ic.

[29] Avdalovic N, Pohl CA, Rocklin RD, Stillian JR. Determination of cations and anions by capillary electrophoresis combined with suppressed conductivity detection. Anal Chem. 1993;65(10):1470–1475.

[30] Madden JE, Haddad PR. Critical comparison of retention models for the optimisation of the separation of anions in ion chromatography: II. Suppressed anion chromatography using carbonate eluents. J Chromatogr A. 1999;850(1):29–41.

[31] Elsa Lundanes LR, Greibrokk T. Chromatography, Basic Principles, Sample Preparations and Related Methods. Wiley-VCH; 2014.

[32] Paull B, Nesterenko PN. Chapter 8 - Ion Chromatography. Fanali S, Haddad PR, Poole CF, Schoenmakers P, Lloyd D, editors. Amsterdam: Elsevier; 2013.

[33] Rapportering i henhold til avtale på møte 27;. (Accessed on 02/19/2018). https://www.mattilsynet.no/fisk_og_akvakultur/fiskevelferd/mattilsynet__rapport_om_vannkvalitet_og_fiskevelferd_2004.5943/binary/Mattilsynet%20-%20Rapport%20om%20vannkvalitet%20og%20fiskevelferd%202004.

[34] Agency TNE. Grenseverdier for klassifisering av vann, sediment og biota; 2016. (Accessed on 02/19/2018). http://www.miljodirektoratet.no/Documents/publikasjoner/M608/M608.pdf.

[35] Thomas R. Practical guide to ICP-MS: a tutorial for beginners. CRC press; 2013.

[36] Hill SJ. Inductively coupled plasma spectrometry and its applications. vol. 8. John Wiley & Sons; 2008.

[37] Kannamkumarath SS, Wrobel K, Wrobel K, B'Hymer C, Caruso JA. Capillary electrophoresis–inductively coupled plasma-mass spectrometry: an attractive complementary technique for elemental speciation analysis. J Chromatogr A. 2002;975(2):245–266.

[38] Laylin JK. Nobel laureates in chemistry, 1901-1992. Chemical Heritage Foundation; 1993.

[39] Robert M Silverstein DJK Francis X Webster, Bryce DL. Spectrometric Identification of Organic Compounds. 8th ed. John Wiley & Sons; 2015.

[40] Survey USG. Introduction to ICP-MS; 2005. (Accessed on 04/12/2018). `https://crustal.usgs.gov/laboratories/icpms/intro.html`.

[41] CHP - Quadrupole Mass Spectrometry;. (Accessed on 04/12/2018). `http://www.tissuegroup.chem.vt.edu/chem-ed/ms/quadrupo.html`.

[42] Railkin AI. Marine biofouling: colonization processes and defenses. CRC press; 2003.

[43] Aldred N, Clare AS. The adhesive strategies of cyprids and development of barnacle-resistant marine coatings. Biofouling. 2008;24(5):351–363.

[44] Yebra DM, Kiil S, Dam-Johansen K. Antifouling technology—past, present and future steps towards efficient and environmentally friendly antifouling coatings. Prog Org Coat. 2004;50(2):75–104.

[45] Leonard N, Blancheton J, Guiraud J. Populations of heterotrophic bacteria in an experimental recirculating aquaculture system. Aquacult Eng. 2000;22(1):109–120.

[46] Babin M, Roesler CS, Cullen JJ. Real-time coastal observing systems for marine ecosystem dynamics and harmful algal blooms: Theory, instrumentation and modelling. Unesco; 2008.

[47] Hagger JA, Depledge MH, Galloway TS. Toxicity of tributyltin in the marine mollusc Mytilus edulis. Mar Pollut Bull. 2005;51(8):811–816.

[48] Manov DV, Chang GC, Dickey TD. Methods for reducing biofouling of moored optical sensors. J Atmos Oceanic Technol. 2004;21(6):958–968.

[49] Letelier ME, Sánchez-Jofré S, Peredo-Silva L, Cortés-Troncoso J, Aracena-Parks P. Mechanisms underlying iron and copper ions toxicity in biological systems: Pro-oxidant activity and protein-binding effects. Chem Biol Interact. 2010;188(1):220–227.

[50] Davidson J, Good C, Welsh C, Summerfelt ST. Abnormal swimming behavior and increased deformities in rainbow trout Oncorhynchus mykiss cultured in low exchange water recirculating aquaculture systems. Aquacult Eng. 2011;45(3):109–117.

[51] Glinel K, Jonas AM, Jouenne T, Leprince J, Galas L, Huck WT. Antibacterial and antifouling polymer brushes incorporating antimicrobial peptide. Bioconjugate Chem. 2008;20(1):71–77.

[52] Kuang J, Messersmith PB. Universal surface-initiated polymerization of antifouling zwitterionic brushes using a mussel-mimetic peptide initiator. Langmuir. 2012;28(18):7258–7266.

[53] Granhag L, Finlay J, Jonsson P, Callow J, Callow M. Roughness-dependent removal of settled spores of the green alga Ulva (syn. Enteromorpha) exposed to hydrodynamic forces from a water jet. Biofouling. 2004;20(2):117–122.

[54] Zuliani C, Diamond D. Opportunities and challenges of using ion-selective electrodes in environmental monitoring and wearable sensors. Electrochim Acta. 2012;84:29–34.

[55] Pal S, Tak YK, Song JM. Does the antibacterial activity of silver nanoparticles depend on the shape of the nanoparticle? A study of the gram-negative bacterium Escherichia coli. Appl Environ Microbiol. 2007;73(6):1712–1720.

[56] Choi O, Deng KK, Kim NJ, Ross Jr L, Surampalli RY, Hu Z. The inhibitory effects of silver nanoparticles, silver ions, and silver chloride colloids on microbial growth. Water Res. 2008;42(12):3066–3074.

[57] Sambhy V, MacBride MM, Peterson BR, Sen A. Silver bromide nanoparticle/polymer composites: dual action tunable antimicrobial materials. J Am Chem Soc. 2006;128(30):9798–9808.

[58] Sondi I, Salopek-Sondi B. Silver nanoparticles as antimicrobial agent: a case study on E. coli as a model for Gram-negative bacteria. J Colloid Interface Sci. 2004;275(1):177–182.

[59] Ivask A, Kurvet I, Kasemets K, Blinova I, Aruoja V, Suppi S, et al. Size-dependent toxicity of silver nanoparticles to bacteria, yeast, algae, crustaceans and mammalian cells in vitro. PloS one. 2014;9(7):e102108.

[60] Milić M, Leitinger G, Pavičić I, Zebić Avdičević M, Dobrović S, Goessler W, et al. Cellular uptake and toxicity effects of silver nanoparticles in mammalian kidney cells. J Appl Toxicol. 2015;35(6):581–592.

[61] silver_database_fauss_sept2_final.pdf;. (Accessed on 02/08/2018). `http://www.nanotechproject.org/process/assets/files/7039/silver_database_fauss_sept2_final.pdf`.

[62] Ahamed M, AlSalhi MS, Siddiqui M. Silver nanoparticle applications and human health. Clin Chim. 2010;411(23-24):1841–1848.

[63] Gliga AR, Skoglund S, Wallinder IO, Fadeel B, Karlsson HL. Size-dependent cytotoxicity of silver nanoparticles in human lung cells: the role of cellular uptake, agglomeration and Ag release. Part Fibre Toxicol. 2014;11(1):11.

[64] Ribeiro F, Van Gestel CA, Pavlaki MD, Azevedo S, Soares AM, Loureiro S. Bioaccumulation of silver in Daphnia magna: Waterborne and dietary exposure to nanoparticles and dissolved silver. Sci Total Environ. 2017;574:1633–1639.

[65] Cebeci FÇ, Wu Z, Zhai L, Cohen RE, Rubner MF. Nanoporosity-driven superhydrophilicity: a means to create multifunctional antifogging coatings. Langmuir. 2006;22(6):2856–2862.

[66] Zhang X, Guo Y, Zhang Z, Zhang P. Self-cleaning superhydrophobic surface based on titanium dioxide nanowires combined with polydimethylsiloxane. Appl Surf Sci. 2013;284:319–323.

[67] Chen Q, Zhou W, Du GH, Peng LM. Trititanate nanotubes made via a single alkali treatment. Adv Mater. 2002;14(17):1208–1211.

[68] Yee MSL, Khiew PS, Lim SS, Chiu WS, Tan YF, Kok YY, et al. Enhanced marine antifouling performance of silver-titania nanotube composites from hydrothermal processing. Colloids Surf, A. 2017;520:701–711.

[69] Koudelka M. Performance characteristics of a planar 'Clark-type'oxygen sensor. Sens Actuators. 1986;9(3):249–258.

[70] Padilla M, Perera A, Montoliu I, Chaudry A, Persaud K, Marco S. Drift compensation of gas sensor array data by orthogonal signal correction. Chemom Intell Lab Syst. 2010;100(1):28–35.

[71] Gan F, Ruan G, Mo J. Baseline correction by improved iterative polynomial fitting with automatic threshold. Chemom Intell Lab Syst. 2006;82(1-2):59–65.

[72] Dietrich W, Rüdel CH, Neumann M. Fast and precise automatic baseline correction of one-and two-dimensional NMR spectra. J Magn Reson (1969). 1991;91(1):1–11.

[73] Alsberg BK. Chemometrics, Compendium for TKJ4175/KJ8175. NTNU;.

[74] Leger MN, Ryder AG. Comparison of derivative preprocessing and automated polynomial baseline correction method for classification and quantification of narcotics in solid mixtures. Appl Spectrosc. 2006;60(2):182–193.

[75] Peng J, Peng S, Jiang A, Wei J, Li C, Tan J. Asymmetric least squares for multiple spectra baseline correction. Anal Chim Acta. 2010;683(1):63–68.

[76] 6.5.6. Interpreting score plots — Process Improvement using Data;. (Accessed on 04/17/2018). https://learnche.org/pid/latent-variable-modelling/principal-component-analysis/interpreting-score-plots-and-loading-plots.

[77] Abarzua S, Jakubowski S. Biotechnological investigation for the prevention of biofouling. I. Biological and biochemical principles for the prevention of biofouling. Mar Ecol Prog Ser. 1995;p. 301–312.

[78] Rosenhahn A, Schilp S, Kreuzer HJ, Grunze M. The role of "inert" surface chemistry in marine biofouling prevention. Phys Chem Chem Phys. 2010;12(17):4275–4286.

[79] Callow ME, Fletcher RL. The influence of low surface energy materials on bioadhesion—a review. Int Biodeterior Biodegrad. 1994;34(3-4):333–348.

[80] Regan F, Barrett A, Briciu-Burghina C, Sullivan T. Antifouling studies and coating strategies for marine deployed structures. In: OCEANS 2017-Aberdeen. IEEE; 2017. p. 1–6.

[81] Merck. 114752 - Spectroquant Ammonium Test;. (Accessed on 05/24/2018). https://www.merckmillipore.com/NO/en/product/Ammonium-Test,MDA_CHEM-114752#anchor_APPL.

[82] Bergheim A, Seymour EA, Sanni S, Tyvold T, Fivelstad S. Measurements of oxygen consumption and ammonia excretion of Atlantic salmon (Salmo salar L.) in commercial-scale, single-pass freshwater and seawater landbased culture systems. Aquacult Eng. 1991;10(4):251–267.

[83] Seymour E. The effects and control of algal blooms in fish ponds. Aquaculture. 1980;19(1):55–74.

[84] Mitra S. Sample preparation techniques in analytical chemistry. vol. 237. John Wiley & Sons; 2004.

A Gan-Ruan-Mo Baseline Correction

The following pseudocode was given in the paper written by F. Gan, G. Ruan and J. Mo [71]:

1. Set polynomial degree to n
2. Let original signal with trend be f_0
3. for k = 1...K_{max} do
4. $d_k = X\hat{b} = XX^TX^{-1}X^Tf_{k-1}$
5. Compare d_k with f_{k-1}
6. if $f_{k-1} > d_kj$ then
7. $f_kj = d_kj$
8. end if
9. $p = \frac{||d_k - d_{k-1}||}{||d_{k-1}||}$
10. if $p \geq \epsilon$ then
11. STOP
12. end if
13. end for

The interpretation of this pseudocode is given in the next two pages. A program for suitable for statistical processing needs to be used. In this case R was used.

baselinecorrection.R

Kristin

Thu May 10 14:56:15 2018

```
rm(list=ls())
dev.off()
```

```
## null device
##           1
```

```
setwd("/Users/Kristin/Desktop/Baseline correction/")

#load the csv file (no3vibtest)
NO3ISEdata=read.csv("no3vibtest.csv")
attach(NO3ISEdata)

#plot NO3ISE=raw data vs Days
par(mfrow=c(2,2)) #to be able to have multiple plots open at the same time.
plot(Hours/24,NO3ISE,"l",ylab = "NO3-N [mg/L]", xlab = "Days", main = "Estimated baseline using MLR" )

#Creating X matrix [1,x,x^2...], the x variable is days/10
n=length(Hours)
days=Hours/(24*10) #days/10 to make shure the matrix is invertable
#Xh=cbind(seq(1,1,len=n),Hours,Hours^2, Hours^3)
Xd=cbind(seq(1,1,len=n),days,days^2, days^3, days^4,days^5,days^6)#,days^7,days^8,days^9,days^10)
#polynomial of choise

#generates XtX
G = t(Xd)%*%Xd
bhat=solve(G)%*%t(Xd)%*%NO3ISE
d=Xd%*%bhat #d is the trend of the baseline

lines(Hours/24,d,"l",col="red") #the trendline based on all data.

g=NO3ISE-d #g is the corrected signal.
g100=g/max(g)*100 #scaled as percentage
plot(Hours/24,g100, "l", xlab = "Days",ylab = "% change in NO3-N",
     main = "The signal after subtraction of MLR baseline")
#plot of the data with baseline correction (not GRM baseline).


#GRM algorithm:

f=matrix(NO3ISE,nrow=length(NO3ISE)) #original signal

for(k in seq(1,100,1)){
  dk=Xd%*%solve(G)%*%t(Xd)%*%f
  for (i in seq(1,length(f),1)){
    if (f[i]>dk[i]){
      f[i]=dk[i]
    }#if
  }#for
```

```
}#for

plot(Hours/24,NO3ISE,"l",ylab = "NO3-N [mg/L]", xlab = "Days", main = "Estimated baseline using GRM"  )
lines(Hours/24,dk, "l",col="blue") #GRM baseline
h=NO3ISE-dk
h100=h/max(h)*100
plot(Hours/24,h100, "l",xlab = "Days", ylab = "% change in NO3-N", main =
       "The signal after subtraction of GRM baseline" )
```

B ICP-MS Results

The concentrations of seven different metals in RAS determined by ICP-MS is given in table B.1. The concentration of silver in the silver release experiment done in the laboratory is given in table B.2.

Table B.1: The concentration in μg/L of 7 different elements quantified by ICP-MS from the RAS system at Nofima. The residual standard errors is based on 10 analysis of each element. The high content of NaCl reduced the sensitivity compared to fresh water samples.

	Cd	Pb	Cr	Ni	Cu	Zn	As
ks0502	0.054 ± 2.4 %	0.000 ± 19.0%	0.11 ± 25.4%	0.42 ± 19.9%	0.66 ± 3.2%	5.64 ± 1.1%	0.875 ± 8.9%
ks0602	0.055 ± 7.9%	-0.001 ± 78.3%	0.16 ± 12.2%	0.53 ± 11.1%	0.81 ± 10.5%	5.59 ± 8.5%	0.930 ± 5.0%
ks0602	0.057 ± 7.9%	0.000 ± 55.4%	0.15 ± 22.9%	0.51 ± 11.1%	0.62 ± 3.9%	4.51 ± 5.4%	0.698 ± 1.7%
ks2602	0.051 ± 5.2%	0.001 ± 18.3%	0.15 ± 3.0%	0.47 ± 5.5%	1.08 ± 5.0%	10.93 ± 4.2%	0.792 ± 13.4%
ks2602	0.053 ± 4.0%	0.000 ± 2.3%	0.16 ± 11.4%	0.53 ± 6.1%	1.09 ± 4.4%	10.68 ± 1.6%	0.709 ± 11.2v
ks0503	0.057 ± 6.9%	0.004 ± 9.9%	0.16 ± 18.4%	0.46 ± 19.8%	1.35 ± 9.5%	18.10 ± 4.3%	0.865 ± 9.3%

Table B.2: The concentration of silver in μg/L analyzed by ICP-MS during the ailver release experiment with PDMS-TiO2-Ag coated caps. The time is given in days after the caps were added the brackish water solution of 12‰NaCl.

Time [day]	Blank 1	Blank 2	Cap 1	Cap 2
0.20	3.14	2.52	3.15	3.18
0.75	3.63	2.48	3.39	3.36
1.75	3.68	2.55	2.62	3.43
3.04	3.53	3.72	3.67	3.51
6.96	3.63	2.95	3.66	3.63
21.00	3.98	2.64	4.08	4.00
21.00	4.19	2.88	3.79	4.63
21.00	4.04	-	-	3.96

C IC Sample Stability

The stability in NH_4-N concentration in a sample stored in the auto sampler is given in figure C.1. The concentration is reduced by 5% after 6 hours. The remaining samples were therefore analyzed within 6 hours after defrosting.

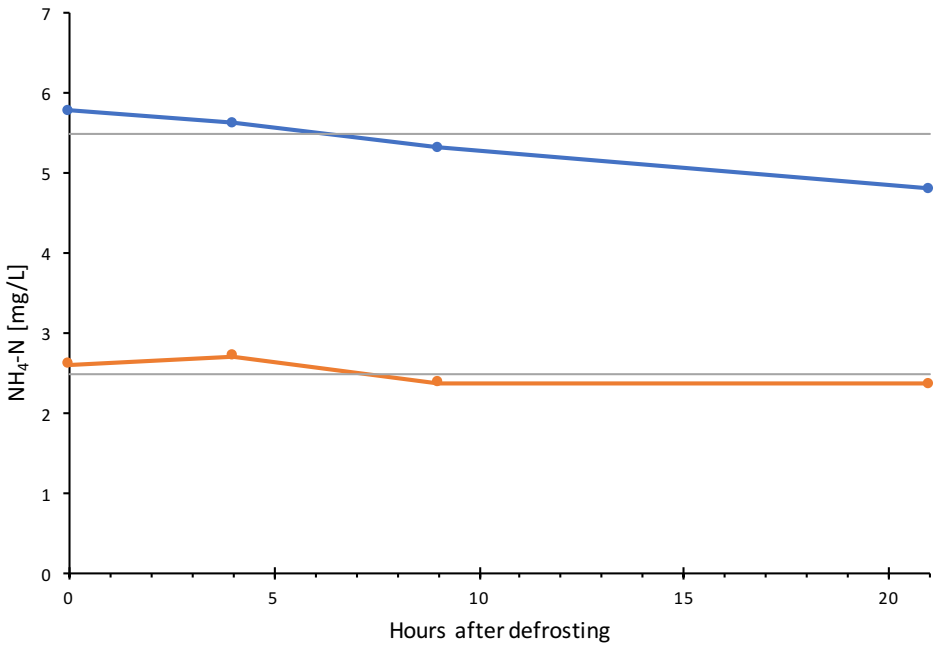

Figure C.1: Investigation of NH4+ stability in samples stored in open vials in room temperature. The blue graph is from a fresh water sample, while the orange is a brackish water sample with 16‰ salinity. The gray lines is the concentration reduced by 5% relative to the first analysis.

D Calibration Curves IC

Calibration curve for NO_3^- and NH_4-N based on peak area is given in figure D.1 and D.2 respectively. The equations on the form $y = ax + b$, where y is the peak area and x is the concentration, and R^2-value is given in table D.1.

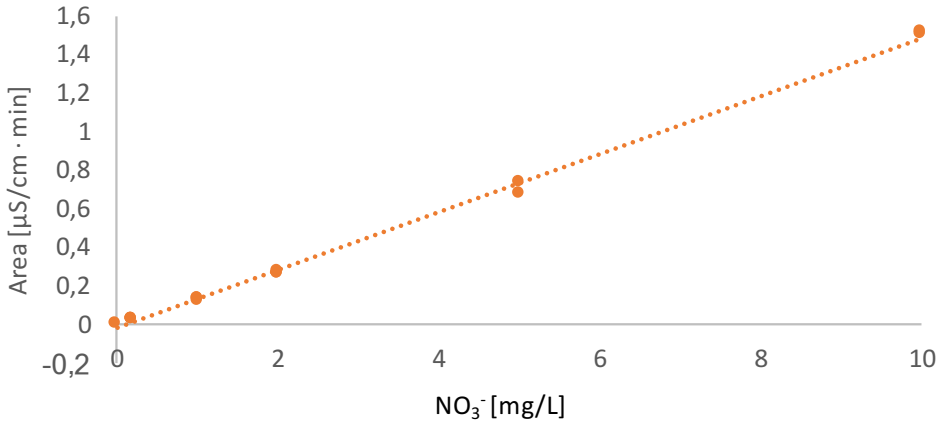

Figure D.1: Calibration curve for NO_3^- analyzed on IC with diluted Fluka Analytical standard for NO_3^-.

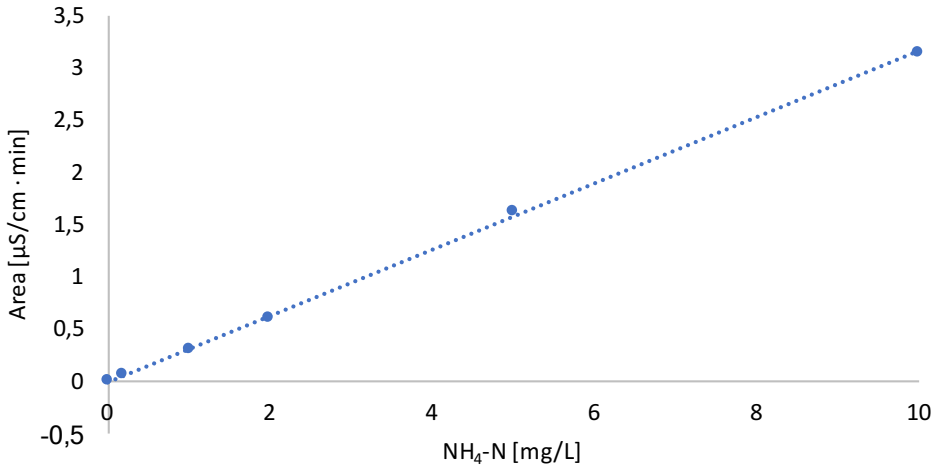

Figure D.2: Calibration curve for NH_4-N analyzed on IC with diluted Fluka Analytical standard for NH_4-N.

Table D.1: The regression lines for NH_4-N and $NO_3{}^-$ based on the calibration points on the form $y = ax + b$, where y is the peak area and x is the concentration

Analyte	a	b	R^2
NH_4-N	0.3158	-0.0047	0.9996
$NO_3{}^-$	0.1512	-0.0244	0.9979

E Signal to Noise Ratio

The signal to noise ratio (S/N) was determined in the lowest calibration standards, as displayed in figure E.2 for NH4 and E.1 for $NO_3{}^-$. The S/N for the samples with smallest peak area was also determined to examine if the signal is above quantification level of S/N>10. The $NH_4{}^+$ peak in sample "ks0905" is presented in figure E.3. The $NO_3{}^-$ peak in sample "anion1503" is presented in figure E.4. The S/N was above 10 in both standards and in the anion sample. The S/N in the cation sample with lowest ammonium concentration was 5.5, and therefore below quantification level.

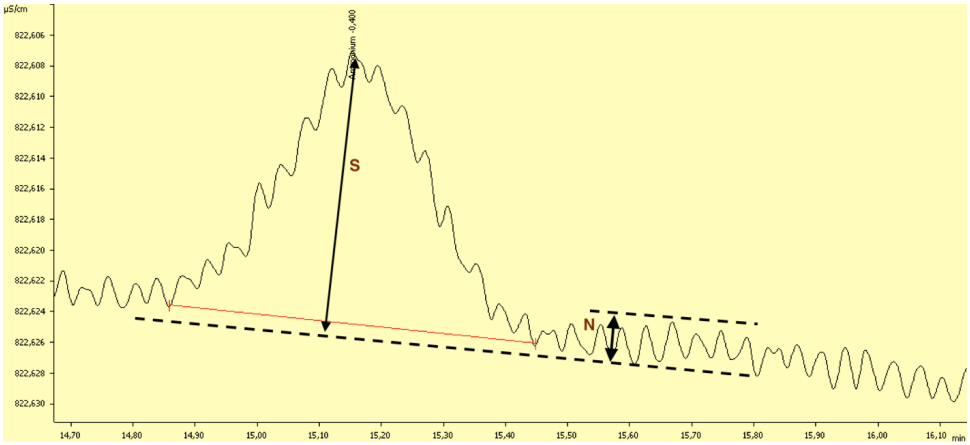

Figure E.1: The NH4+ peak in a sample with lowest concentration used to calculate the signal to noise ratio. The signal to noise ratio was 5.5.

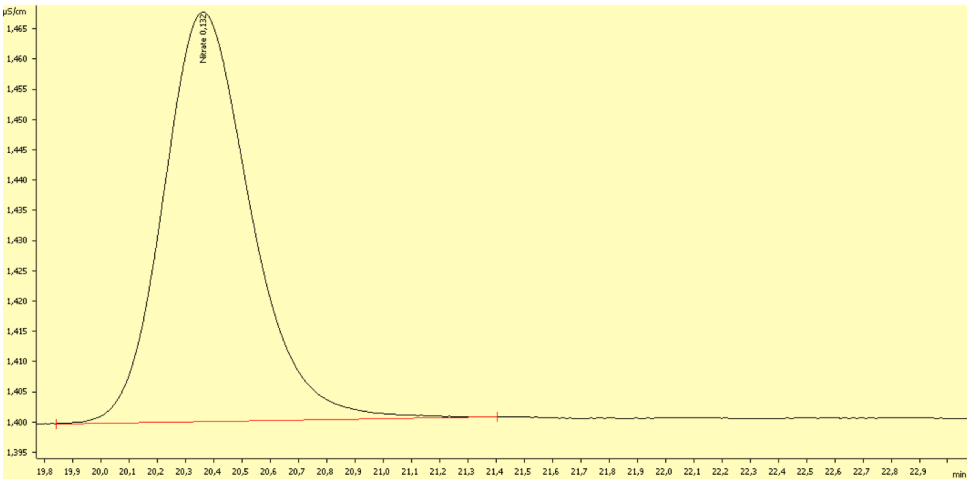

Figure E.2: The NO3- peak in the lowest calibration standard. The signal is obviously above the quantification level at 10 times the signal to nise ratio.

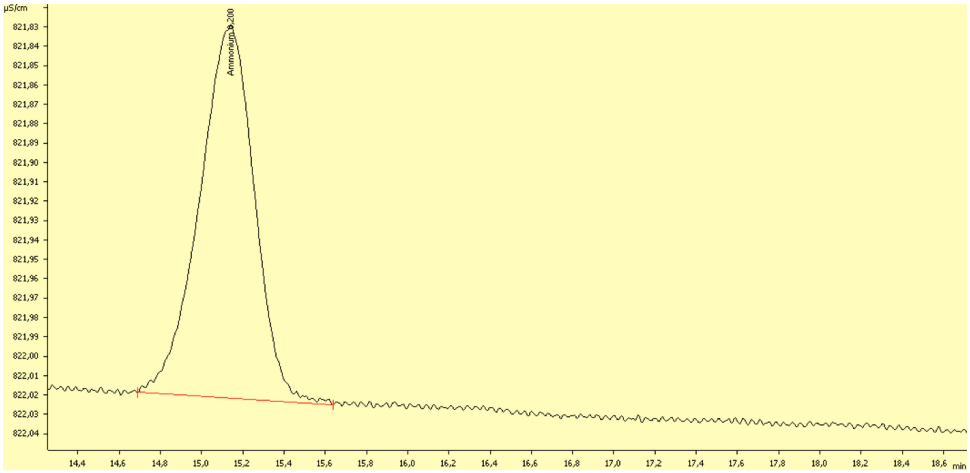

Figure E.3: The standard solution with lowest concentration (0.2 mg/L) of NH4+. The signal to noise ratio was 31.5.

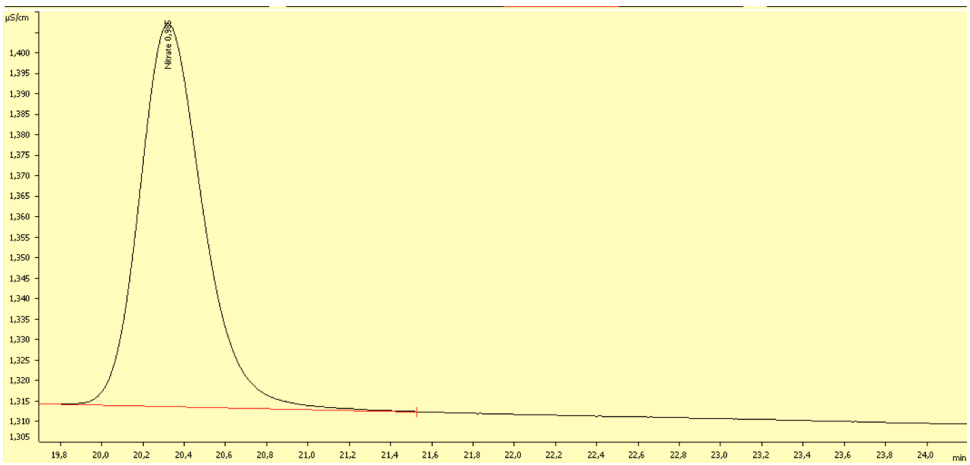

Figure E.4: The NO3- peak in the sample with lowest concentration. The signal is obviously above the quantification level at 10 times the signal to nise ratio.

F Validation of the IC Analysis

As a fast validation of the IC instrument, the calibration standards for nitrate used to calibrate the ISE was analyzed by IC. The calibration solutions had a concentration of NO_3-N equal to 10 and 100 mg/L. Also the calibration solution from the IC calibration curve was analyzed, to make sure the instrument was working properly.

Table F.1: The validation of the IC analysis. The calibration solutions for IC and ISE were analyzed as samples. The concentration of the IC standard is given as $NO_3{}^-$, while the ISE is given as nitrate nitrogen (NO_3-N).

Standard	Target concentration [mg/L]	Measured concentration	Unit
IC calibration solution	10	10.368	$NO_3{}^-$
IC calibration solution	10	10.217	$NO_3{}^-$
ISE standard	10	11.402	NO_3-N
ISE standard	10	10.952	NO_3-N
ISE standard	100	102.622	NO_3-N
ISE standard	100	102.806	NO_3-N

G IC Results

Table G.1: The results from the IC analysis of nitrate. The sample date is given in the sample name as day and month. The retention time changed slightly due to unstable mixing of eluent.

Sample name	System	Retention time	Area	Dilution	NO_3-N [mg/L]
anion0502	RAS	20.29	0.253	20	8.240
anion0502rep	RAS	20.29	0.246	20	8.032
anion0602	RAS	30.79	0.624	10	9.630
anion0902	RAS	20.28	0.123	20	4.378
anion1302	RAS	20.30	0.084	20	3.220
anion1502	RAS	20.29	0.222	20	7.319
anion2602	RAS	27.58	1.580	5	11.914
anion2602rep	RAS	29.39	1.561	5	11.773
anion0503	RAS	20.24	0.348	20	11.062
anion0903	FTS	20.31	0.041	5	0.486
anion1303	FTS	20.40	0.013	10	0.555
anion1503	FTS	20.31	0.033	5	0.426
anion2103	FTS	20.34	0.017	10	0.615
anion0803	FTS	28.10	1.011	5	7.689
anion1804	FTS	27.90	0.042	5	0.493
anion2004	FTS	20.36	0.016	10	0.600
anion2504	FTS	27.63	0.031	5	0.411
anion2504rep	FTS	29.38	0.031	5	0.411
anion0205	FTS	30.33	0.040	5	0.478
anion0905	FTS	20.36	0.018	10	0.630
anion0905rep	FTS	20.36	0.017	10	0.615
anion0905rep2	FTS	20.35	0.017	10	0.615
test standard	-	29.10	0.133	10	2.338

Table G.2: The results from the IC analysis of ammonium. Just a selection of the samples were analyzed for cations because of a limited amount of eluent.

Sample name	System	Area	Dilution	NH_4-N [mg/L]
ks0804	FTS	NA	NA	NA
ks0903	FTS	0	2	0
ks0905	FTS	0.005	1	0.030
ks0205	FTS	0.007	1	0.036
ks0602	RAS	0.038	5	0.671
ks0502	RAS	0.024	5	0.454
ks0902	RAS	0.010	5	0.225
ks2602	RAS	0.015	5	0.313
ks0503	RAS	0.011	10	0.510
ren std.	-	1.039	3	9.916

H Chromatograms - Anions

The quantification was done in Microsoft Excel, and the given concentrations in the following tables are not correct. The given areas were used to calculate the concentrations using the calibration curves in appendix D. The concentrations are given in appendix G.

MagIC Net

2018-06-05 09:53:44

Sample data

Ident	anion0205	
Sample type	Sample	
Determination start	2018-05-19 09:20:11 UTC+2	
Method	Logisk fortynning NTNU Kjemisk	
Operator		

Anions

Data source	Conductivity detector 1 (940 Professional IC Vario 1)	
Channel	Conductivity	
Recording time	38,0	min
Integration	Automatically	
Column type	Metrosep A Supp 7 - 250/4.0	
Eluent composition	Anion Eluent - 3,6 mM Na2CO3	
Flow	0,700	mL/min
Maximum flow monitored	yes	
Pressure	10,02	MPa
Maximum pressure monitored	yes	
Temperature	45,0	°C

Anions

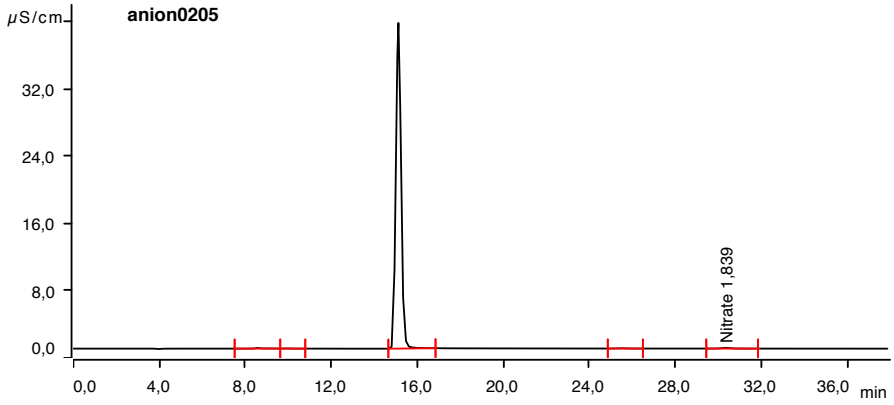

Peak number	Retention time min	Area (µS/cm) x min	Height µS/cm	Concentration mg/L	Component name
1	8,573	0,0352	0,080	invalid	
2	9,933	0,0083	0,020	invalid	
3	15,117	10,7963	38,724	invalid	
4	25,472	0,0132	0,030	invalid	
5	30,328	0,0403	0,078	1,839	Nitrate

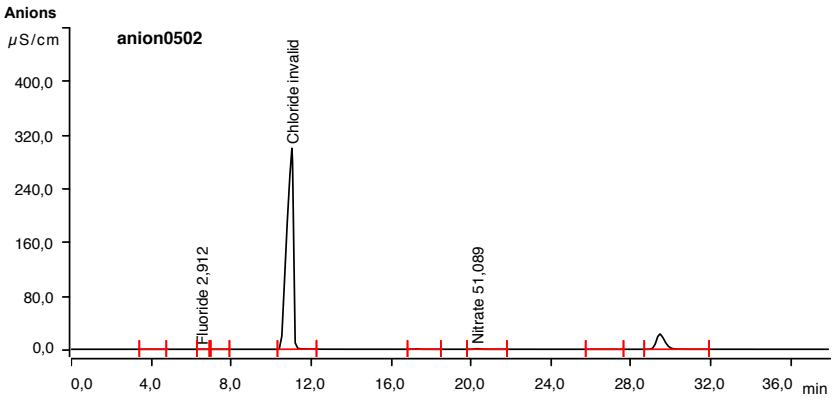

Peak number	Retention time min	Area (µS/cm) x min	Height µS/cm	Concentration mg/L	Component name
1	3,853	0,0104	0,047	invalid	
2	6,507	0,0103	0,057	2,912	Fluoride
3	7,437	0,0036	0,012	invalid	
4	11,037	112,3031	299,146	invalid	Chloride
5	17,250	0,1428	0,477	invalid	
6	20,290	0,2528	0,737	51,089	Nitrate
7	26,462	0,0130	0,022	invalid	
8	29,440	11,1943	22,672	invalid	

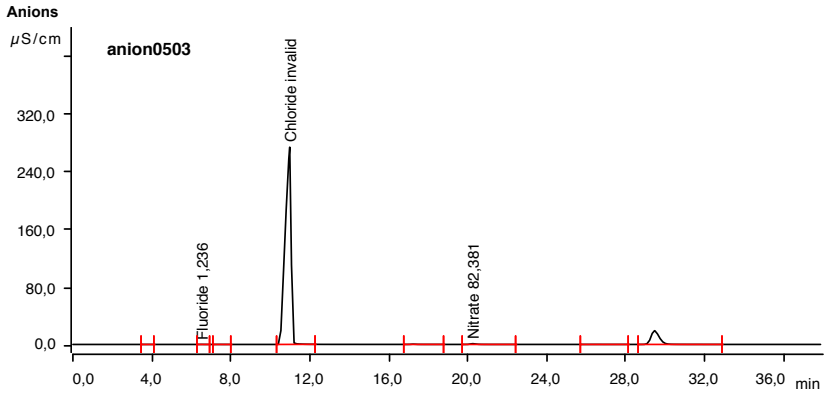

Peak number	Retention time min	Area (µS/cm) x min	Height µS/cm	Concentration mg/L	Component name
1	3,860	0,0027	0,015	invalid	
2	6,508	0,0088	0,050	1,236	Fluoride
3	7,433	0,0035	0,013	invalid	
4	10,980	92,9538	272,989	invalid	Chloride
5	17,232	0,1148	0,382	invalid	
6	20,238	0,3476	1,021	82,381	Nitrate
7	26,428	0,0202	0,039	invalid	
8	29,448	9,2880	18,996	invalid	

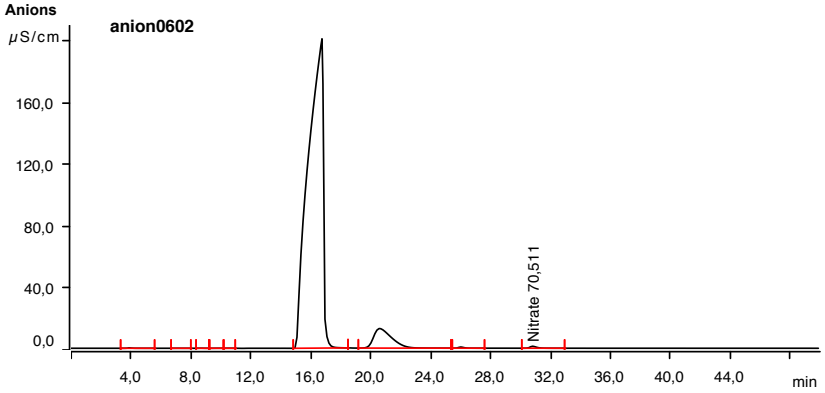

Peak number	Retention time min	Area (µS/cm) x min	Height µS/cm	Concentration mg/L	Component name
1	3,853	0,0846	0,276	invalid	
2	7,143	0,0049	0,012	invalid	
3	8,628	0,0196	0,056	invalid	
4	9,875	0,0084	0,021	invalid	
5	10,472	0,0095	0,025	invalid	
6	16,738	231,3358	200,096	invalid	
7	20,587	17,5596	12,645	invalid	
8	26,000	0,3045	0,732	invalid	
9	30,793	0,6237	1,259	70,511	Nitrate

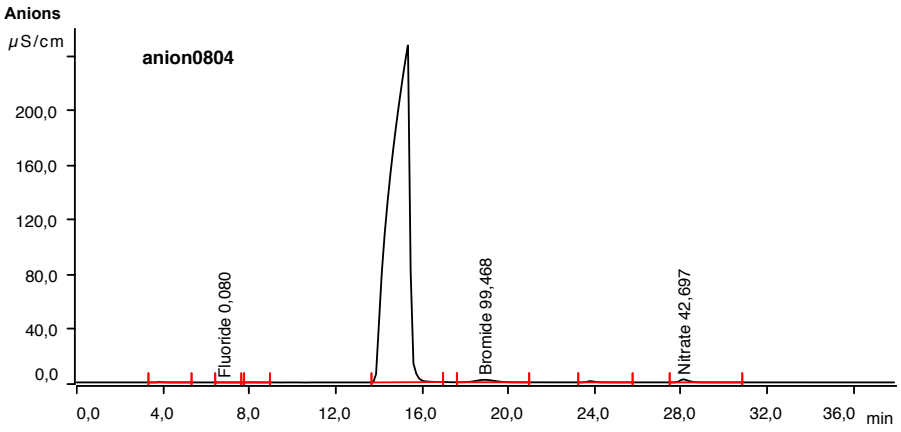

Peak number	Retention time min	Area (µS/cm) x min	Height µS/cm	Concentration mg/L	Component name
1	3,833	0,0867	0,294	invalid	
2	6,810	0,0050	0,014	0,080	Fluoride
3	8,082	0,0239	0,070	invalid	
4	15,347	254,2474	246,461	invalid	
5	18,897	1,7978	1,803	99,468	Bromide
6	23,797	0,3418	0,887	invalid	
7	28,100	1,0114	2,208	42,697	Nitrate

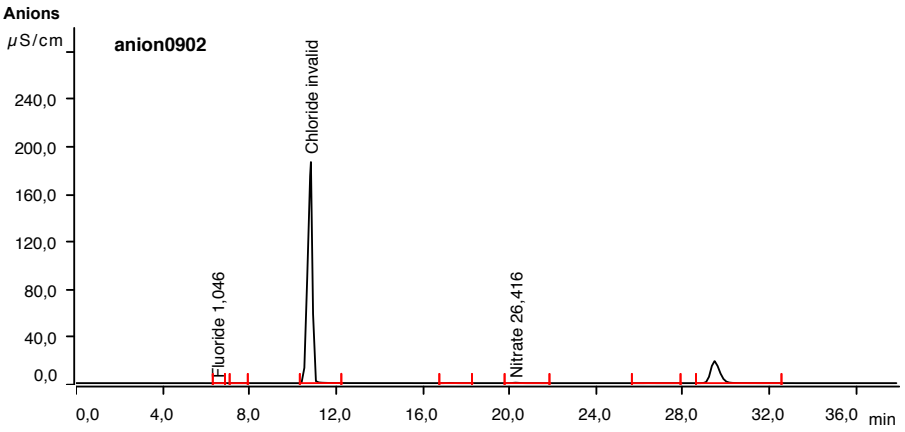

Peak number	Retention time min	Area (µS/cm) x min	Height µS/cm	Concentration mg/L	Component name
1	6,513	0,0051	0,030	1,046	Fluoride
2	7,428	0,0035	0,013	invalid	
3	10,837	46,7959	185,877	invalid	Chloride
4	17,238	0,0504	0,164	invalid	
5	20,282	0,1234	0,354	26,416	Nitrate
6	26,417	0,0154	0,029	invalid	
7	29,455	9,0183	18,446	invalid	

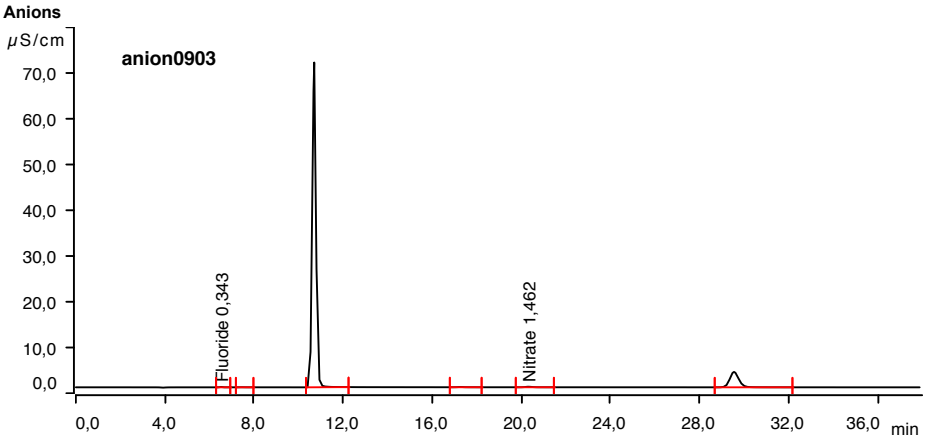

Peak number	Retention time min	Area (µS/cm) x min	Height µS/cm	Concentration mg/L	Component name
1	6,515	0,0115	0,073	0,343	Fluoride
2	7,425	0,0043	0,017	invalid	
3	10,700	13,7073	70,990	invalid	
4	17,248	0,0165	0,052	invalid	
5	20,312	0,0410	0,116	1,462	Nitrate
6	29,537	1,5874	3,372	invalid	

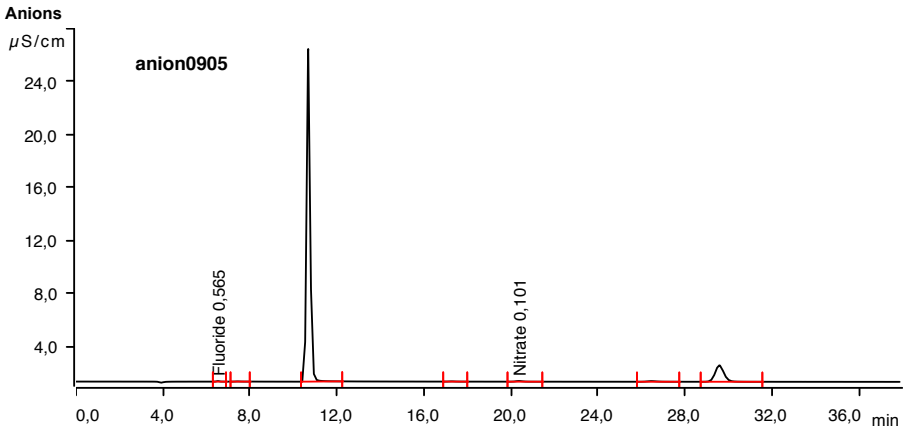

Peak number	Retention time	Area	Height	Concentration	Component name
	min	(µS/cm) x min	µS/cm	mg/L	
1	6,518	0,0067	0,043	0,565	Fluoride
2	7,430	0,0039	0,015	invalid	
3	10,675	4,7651	25,135	invalid	
4	17,277	0,0057	0,018	invalid	
5	20,355	0,0183	0,051	0,101	Nitrate
6	26,445	0,0248	0,047	invalid	
7	29,568	0,5868	1,244	invalid	

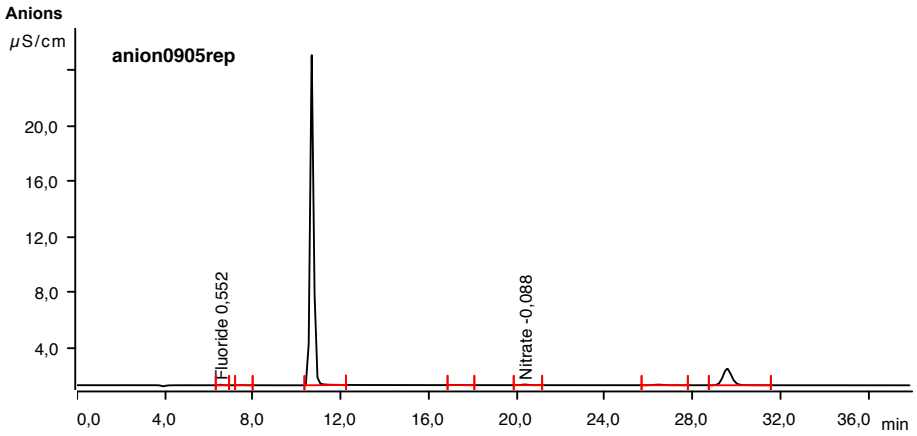

Peak number	Retention time	Area	Height	Concentration	Component name
	min	(µS/cm) x min	µS/cm	mg/L	
1	6,518	0,0062	0,039	0,552	Fluoride
2	7,430	0,0030	0,012	invalid	
3	10,673	4,5193	23,765	invalid	
4	17,275	0,0055	0,017	invalid	
5	20,355	0,0168	0,047	-0,088	Nitrate
6	26,442	0,0210	0,041	invalid	
7	29,565	0,5602	1,186	invalid	

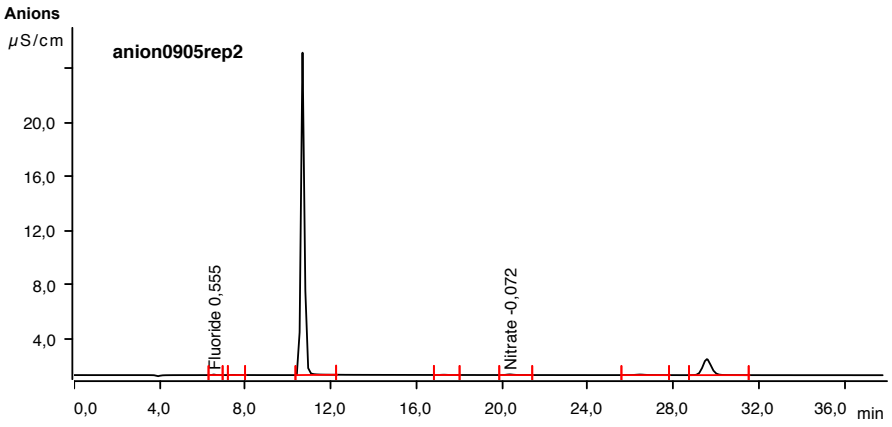

Peak number	Retention time min	Area (µS/cm) x min	Height µS/cm	Concentration mg/L	Component name
1	6,517	0,0063	0,040	0,555	Fluoride
2	7,432	0,0031	0,012	invalid	
3	10,672	4,5204	23,840	invalid	
4	17,275	0,0055	0,017	invalid	
5	20,347	0,0170	0,047	-0,072	Nitrate
6	26,435	0,0212	0,041	invalid	
7	29,558	0,5572	1,182	invalid	

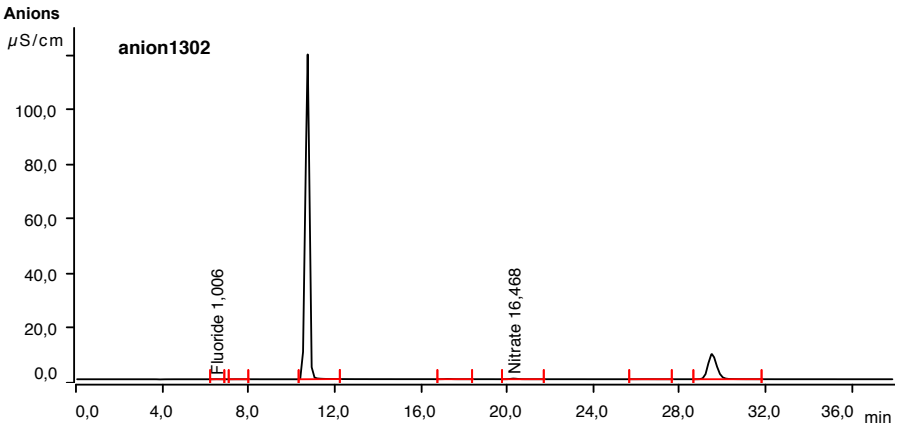

Peak number	Retention time min	Area (µS/cm) x min	Height µS/cm	Concentration mg/L	Component name
1	6,513	0,0043	0,026	1,006	Fluoride
2	7,428	0,0036	0,014	invalid	
3	10,748	24,7509	118,953	invalid	
4	17,247	0,0293	0,093	invalid	
5	20,297	0,0835	0,238	16,468	Nitrate
6	26,417	0,0088	0,017	invalid	
7	29,498	4,3953	9,217	invalid	

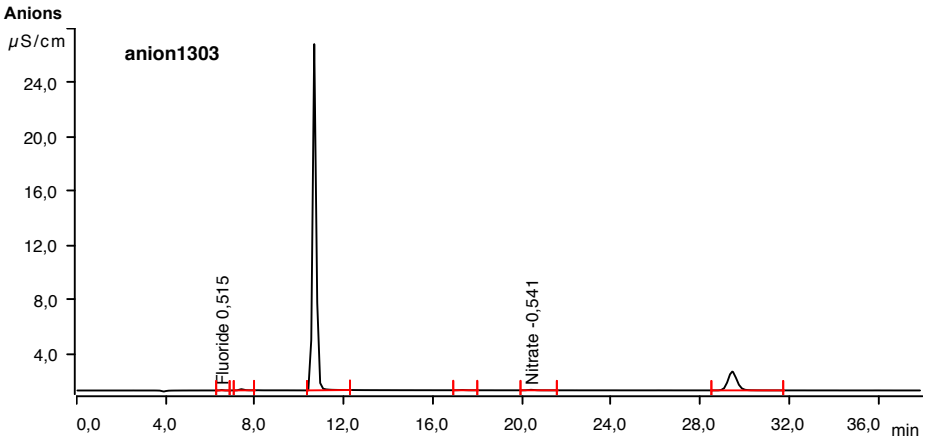

Peak number	Retention time	Area	Height	Concentration	Component name
	min	(µS/cm) x min	µS/cm	mg/L	
1	6,502	0,0048	0,030	0,515	Fluoride
2	7,397	0,0199	0,085	invalid	
3	10,668	4,8683	25,554	invalid	
4	17,310	0,0058	0,018	invalid	
5	20,400	0,0132	0,036	-0,541	Nitrate
6	29,433	0,6536	1,388	invalid	

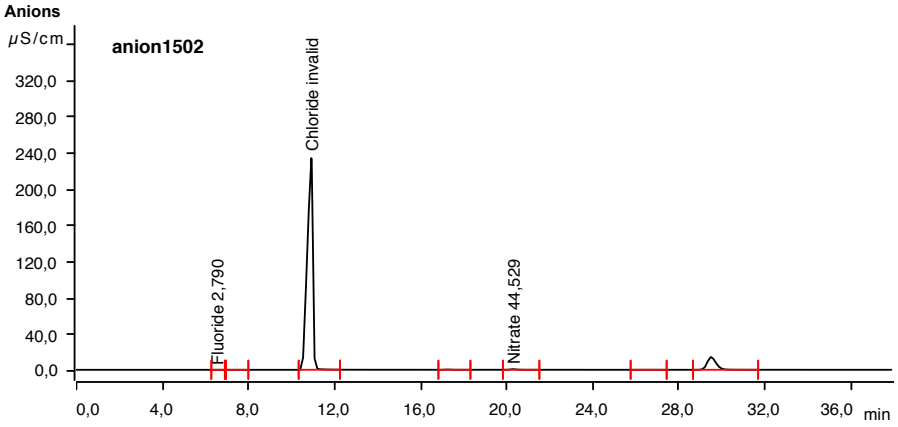

Peak number	Retention time	Area	Height	Concentration	Component name
	min	(µS/cm) x min	µS/cm	mg/L	
1	6,510	0,0078	0,046	2,790	Fluoride
2	7,433	0,0041	0,014	invalid	
3	10,918	68,8912	233,013	invalid	Chloride
4	17,255	0,0862	0,284	invalid	
5	20,290	0,2222	0,648	44,529	Nitrate
6	26,457	0,0119	0,022	invalid	
7	29,490	6,7320	13,958	invalid	

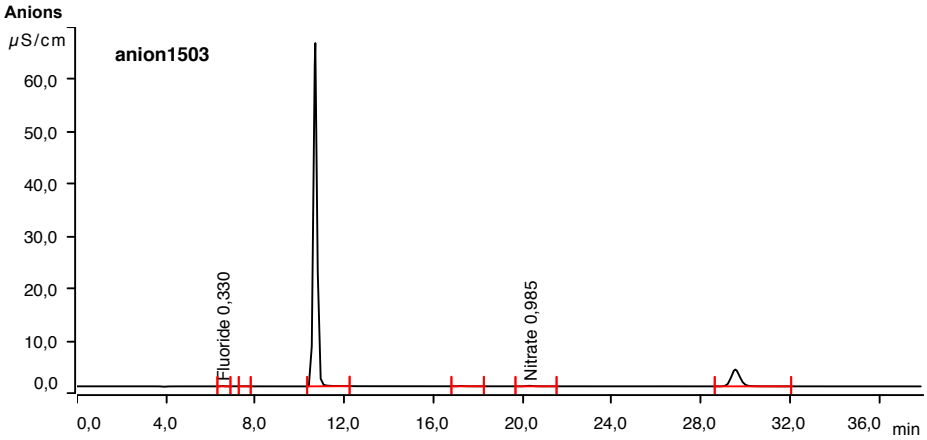

Peak number	Retention time min	Area (µS/cm) x min	Height µS/cm	Concentration mg/L	Component name
1	6,515	0,0105	0,066	0,330	Fluoride
2	7,425	0,0029	0,014	invalid	
3	10,693	12,6178	65,641	invalid	
4	17,248	0,0152	0,048	invalid	
5	20,312	0,0333	0,093	0,985	Nitrate
6	29,538	1,5127	3,214	invalid	

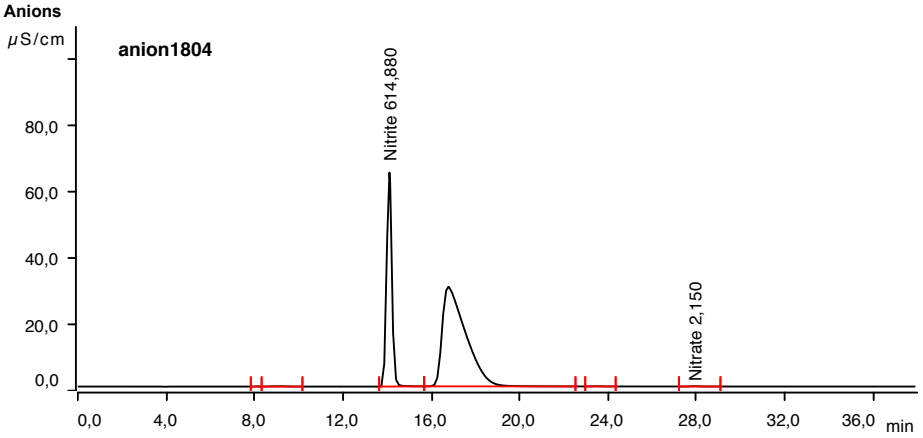

Peak number	Retention time min	Area (µS/cm) x min	Height µS/cm	Concentration mg/L	Component name
1	8,098	0,0130	0,070	invalid	
2	9,032	0,0758	0,086	invalid	
3	14,102	17,6942	64,681	614,880	Nitrite
4	16,765	36,9520	30,075	invalid	
5	23,483	0,0217	0,054	invalid	
6	27,902	0,0421	0,090	2,150	Nitrate

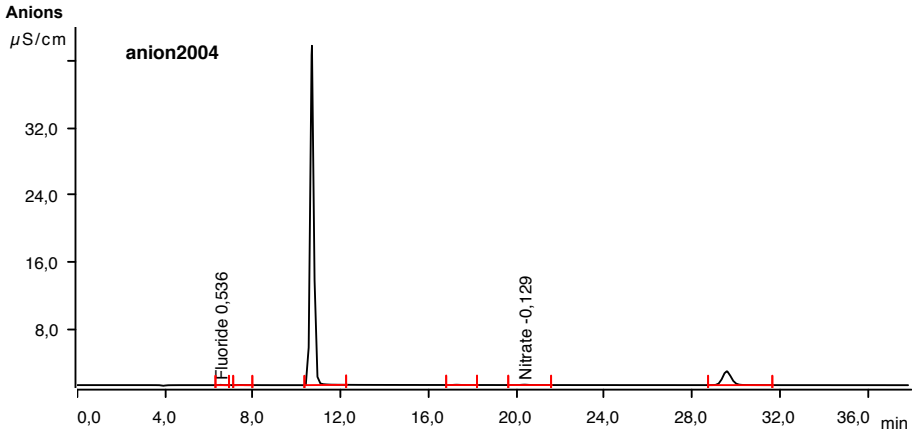

Peak number	Retention time min	Area (µS/cm) x min	Height µS/cm	Concentration mg/L	Component name
1	6,517	0,0056	0,035	0,536	Fluoride
2	7,430	0,0035	0,014	invalid	
3	10,683	7,7299	40,450	invalid	
4	17,273	0,0094	0,029	invalid	
5	20,357	0,0165	0,046	-0,129	Nitrate
6	29,567	0,7780	1,650	invalid	

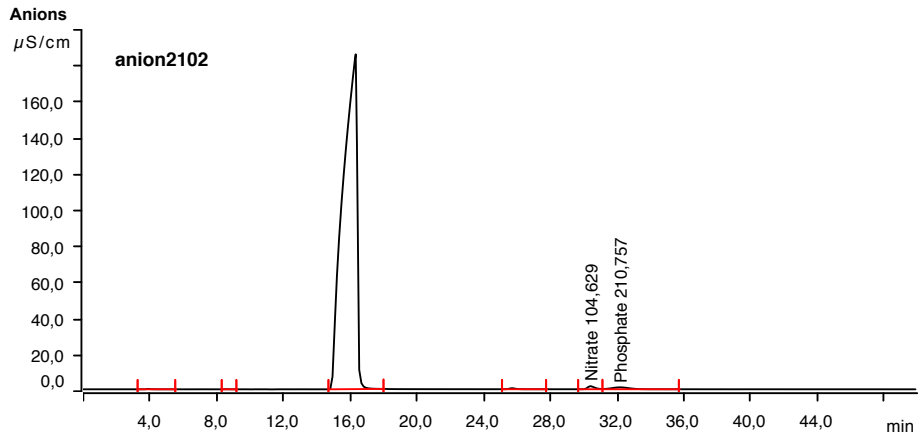

Peak number	Retention time min	Area (µS/cm) x min	Height µS/cm	Concentration mg/L	Component name
1	3,867	0,0625	0,208	invalid	
2	8,590	0,0170	0,053	invalid	
3	16,323	179,5064	185,238	invalid	
4	25,688	0,2353	0,560	invalid	
5	30,388	0,8461	1,717	104,629	Nitrate
6	32,155	1,2899	1,054	210,757	Phosphate

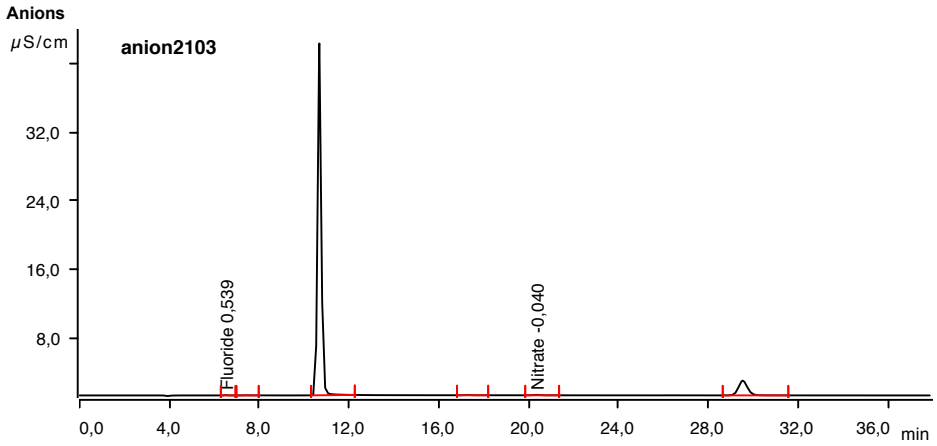

Peak number	Retention time min	Area (µS/cm) x min	Height µS/cm	Concentration mg/L	Component name
1	6,513	0,0057	0,036	0,539	Fluoride
2	7,425	0,0038	0,014	invalid	
3	10,675	7,8183	41,004	invalid	
4	17,263	0,0095	0,030	invalid	
5	20,340	0,0172	0,048	-0,040	Nitrate
6	29,523	0,8085	1,720	invalid	

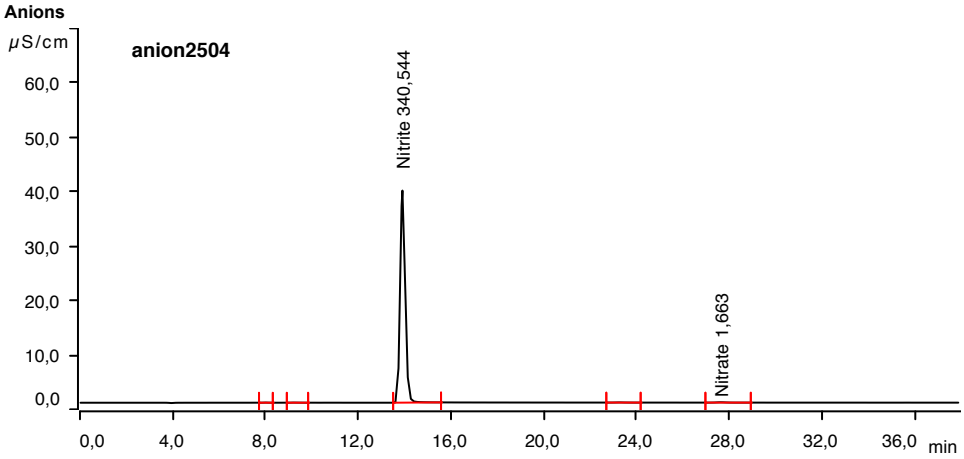

Peak number	Retention time min	Area (µS/cm) x min	Height µS/cm	Concentration mg/L	Component name
1	8,013	0,0047	0,027	invalid	
2	9,242	0,0062	0,022	invalid	
3	13,903	9,7997	38,966	340,544	Nitrite
4	23,258	0,0121	0,030	invalid	
5	27,627	0,0312	0,067	1,663	Nitrate

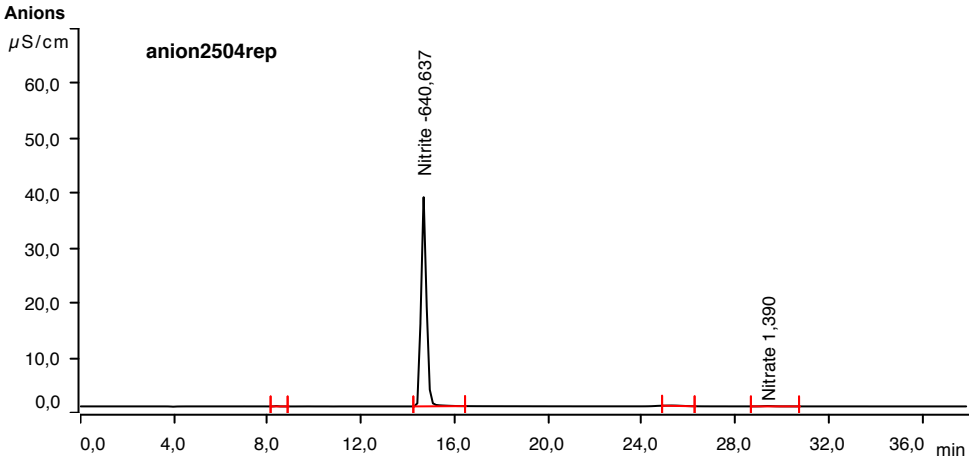

Peak number	Retention time	Area	Height	Concentration	Component name
	min	(µS/cm) x min	µS/cm	mg/L	
1	8,365	0,0112	0,063	invalid	
2	14,673	10,2319	38,114	-640,637	Nitrite
3	25,273	0,0484	0,065	invalid	
4	29,375	0,0312	0,063	1,390	Nitrate

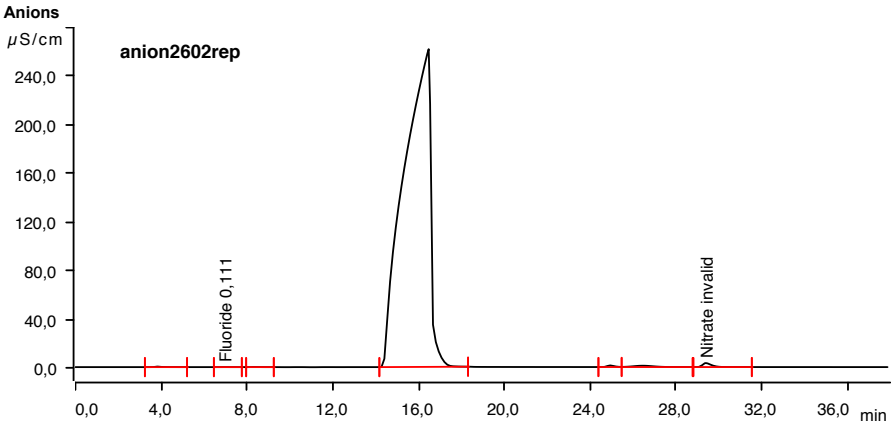

Peak number	Retention time	Area	Height	Concentration	Component name
	min	(µS/cm) x min	µS/cm	mg/L	
1	3,812	0,1385	0,445	invalid	
2	6,963	0,0069	0,016	0,111	Fluoride
3	8,292	0,0359	0,088	invalid	
4	16,467	374,0975	260,886	invalid	
5	24,925	0,5140	1,308	invalid	
6	26,442	1,2128	1,085	invalid	
7	29,387	1,5610	3,278	invalid	Nitrate

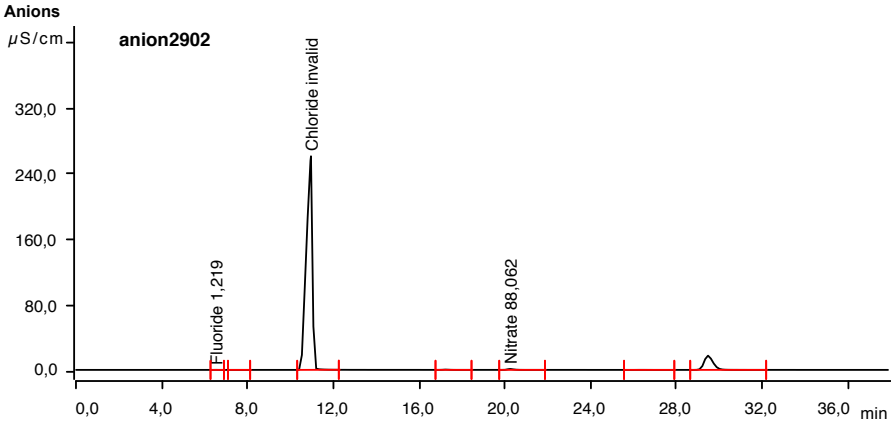

Peak number	Retention time	Area	Height	Concentration	Component name
	min	(µS/cm) x min	µS/cm	mg/L	
1	6,510	0,0085	0,049	1,219	Fluoride
2	7,438	0,0031	0,011	invalid	
3	10,957	84,5952	260,120	invalid	Chloride
4	17,232	0,1049	0,349	invalid	
5	20,233	0,3704	1,090	88,062	Nitrate
6	26,422	0,0205	0,040	invalid	
7	29,462	8,4009	17,285	invalid	

I Chromatograms - Cations

The quantification was done in Microsoft Excel, and the given concentrations in the following tables are not correct. The given areas were used to calculate the concentrations using the calibration curves in appendix D. The concentrations are given in appendix G.

MagIC Net

2018-06-05 11:17:11

Sample data

Ident	ks0902	
Sample type	Sample	
Determination start	2018-05-14 23:51:12 UTC+2	
Method	Kationer logisk 2018	
Operator		

Kationer

Data source	Conductivity detector 1 (940 Professional IC Vario 1)	
Channel	Conductivity	
Recording time	42,0	min
Integration	Automatically	
Column type	Metrosep C 6 - 250/4.0	
Eluent composition	Anion Eluent - 3,6 mM Na2CO3	
Flow	0,900	mL/min
Maximum flow monitored	yes	
Pressure	10,19	MPa
Maximum pressure monitored	yes	
Temperature	30,0	°C

Kationer - logical

Data source	Conductivity detector 1 (940 Professional IC Vario 1)	
Channel	Conductivity	
Recording time	42,0	min
Integration	Automatically	
Column type	Metrosep C 6 - 250/4.0	
Eluent composition	Anion Eluent - 3,6 mM Na2CO3	
Flow	0,900	mL/min
Maximum flow monitored	yes	
Pressure	10,19	MPa
Maximum pressure monitored	yes	
Temperature	30,0	°C

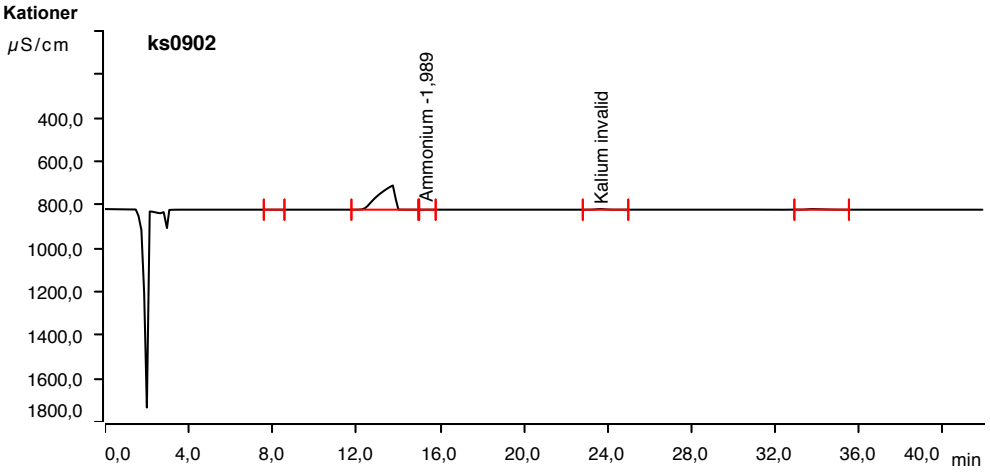

Peak number	Retention time min	Area (µS/cm) x min	Height µS/cm	Concentration mg/L	Component name
1	8,223	0,0058	0,012	invalid	
2	13,732	100,9305	111,186	invalid	
3	15,282	0,0095	0,035	-1,989	Ammonium
4	23,625	1,4443	2,812	invalid	Kalium
5	33,737	2,4110	2,676	invalid	

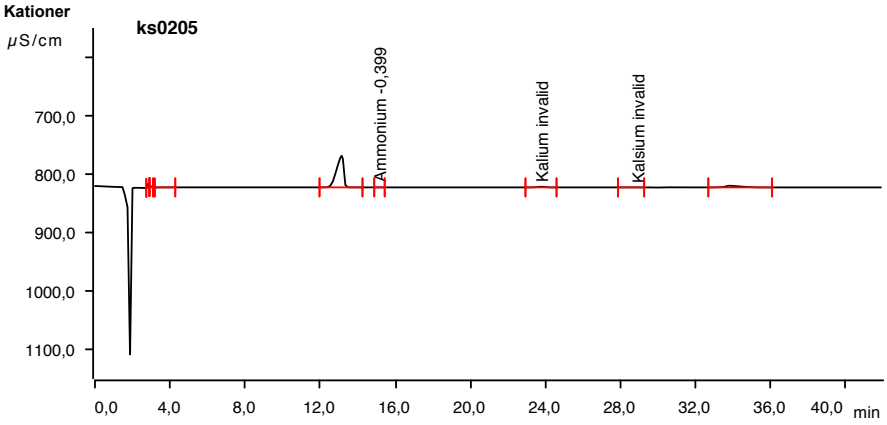

Peak number	Retention time min	Area (µS/cm) x min	Height µS/cm	Concentration mg/L	Component name
1	2,827	0,4653	6,305	invalid	
2	2,968	0,1520	1,725	invalid	
3	3,613	0,0937	0,133	invalid	
4	13,138	24,1682	54,234	invalid	
5	15,163	0,0068	0,025	-0,399	Ammonium
6	23,768	0,5630	1,113	invalid	Kalium
7	28,897	0,0191	0,032	invalid	Kalsium
8	33,792	2,6372	2,809	invalid	

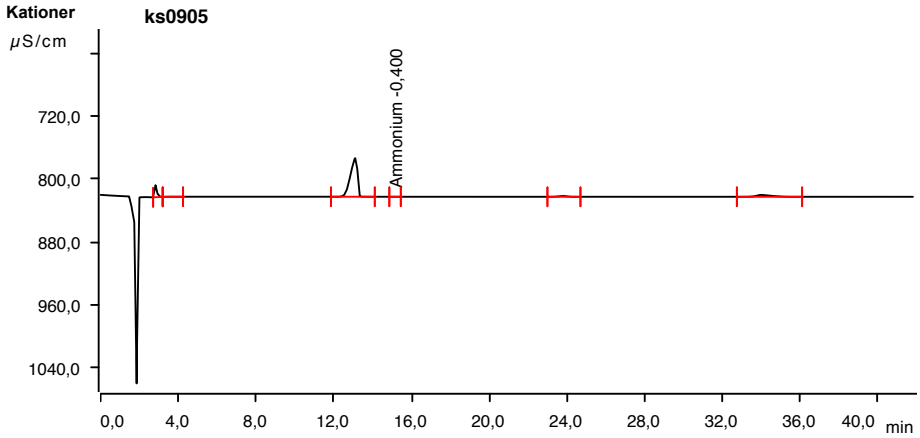

Peak number	Retention time min	Area (µS/cm) x min	Height µS/cm	Concentration mg/L	Component name
1	2,828	1,9238	15,270	invalid	
2	3,590	0,0717	0,110	invalid	
3	13,098	20,4914	48,923	invalid	
4	15,147	0,0048	0,018	-0,400	Ammonium
5	23,787	0,4875	0,962	invalid	
6	33,967	2,1236	2,366	invalid	

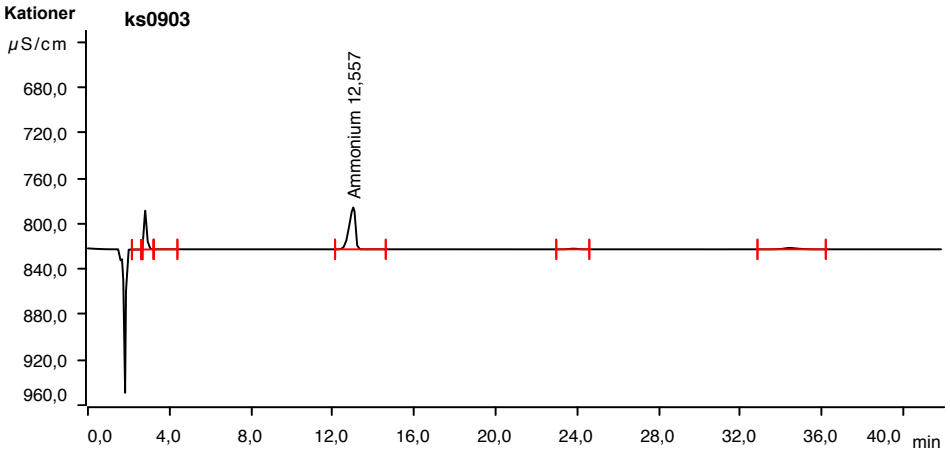

Peak number	Retention time min	Area (µS/cm) x min	Height µS/cm	Concentration mg/L	Component name
1	2,357	0,0299	0,097	invalid	
2	2,812	4,3052	34,189	invalid	
3	3,537	0,0406	0,065	invalid	
4	13,010	13,5163	36,823	12,557	Ammonium
5	23,810	0,3038	0,594	invalid	
6	34,385	0,9654	1,185	invalid	

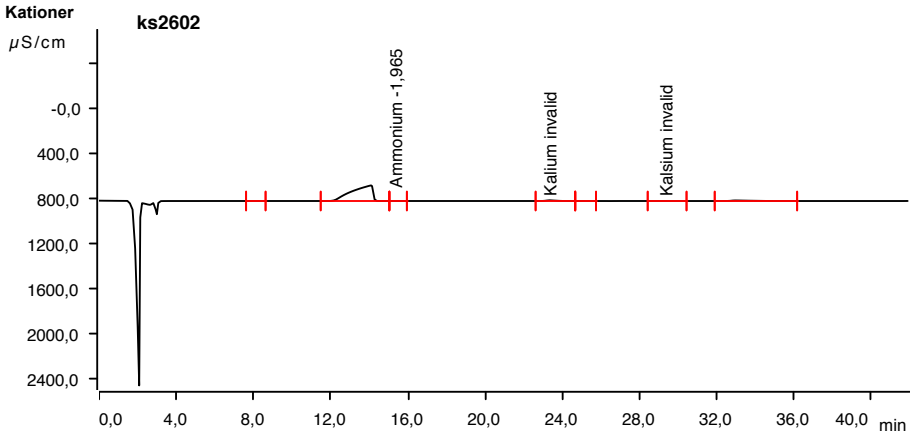

Peak number	Retention time min	Area (µS/cm) x min	Height µS/cm	Concentration mg/L	Component name
1	8,187	0,0112	0,016	invalid	
2	14,087	174,8959	138,491	invalid	
3	15,330	0,0194	0,073	-1,965	Ammonium
4	23,320	3,4489	6,196	invalid	Kalium
5	25,383	0,0151	0,031	invalid	
6	29,055	0,0208	0,015	invalid	Kalsium
7	32,927	5,6799	4,987	invalid	

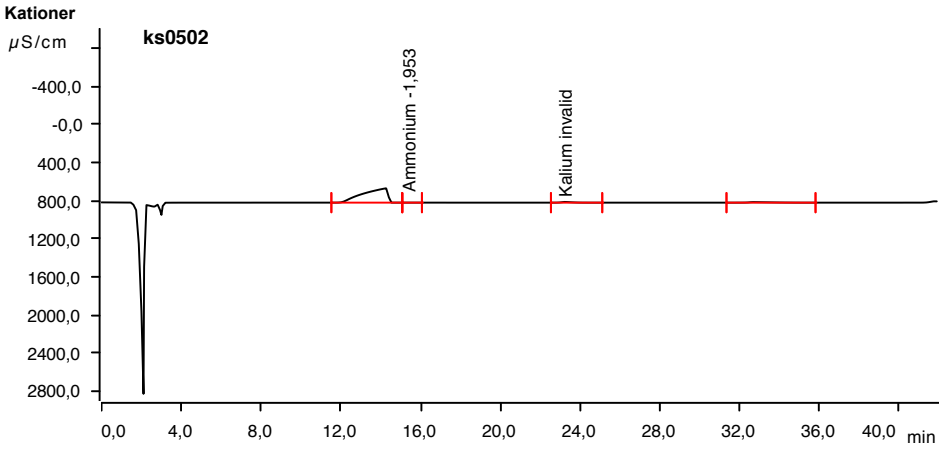

Peak number	Retention time min	Area (µS/cm) x min	Height µS/cm	Concentration mg/L	Component name
1	14,255	215,7330	149,950	invalid	
2	15,372	0,0243	0,088	-1,953	Ammonium
3	23,215	4,2467	7,375	invalid	Kalium
4	32,657	6,8422	5,654	invalid	

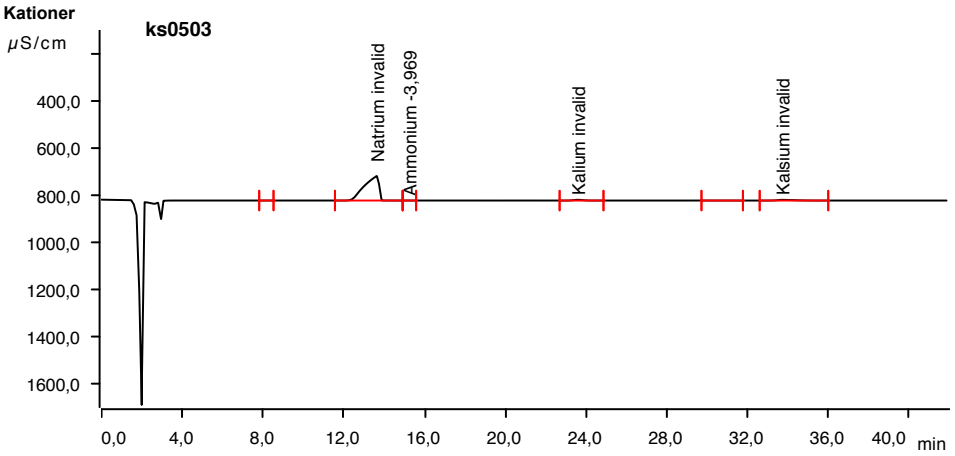

Peak number	Retention time min	Area (µS/cm) x min	Height µS/cm	Concentration mg/L	Component name
1	8,215	0,0055	0,014	invalid	
2	13,632	86,5397	103,913	invalid	Natrium
3	15,233	0,0114	0,043	-3,969	Ammonium
4	23,570	1,6615	3,218	invalid	Kalium
5	30,508	0,0274	0,023	invalid	
6	33,697	2,8215	2,983	invalid	Kalsium

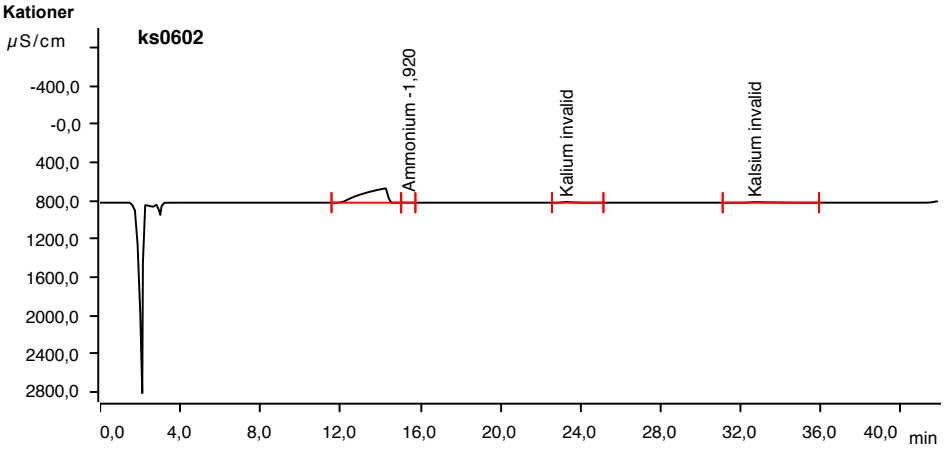

Peak number	Retention time min	Area (µS/cm) x min	Height µS/cm	Concentration mg/L	Component name
1	14,250	213,7886	149,414	invalid	
2	15,372	0,0377	0,143	-1,920	Ammonium
3	23,232	4,2062	7,314	invalid	Kalium
4	32,645	6,9871	5,732	invalid	Kalsium